PROCESS ANALYSIS AND OPTIMIZATION OF BIODIESEL PRODUCTION

FROM VEGETABLE OILS

A Thesis

by

LAY L. MYINT

Submitted to the Office of Graduate Studies of
Texas A&M University
in partial fulfillment of the requirements for the degree of

MASTER OF SCIENCE

May 2007

Major Subject: Chemical Engineering

PROCESS ANALYSIS AND OPTIMIZATION OF BIODIESEL PRODUCTION

FROM VEGETABLE OILS

A Thesis

by

LAY L. MYINT

Submitted to the Office of Graduate Studies of
Texas A&M University
in partial fulfillment of the requirements for the degree of

MASTER OF SCIENCE

Approved by:

Chair of Committee,	Mahmoud El-Halwagi
Committee Members,	Sam Mannan
	Guy Curry
Head of Department,	N.K.Anand

May 2007

Major Subject: Chemical Engineering

ABSTRACT

Process Analysis and Optimization of Biodiesel Production

from Vegetable Oils. (May 2007)

Lay L. Myint, B.S., Purdue University

Chair of Advisory Committee: Dr. Mahmoud M. El-Halwagi

The dwindling resources of fossil fuels coupled with the steady increase in energy consumption have spurred research interest in alternative and renewable energy sources. Biodiesel is one of the most promising alternatives for fossil fuels. It can be made from various renewable sources, including recycled oil, and can be utilized in lieu of petroleum-based diesel. To foster market competitiveness for biodiesel, it is necessary to develop cost-effective and technically sound processing schemes, to identify related key design criteria, and optimize performance.

The overall goal of this work was to design and optimize biodiesel (Fatty Acid Methyl Ester "FAME") production from vegetable oil. To achieve this goal, several inter-connected research activities were undertaken. First, a base-case flow sheet was developed for the process. The performance of this flow sheet along with the key design and operating criteria were identified by conducting computer-aided simulation using ASPEN Plus. Various scenarios were simulated to provide sufficient understanding and insights. Also, different thermodynamic databases were used for different sections of the process to account for the various characteristics of the streams throughout the process. Next, mass and energy integration studies were performed to reduce the consumption of material and energy utilities, improve environmental impact, and enhance profitability. Finally, capital cost estimation was carried out using the ICARUS Process Evaluator computer-aided tools linked to the results of the ASPEN simulation.

The operating cost of the process was estimated using the key information on process operation such as raw materials, utilities, and labor. A profitability analysis was carried out by examining the ROI (Return of Investment) and PP (Payback Period). It was determined that the single most important economic factor is the cost of soybean oil, which accounted for more than 90% of the total annualized cost. Consequently, a

sensitivity analysis was performed to examine the effect of soybean oil cost on profitability. It was determined that both ROI and PP quickly deteriorate as the cost of soybean oil increases.

ACKNOWLEDGEMENTS

I am very thankful to my parents, Mr. and Mrs. Tsung Aung, for their unconditional love and encouraging me to continue my journey of learning. They have taught me that no matter how hard life has become, determination and hard work will steer me towards my destination. I am forever indebted to my husband, Thuya Aung, for his patience, unlimited understanding, and true love. He has helped me every possible way to make my life easier and been there for me not only as my life partner but also as my guiding spirit.

My special thank to my wonderful graduate advisor and role model, Dr. El-Halwagi, who has inspired me to become a true passionate chemical engineer. I sincerely appreciate his moral support, guidance and abundant help through out my graduate school year. I am also thankful to all my professors, especially Dr. West, Dr. Baldwin and Mr. Bradshaw, who have helped me with my research work and guided my steps towards my goal.

I am thankful to my group members for their help and guidance. My special thank to Arwa for her moral support and all the helps she has provided during my school year.

I am grateful to USDA for funding my research.

TABLE OF CONTENTS

LIST OF FIGURES

LIST OF TABLES

TABLE   Page

CHAPTER I

INTRODUCTION

Recently, developing countries such as India and China have experienced a significant increase in energy demand. In addition, some of the world's largest producers of oil have suffered from warfare and political and social instability. Diminishing fossil fuel resources, coupled with the steady increase in energy consumption, has spurred research interest in alternative and renewable energy sources. Biodiesel is among the most promising fossil fuel alternatives. Various renewable sources, including recycled oil, can be utilized as feedstocks. Of significant import is biodiesel's capability to be used in lieu of petroleum-based diesel.

Potentially, there is a very large market for alternative fuels. According to International Energy Outlook 2006 report, the global demand for oil will grow from 80 million barrels per day in 2003 to 98 million barrels per day in 2015 and 118 million barrels per day in 2030. Although current oil prices are already 35% higher than the 2025 projected prices of the previous year, global demand for oil continues to rise steadily. In order to meet the projected increase in world oil demand, total petroleum supply in 2030 will need to increase by 38 million barrels per day, from 80 million barrels per day in 2003 to 118 million barrels per day in 2030. Members of the Organization of Petroleum Exporting Countries (OPEC) are expected to provide 14.6 million barrels per day of the increase. Higher oil prices have also induced substantial increase in non-OPEC oil production in the amount of 23.7 million barrels per day. Figure (1.1) illustrates the projected increase in global energy demand.

_____

This thesis follows the style of Bioresource Technology.
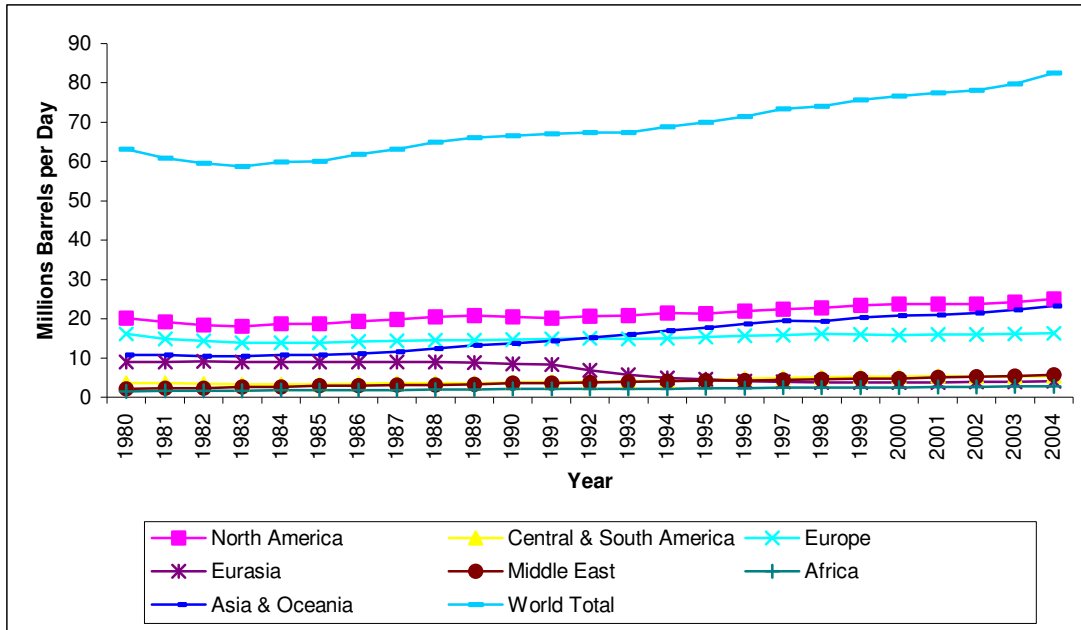
Figure 1.1 Increase in Global Petroleum Consumption (EIA, 2005)

Current petroleum consumption in the US is 20 million barrels of oil per day. Nearly a quarter of this amount is refined into diesel fuel and heating oil for use in trucks, boats, and heavy equipments. Highway diesel fuel consumption alone stands at 136 million gallons per day (EIA, 2005). Although Biodiesel production can replace only a small percentage of the nation's fuel supply, the petroleum market has a tendency to be sensitive to small fluctuations in supply (West et al., 2006). This instability of petroleum price can be seen clearly in Figure (1.2). Therefore, additional sources of fuel can potentially have a large impact on fuel price stability.
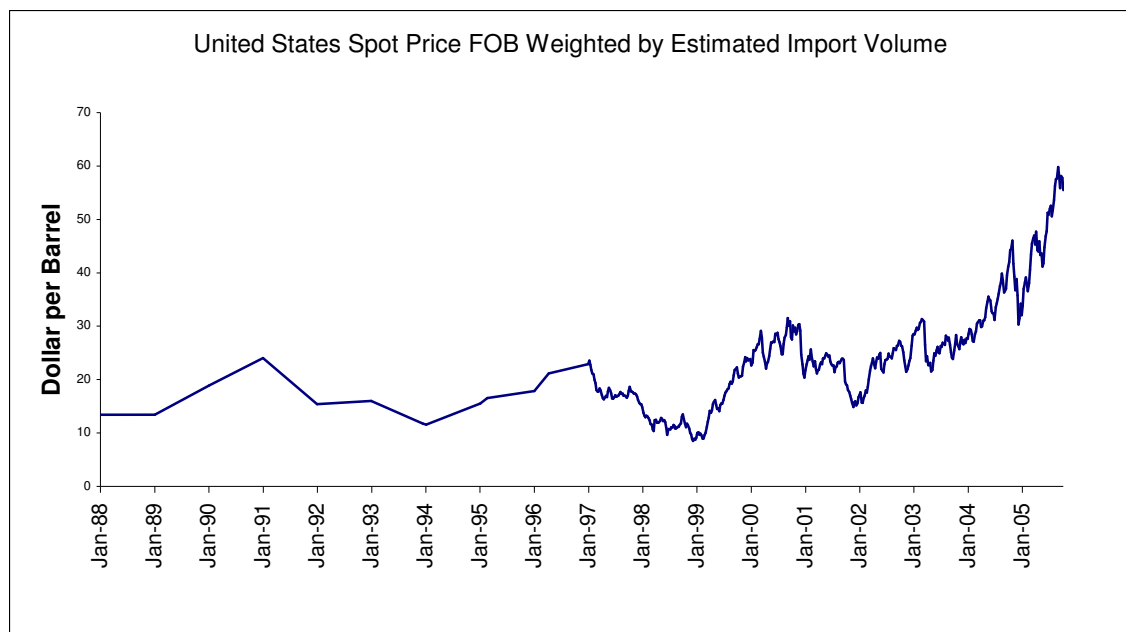
Figure 1.2 Changing Oil Prices in the United States (EIA, 2006)

Another major contributing factor to the importance of Biodiesel production is reduction of green house gas emissions. Combustion of fossil fuel over the past century has dramatically increased the emission of carbon dioxide and other green house gases into the atmosphere. These gases trap heat, thereby contributing to global warming. Since Biodiesel is manufactured from plants, which obtain carbon dioxide from the air during photosynthesis, its use reduces overall CO_2 emission. Life cycle analysis of Biodiesel demonstrates that overall CO_2 emissions are reduced by 78% when Biodiesel is utilized as opposed to petroleum-based diesel fuel (Gerpen, 2005).

Combustion of fossil fuel deposits sulfuric, carbonic, and nitric acids into the atmosphere, increasing the probability of acid rain production. Other pollutants, such as oxygen oxides, sulfur dioxide, volatile organic compounds, and heavy metals, generated by the use of fossil fuels are very harmful to our health and environment.

One of the main pollutants contained in diesel fuel is sulfur. High levels of sulfur in diesel are detrimental to the environment through contributions to low-level pollution such as smog. Diesel fuel sulfur content, which ranges from 300 to 500 ppm, has not been regulated until recently. The Environmental Protection Agency (EPA) has mandated a standard known as Ultra Low Sulfur Diesel (ULSD), requiring diesel fuels used in both

on and off road vehicles to be lowered to 15 ppm of sulfur (API, 2006). Removal of sulfur from diesel fuel tremendously decreases the fuel's lubricity. As a result of this change in lubricity, engine efficiency and lifespan decrease significantly. Consequently, additives are needed to regain the appropriate level of lubricity. It has been determined that blending ultra low sulfur diesel with Biodiesel recovers the lost lubricity (Kotrba, 2006). Therefore, the use of additional device to control diesel particulate emissions and additives to regain lubricity can be avoided through use of biodiesel.

In an effort to decrease dependence on foreign oil, the United States Federal Government has been supportive of growth in the biodiesel industry. The following factors have been identified as contributers to the viability of Biodiesel market opportunities in the United States (Earth Biofuels, 2006):

- Strains on U.S. oil refineries to meet demand
- Ratification of the ASTM (American Society for Testing and Materials) Biodiesel quality standard
- Current and future EPA emission standards
- New clean diesel engine technologies
- Excise tax credit for biodiesel mandates
- Passage of the 2005 Energy Bill
- Health risks associated with petrodiesel emissions

Biodiesel production has increased exponentially from 0.5 million gallons in 1999 to 75 million gallons in 2005 as shown in Figure (1.3).
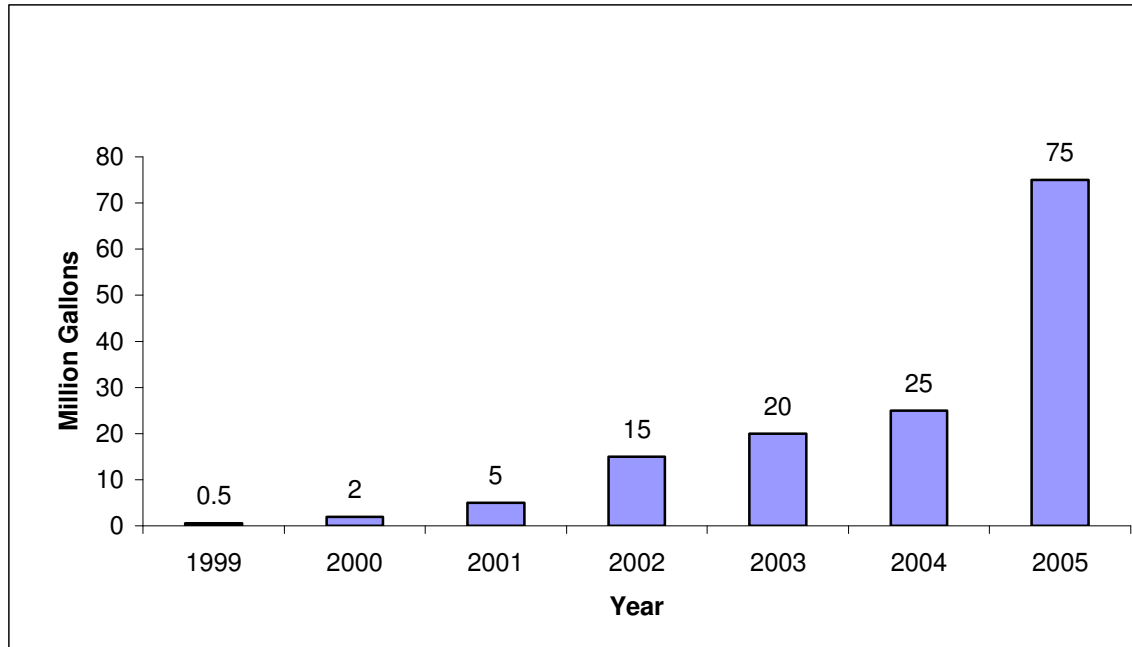
Figure 1.3 Estimated Biodiesel Production in the United States (NBB, 2006)

Figure (1.4) shows the current Biodiesel production plants in the United States as of November 2006.
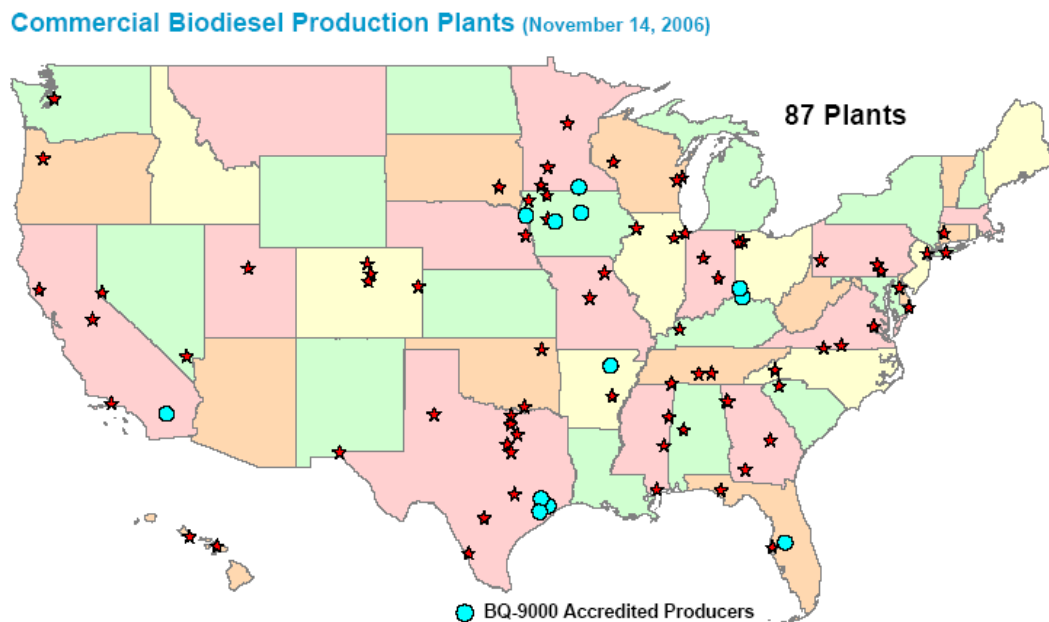
Figure 1.4 Biodiesel Production Plants in the United States (NBB, 2006)

CHAPTER II

BACKGROUND AND LITERATURE SURVEY

2.1 Biofuels History

The concept of using alternative fuels is not contemporary in its nature; it has existed for many years. Alternative diesel engine fuels that have been researched over the years range from coal to peanut oil. During the 1900 Paris World Fair, the French Otto Company ran the Diesel Engine on peanut oil at the request of the French government. A Belgian patent granted in 1937 to G. Chavanne displays the early existence of the use of ethyl esters extracted from palm oil (Knothe et al., 1997).

However, inexpensive petroleum-based fuels prevented biodiesel fuels from receiving much consideration, resulting in adoption of a diesel engine to specifically burn petroleum diesel. Interruption of cheap oil supplies resulting from the 1973 oil embargo as well as the 1990 Gulf War sparked a renewed interest and research in using domestically grown and renewable sources for fuel production. Although the use of biodiesel did not receive much attention in the United States until the late 1990s, it has been used extensively in Europe for nearly a quarter of a century.

It is important to understand how a diesel engine functions in order to understand the necessary characteristics of biodiesel and why biodiesel is a suitable alternative fuel for petrodiesel.

2.2 Mechanism of Diesel Engine

As opposed to a typical engine, a diesel engine does not employ spark plugs. Therefore, extreme temperature and pressure is required to ignite the fuel. Diesel engines utilize internal combustion. In this process, burning of a fuel occurs in a confined space called a combustion chamber. When the gas is compressed, the pressure rises, affecting a resultant increase in temperature. In a diesel engine, air is drawn into a cylinder and compressed by a rising piston at a much higher compression ratio (25:1) than for a spark ignition engine. The air temperature reaches 700ºC to 900ºC. At the top of the piston stroke, the diesel fuel is injected into the combustion chamber at high pressure via an atomizing nozzle, mixing with hot, high-pressured air. The resulting mixture ignites and

burns very rapidly. This contained combustion causes the gas in the chamber to heat up rapidly, resulting in an increase in pressure, thereby forcing the piston downwards. The piston is connected to rods through which it delivers rotary power at the output end of the crankshaft. This engine system is known as a Direct Injection system (DI). A DI system utilizes diesel since diesel oil has a much lower flash point than gasoline (Billen et al., 2004). Another type of engine is the Indirect Injection Diesel (IID) engine in which fuel is preheated in a different chamber prior to contact with the hot air. Injection takes place at a lower pressure and the spraying holes are larger than those in a DI system (Billen et al., 2004). Modern diesel engines are typically of the DI type.

2.3 Viscosity

Viscosity is a measure of a fuel's adhesive or cohesive property and is the key factor in estimating the required temperature for pumping, injection, storage, and transfer of the fuel. A viscosity comparison of petrodiesel, biodiesel, and vegetable oils is shown in Table (2.1).

Table 2.1 Comparison of Viscosity among Diesel, Bioidiesel and Vegetable Oils (Knothe et al., 1997)

Type	Heat of Combustion (MJ/Kg)	Kinetic Viscosity (mm^2/s)	Iodine Value	Flash Point (ºC)
Diesel	427	1-4	-	80
Biodiesel	372	4-6	<115	100
Jatropha Oil	396	757	13	340
Rapeseed Oil	376	74	94-110	317
Sunflower Oil	371	66	118-144	316
Soya Oil	371	63.5	114-138	350
Olive Oil	378	83.8	76-90	-
Cottonseed Oil	368	89.4	90-117	320
Nut Oil	372	71	103	340
Coconut Oil	353	21.7	10-Jul	-
PalmOil(butter)	37	29.4	34-61	267
Palm Oil (fat)	355	21.5	14-22	-

Vegetable oils are characterized by much higher viscosities and lower volatilities than diesel fuel, which elicits incorrect vaporization and atomization and incomplete combustion. These DI engines are optimized for diesel fuel and therefore might not perform well with vegetable oils. Potential issues include improper operation and deposition on the injectors and in the combustion chamber, leading to poor performance, higher emissions, and shorter engine life.

The following are difficulties associated with the use of vegetable oils as fuel:

1. Coking and trumpet formation on the injectors to such an extent that fuel atomization does not occur properly or is even prevented due to plugged orifices
2. Carbon deposition
3. Oil ring sticking
4. Thickening or gelling of the lubricating oil as a result of contamination by vegetable oils
5. Lubrication problems.

Vegetable oils or grease that are blended at even a level of 10 to 20% can result in engine deposits, ring sticking, lube oil gelling, and other maintenance problems that can shorten the engine's life (Tyson et al., 2006).

2.4 Petroleum Diesel

Petrodiesel is processed from crude oil, a fossil fuel with broad variations in color, from clear to tar-black, and viscosity, from that of water to almost a solid. Crude oil contains a complex mixture of hydrocarbons comprised of differing chain lengths and physical and chemical properties. The hydrocarbons can be divided into 5 total groupings consisting of three predominant groups (paraffins, aromatics, and naphthenes) and 2 minor groups (alkenes, dienes and alkynes) as shown in Table (2.2) (OTM, 1999). Crude oils are composed of 80 to 90% hydrogen saturated aliphatic alkanes (paraffins) and cycloalkanes (naphthenes). Aromatic hydrocarbons and alkenes (olefins) comprise 10-20% and 1%, respectively, of crude oil composition (ATSDR, 1995). Hydrocarbons containing up to four carbon atoms are gaseous in nature, those with 5 to 19 carbon atoms

are usually found in liquid form, and those with a carbon composition greater than 19 are found as solids.

Table 2.2 Hydrocarbon Contents in Crude Oil (ATSDR, 1995; OTM, 1999)

HYDROCARBONS	GENERAL FORMULA	CHAIN TYPE	STATE (Room temp)	EXAMPLES
Paraffins (Aliphatic)	C_nH_{2n+2} (n:1 to20)	Linear or Branched	Gas or Liquid	Methane, Propane Hexane
Aromatic	C6H5-Y	One or More Benzene Rings wt Long Chains Ys	Liquid	Benzene Napthalene
Napthenes (Cycloalkanes)	C_nH_{2n}	One or More Cycloalkane Rings	Liquid	Cyclohexane Methyl Cyclohexane
Alkenes (Olefin)	C_nH_{2n}	Liner or Branched One or More Double Bond	Gas or Liquid	Ethylene Butene Isobutene
Dienes and Alkynes	C_nH_{2n-2}	Triple Bond	Gas or Liquid	Butadiene Acetylene

Products resulting from fractional distillation are shown in Table (2.3). These products undergo further processing (cracking, unification, and alteration) in order to acquire desired compounds.

Table 2.3 Physical Properties of Petroleum Products (Freudenrich, 2001)

Product Types	Boiling Range °C	Chain Type
Petroleum Gas	Less than 40	Alkanes (1 to 4 carbon atoms)
Naptha	60 to 100	Alkanes (5 to 9 carbon atoms)
Gasoline	40 to 205	Alkanes (5 to 12 carbon atoms) and Cycloalkane
Kerosene	175 to 325	Alkanes (10 to 18 carbon atoms) and Aromatics
Diesel Distillate	250 to 350	Alkanes(12 or more carbon atoms), Aromatic, Cycloakanes
Lubricating Oil	300 to 370	Alkanes (20 to 50 carbon atoms), Aromatic, Cycloakanes
Heavy Gas Oil	370 to 600	Alkanes (20 to 70 carbon atoms), Aromatic Cycloakanes
Residuals (coke, asphalt,tar, wax)	Greater than 600	Multiple-ringed compounds (70 or more carbon atom)

Petroleum derived diesel is composed of 64% hydrocarbons, 35% aromatic hydrcarbons, and 1-2% olefinic hydrocarbons (ATSDR, 1995). Conversely, diesel fuel composition is quite variable, depending upon supplier and season (from summer to winter). This variation results from supplier and seasonal dissimilarities in refining and blending practices.

2.5 Biodiesel

In order for vegetable oils and fats to be compatible with the diesel engine, it is necessary to reduce their viscosity. This can be accomplished by breaking down triglyceride bonds, with the final product being referred to as biodiesel. There are at least four ways in which oils and fats can be converted into Biodiesel (Ghadge and Raheman, 2006):

1. Transesterification
2. Blending
3. Microemulsions
4. Pyrolysis.

Among these processes, transesterification is the most commonly used method. The transesterification process is achieved by reaction of a triglyceride molecule with an excess of alcohol in the presence of a catalyst to produce glycerin and fatty esters. The chemical reaction with methanol is shown schematically in Figure (2.1).
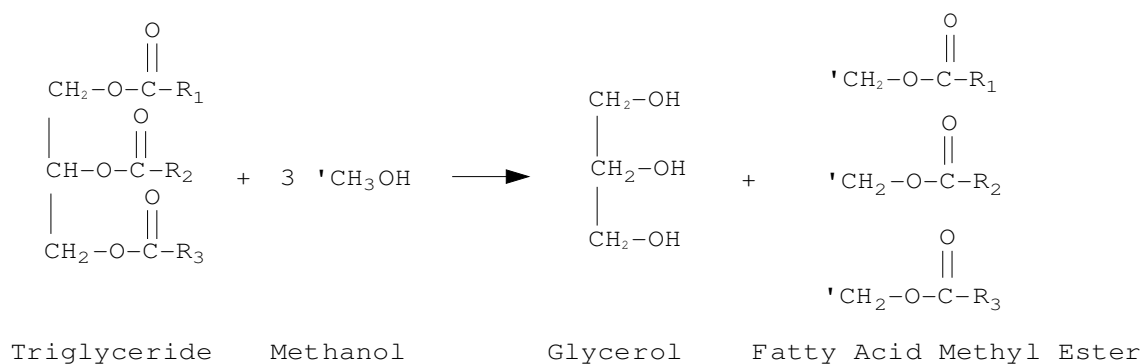
Figure 2.1 Overall mechanism of Transesterification (Gerpen, 2005)

2.6 Comparison of Diesel and Biodiesel

When Biodiesel is blended with petrodiesel, the concentration of Biodiesel is always written as BXX. The 'XX' refers to the percentage volume of Biodiesel or ethanol. For example, pure 100 % Biodiesel will be named B100. B20 is 20% Biodiesel and 80% petroleum diesel. Table (2.4) presents properties comparison for diesel, B20, and B100.

Table 2.4 Properties of Diesel and Biodiesel (Tyson et al., 2004)

Fuel Type	Density (g/cm^3)	Avg Net Heating Value (Btu/gal)	% Difference from No.2 Petro Diesel
No 2 Petro Diesel	0.85	129,500	
Pure Biodiesel (B100)	0.88	118,296	8.65%
Blend Diesel (B20)	0.856	127,259	1.73%
Blend Diesel (B2)	0.851	129,276	0.17%

Energy content of petrodiesel can vary up to 15%. The energy content of Biodiesel is much less variable than that of petrodiesel. The feedstock utilized has a greater effect on the energy content of biodiesel than a particular processing method. Pure biodiesel contains about 8 % less energy per gallon than No. 2 petrodiesel, or 12.5 % less energy per pound. This difference results from the slightly higher density of biodiesel than petrodiesel, 0.88 kg/L vs. 0.85 kg/L. As the ratio of biodiesel to petrodiesel becomes lower, any difference between the biodiesel and petrodiesel becomes less significant. B20 and B2 have 1.73 % and 0.17% less energy per gallon from the petrodiesel, respectively, and do not exhibit a noticeable difference in performance (Tyson et al., 2004).

Pure biodiesel contains up to 10-12 % weight of oxygen, while diesel contains almost 0 % oxygen. The presence of oxygen allows more complete combustion, which reduces hydrocarbons (HC), carbon monoxide (CO), and particulate matter (PM) emission. However, higher oxygen content increases nitrogen oxides (NOx) emissions.

The primary reason biodiesel is suitable as an alternative fuel for petrodiesel lies in the cetane number. The cetane number indicates the ignition quality of a diesel fuel. It measures a fuel's ignition delay, which is a period between the start of injection and start of combustion (ignition) of the fuel. Fuels with a higher cetane number have shorter

ignition delays, providing more time for the fuel combustion process to be completed. The term "cetane number" is derived form a straight chain alkane with 16 carbons ($C_{16}H_{34}$), hexadecane or cetane which is shown in Figure (2.2).
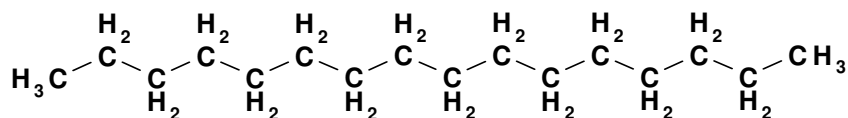
Figure 2.2 Hexadecane

This long unbranched hexadecane is the high quality standard on the cetane scale and has been assigned as having a cetane number of 100. On the other hand, highly branched alkanes are low quality compounds on the cetane scale and have low cetane numbers. Biodiesel's long chain fatty acids methyl ester are similar to long chain alkanes with number of carbons ranging from 14 to 22 (Figure 2.3). This makes biodiesel suitable for alternative diesel fuel (Gerpen et al., 2004).
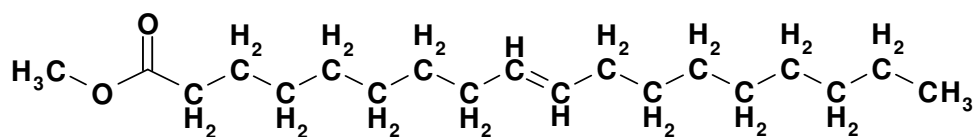
Figure 2.3 Fatty Acid Methyl Ester

2.7 Feedstock

There are different types of oils and fats that can be used as feedstocks for Biodiesel production. The types of fatty acids in different fats and oils are listed in Table (2.5) with their respective compositions listed in Table (2.6).

Table 2.5 Molecular Formula of Various Fatty Acids in Vegetable Oils (Tyson et al., 2004)

Name	Components		Acid	Ester
Myristic acid	C14:0		$C_{14}H_{28}O_2$	$C_{15}H_{30}O_2$
Palmitic Acid	C16:0		$C_{16}H_{32}O_2$	$C_{17}H_{34}O_2$
Palmitoleic	C16:1	c9	$C_{16}H_{30}O_2$	$C_{17}H_{32}O_2$
Hexadecadienoic	C16:2	c5,c9	$C_{16}H_{28}O_2$	$C_{17}H_{30}O_2$
Hexadecatrienoic	C16:3	c7,c10,c13	$C_{16}H_{26}O_2$	$C_{17}H_{28}O_2$
Hexadecatetraoic	C16:4	c6,c9,c12,c15	$C_{16}H_{24}O_2$	$C_{17}H_{26}O_2$
Stearic acid	C18:0		$C_{18}H_{36}O_2$	$C_{19}H_{38}O_2$
Heptadecinoic acid	C18:1n-7	c11	$C_{18}H_{34}O_2$	$C_{19}H_{36}O_2$
Oleic Acid	C18:1n-9	c9	$C_{18}H_{34}O_2$	$C_{19}H_{36}O_2$
Linoleic acid	C18:2n-6	c9,c12	$C_{18}H_{32}O_2$	$C_{19}H_{34}O_2$
Linolenic acid	C18:3n-3	c9,c12,c15	$C_{18}H_{30}O_2$	$C_{19}H_{32}O_2$
Eiscosenoic acid	C20:1n9	c11	$C_{20}H_{38}O_2$	$C_{21}H_{40}O_2$
Erucic acid	C22:1n-9	c13	$C_{22}H_{42}O_2$	$C_{23}H_{44}O_2$

In these tables, the number in front of the colon is the number of carbon atoms contained in the fatty acid. The number following the colon is the number of double bonds. For example, C16:2 represents 16 carbon atoms and 2 double bonds.

Table 2.6 Compositions of Various Oils and Fats (Knothe et al., 1997)

Oil or Fat	Fatty Acid [C-O-O-R] Compositions (Wt.-%)								
	C12:0	**C14:0**	**C16:0**	**C18:0**	**C18:1**	**C18:2**	**C18:3**	**C20:1**	**C22:1**
Babassu	44-45	15-17	5.8-9	2.5-5.5	12-16	1.4-3			
Canola			4-5	38719	55-63	20-31	9-10		1-2
Coconut	44-51	13-18.5	7.5-10.5	1-3	5-8.2	1.0-2.6			
Corn		1-2	7-13	2.5-3	30.5-43	39-52	Trace		
Cottonseed		0.8-1.5	22-24	2.6-5	19	50-52.5			
Linseed			6	3.2-4	13-37	5-23	26-60		
Olive		1.3	7-18.3	1.4-3.3	55.5-85	4-19			
Palm		0.6-2.4	32-46.3	4-6.3	37-53	6-12			
Peanut		0.5	6-12.5	2.5-6	37-61	13-41			1
Rapeseed		1.5	1-4.7	1-3.5	13-38	9.5-22	1-10		40-64
Safflower			6.4-7.0	2.4-29	9.7-13.8	75-80.5			
Safflower, high-oleic			4-8	2.3-8	73.6-79	11-19			
Sesame			7.2-9.2	5.8-7.7	35-46	35-48			
Soybean			2.3-11	2.4-6	22-30.8	49-53	2-10.5		
Sunflower			3.5-6.5	1.3-5.6	14-43	44-68.7			
Butter		7-10	24-26	10-13	28-31	1-2.5	0.2-0.5		
Lard		1-2	28-30	12-18	40-50	7-13	0-1		
Yellow Grease		1.27	17.44	12.38	54-67	7.96	0.69	0.25	0.52
Tallow (beef)		3-6	25-37	14-29	26-50	1-2.5			

Figure (2.4) compares monthly prices of different feedstocks. It can be seen that price fluctuation is a function of supply and demand, rather than the crop's season.
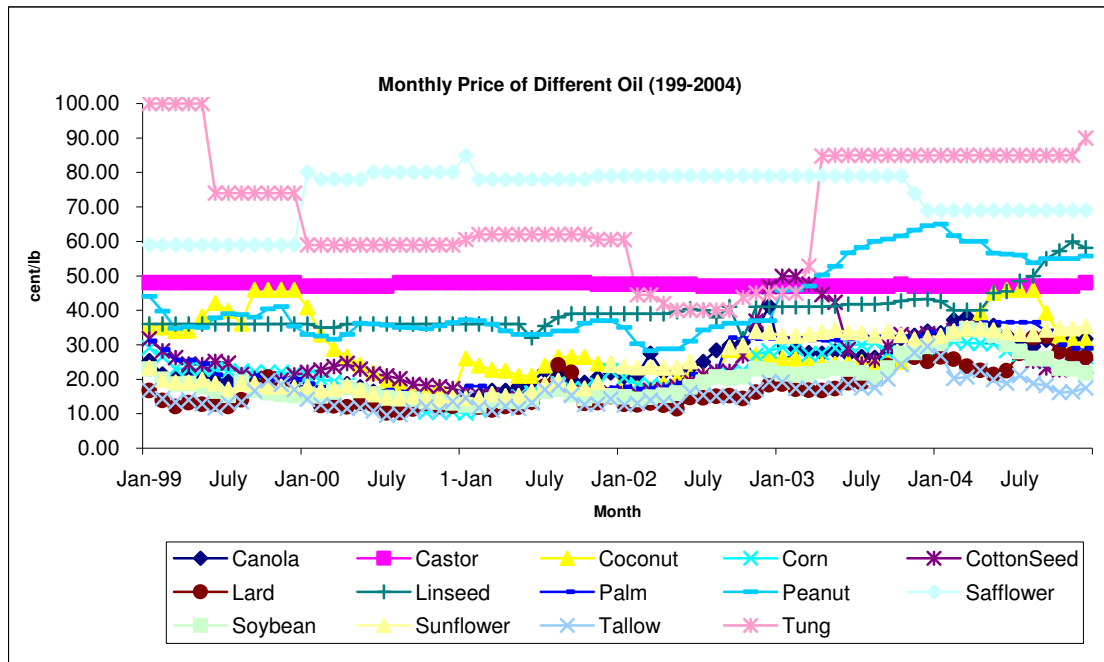
Figure 2.4 Comparison of Different Oil Prices in the United States (USDA, 2006)

Among all the feedstocks in Figure 2.4, biodiesel production from soybean is the highest, 374.45 mmgpy out of 541.05 mmgpy total production as of November 2006, as seen in Figure (2.5). Total biodiesel production capacity was 582 million gallons for 2006. The total shown in Figure 2.5 excludes the plants that did not report their production capacities.

Commercial Biodiesel Production Plant (Nov2006)
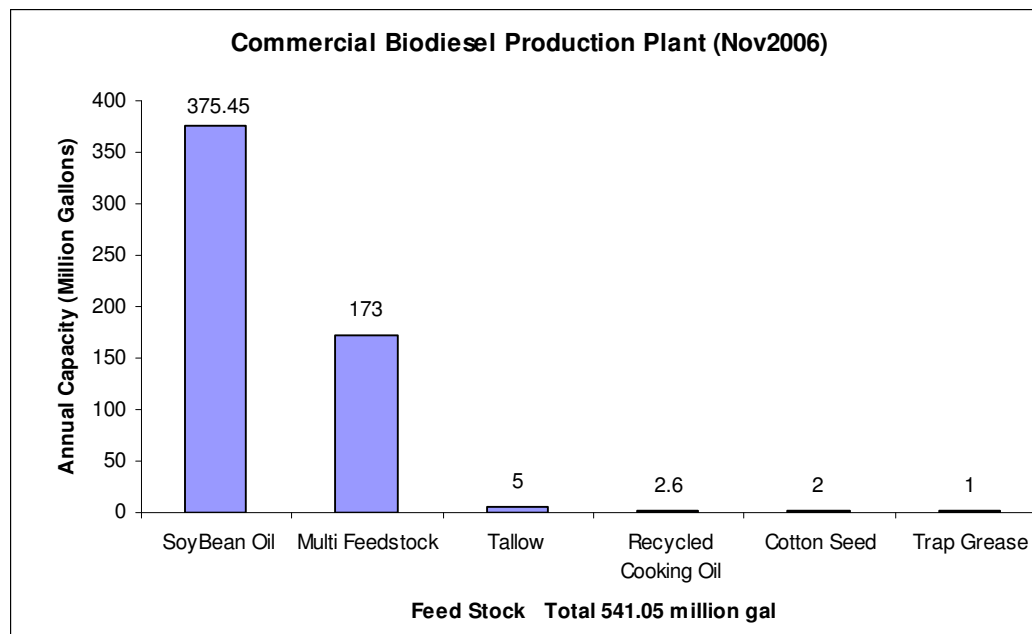
Figure 2.5 Biodiesel Production Plant Capacities using Different Feedstocks

2.8 Catalyst Options

Catalysts are used to accelerate a chemical reaction by reducing the activation energy, which is the energy needed to initiate the reaction. There are two different types of catalyst systems, heterogeneous and homogeneous systems (Vicente et al., 2004). The heterogeneous catalyst system includes:

- Enzymes
- Titanium silicates
- Alkaline-earth metal compounds
- Anion exchange resins
- Guanadines heterogenized on organic polymers

Currently, heterogeneous catalysts are not very popular due to high cost or inability to complete the degree of reaction required by the ASTM specification standard (Gerpen et al., 2004). Homogeneous system includes acids and bases. However, acid catalysts are not preferred compared to base catalysts due to a much slower transesterification process of triglycerides into fatty acid methyl ester. The catalyst results in very high yields, but

the reaction rate is very slow, requiring more time and high temperatures to complete the reaction. Therefore, acid catalysts are commonly used for pre-treating high free fatty acid feedstocks. During this pretreatment, fatty acids are converted to fatty acid ester (Gerpen et al., 2004).

Although different kinds of base and acid catalysts are available for transesterification processes, virtually almost all commercial biodiesel producers use base catalysts. The most common alkali catalysts are:

- Sodium hydroxide (NaOH)
- Potassium hydroxide (KOH)
- Sodium methoxide (NaOCH$_3$)
- Potassium methoxide (KOCH$_3$)

Methoxide ion has been described as the preferred catalyst for the transesterification process of biodiesel production. Methoxide ions can be obtained via several different methods (Jackson, 2006). The traditional method entails preparation of the catalyst solution within the biodiesel plant by mixing either sodium hydroxide or potassium hydroxide with methanol as shown below.

$$\text{NaOH} + \text{H}_3\text{C-OH} \rightleftharpoons \text{H}_3\text{CO}^- + \text{Na}^+ + \text{H}_2\text{O}$$

$$\text{KOH} + \text{H}_3\text{C-OH} \rightleftharpoons \text{H}_3\text{CO}^- + \text{K}^+ + \text{H}_2\text{O}$$

Another method is to place sodium methoxide in a methanol solution as shown below. Sodium methoxide is known by many names, such as alcholate, methoxide, and methylate.

$$\text{(methanol solution)}$$
$$\text{H}_3\text{C-O-Na} \rightleftharpoons \text{H}_3\text{C-O}^- + \text{Na}^+$$

The main advantage of using sodium methoxide over sodium hydroxide is the virtually water free character of the catalyst solution. When mixing traditional hydroxides

with methanol, water is generated, initiating unwanted side reactions such as saponification.

2.8.1 Saponification

The higher the soap formation or saponifacation, the more complicated and costly it becomes to separate biodiesel during the purification steps. In order to maximize the yield of biodiesel production, it is essential to reduce formation of soap. Soap has both long hydrocarbon nonpolar ends (tail) and polar carboxylate salt ends (head) as shown in Figure (2.6).
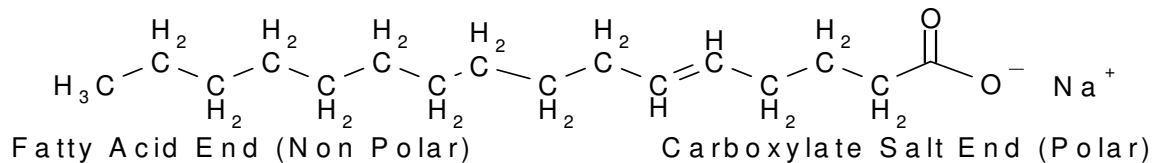
Figure 2.6 Molecular Structure of Soap

A nonpolar tail can readily attach (or dissolve) to nonpolar molecules such as grease or oil, while a polar head can dissolve in polar molecules such as water or glycerol, as shown in Figure (2.7).
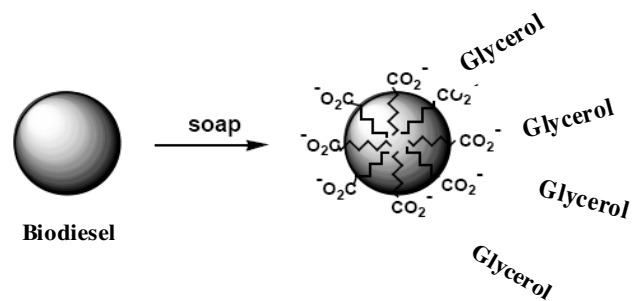
Figure 2.7 Emulsification of Bioidiesel by Soap

This process is known as emulsification and it enhances the biodiesel solubility in the glycerol layer and decreases the yield.

Soap can be formed in two different ways in the Biodiesel process:

1. Triglyceride saponification
2. Neutralization of free fatty acid

Presence of water from the feedstock or the catalyst can contribute to saponification. When a base catalyst such as NaOH or KOH is used, it is first mixed with methanol, with water being formed during the process as shown below.

$$NaOH \ + \ H_3C\text{-}OH \ \rightleftharpoons \ H_3CO^- \ Na^+ \ + \ H^+ \ OH^-$$

The presence of OH⁻ ion from water promotes the reaction of sodium with triglycerides, allowing soap to be formed, as seen below (Zadra, 2006).
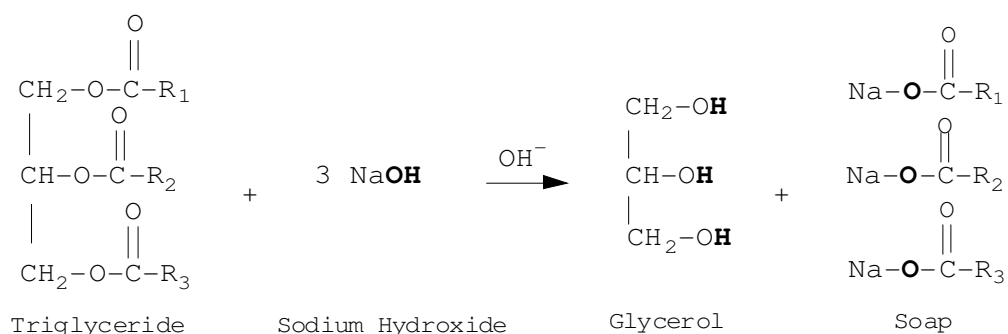
When there is free fatty acid in the feedstock, it reacts with a base catalyst to form soap and water. The formation of water (seen below), further promotes the triglyceride saponification (Zadra, 2006).
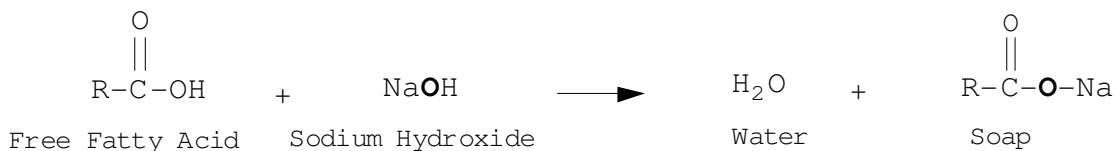
Therefore, soap formation decreases the amount of triglyceride reactants and NaOH catalyst in transesterification reaction. Formation of soap not only contributes to a decrease in biodiesel yield, but also results in higher glycerol purification costs if high quality product is needed (Vicente et al., 2004).

2.9 Reaction Mechanism

The mechanism of **acid catalyzed transesterification** is described below (Meher, 2006). Transesterification can be catalyzed by sulfuric or sulfonic acids. The first step involves the protonation of a carbonyl group, which results in the formation of a carbon cation.
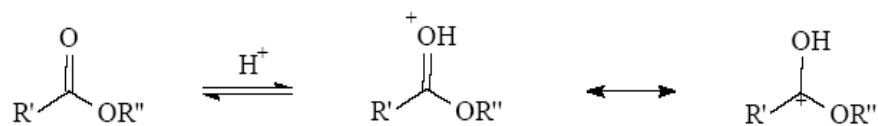
The second step involves the nucleophilic attack of alcohol, producing a tetrahedral intermediate.
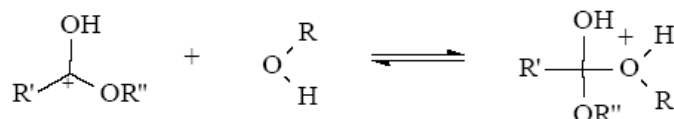
The tetrahedral intermediate rearranges, releasing an alkyl ester and proton catalyst.
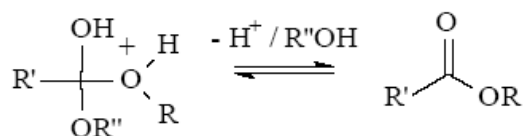
The mechanism of **alkali-catalyzed transesterification** is described as follows (Schuchardt et al., 1997). The first step involves the reaction of a base with alcohol, producing an alkoxide with protonated catalyst.

$$ROH + B \rightleftharpoons RO^- + BH^+$$

The second step is nucleophilic attack of the carbonyl carbon of the triglyceride molecule by the alkoxide ion, resulting in the formation of a tetrahedral intermediate.
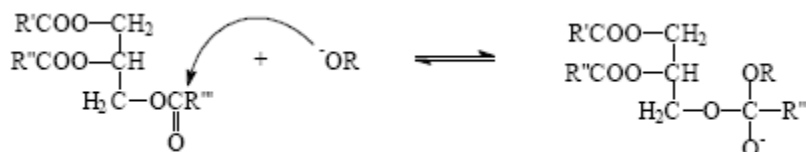
In the last step, the rearrangement of the tetrahedral intermediate gives rise to an alkyl ester and a corresponding diglyceride anion.
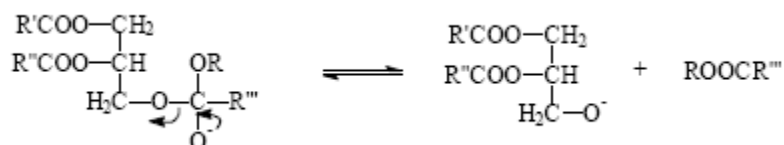
The diglyceride anion deprotonates the catalyst, forming active catalyst and diglyceride.
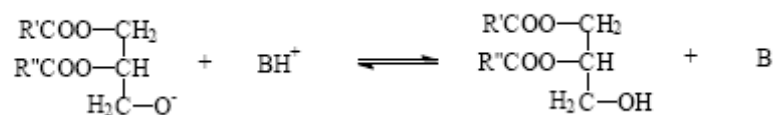
The above mechanism taking placed in each of the following intermediate steps as shown in Figure (2.8).
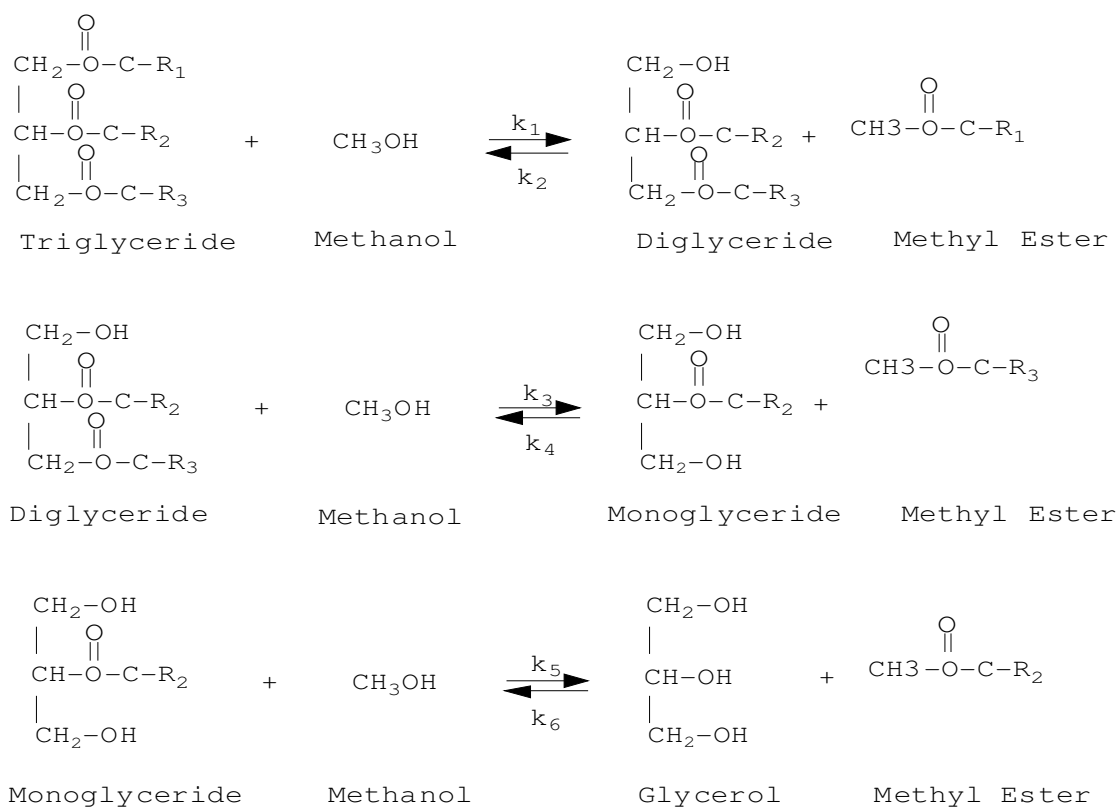
Figure 2.8 Intermediate steps in Biodiesel Transesterification (Allen et al, 2006)

Kinetics of the intermediate steps was studied by Noureddini and Zhu (1997). The resulting kinetic parameters are displayed in Table (2.7).

Table 2.7 Activation Energies and Rate Constants (Noureddini et al., 1997)

Soy bean oil @ 50 °C				
		1/(mol min)		Cal/(mol K)
First	k_1	0.050	E1	13145
Step	k_2	0.11	E2	9932
Second	k_3	0.215	E3	19860
Step	k_4	1.228	E4	14639
Third	k_5	0.242	E5	6241
Step	k_6	0.007	E6	9588

The values of reaction constants (k) and activation energies (E) are for soybean transesterification at 50 ºC with a methanol to oil ratio of 6:1. In general, reactions with high activation energies are favored by high temperature. Therefore, the first two steps favor forward reaction at high temperature (larger E1 and E3). Analysis of the third step is more complex. Although the reverse reaction is favored at high temperature (smaller E6), the higher concentrations of monoglycerides offset this effect and the overall reaction is favored at higher temperatures in the kinetically controlled region (Noureddini et al., 1997). The reaction rate constant for the forward reaction in the last step (k_5) is much higher than the backward reaction (k_6).

2.10 ASTM Standard

The American Society for Testing and Materials International (ASTM) specification for biodiesel (B100) is ASTM D 6751-03, for diesel it is ASTM D 975. ASTM standards and properties for petrodiesel and biodiesel are summarized in the first part of Table (2.8).

Table 2.8 Comparison of Petrodiesel and Biodiesel ASTM Standards and Properties (Tyson, 2006)

Fuel Property		Diesel (No 2 D)			Biodiesel (B100)	
	Unit	ASTM Method	Limits	ASTM Method	Limits	
Fuel Standard		ASTM D 975		ASTM D 6751		
Flash Point (min)	°C	D 93	52	D 93	130	
Water and Sediments	% vol	D 2709	0.05	D 2709	0.05	
Kinematics Viscosity @ 40 °C	mm^2/s	D 445	1.9 - 4.1	D 445	1.9 -6.0	
Ash	% mass	D 482	0.01 - 0.1	D 874	0.02	
Sulfur	% mass	D 129	15ppm	D 5453	0.0015 (S15) 0.05 (S500)	
Copperstrip Corrosion		D 130	No.3 Max	D 130	No.3 Max	
Cetane Number (min)		D 613	40	D 613	47	
Cloud Point	°C	D 2500	varies	D 2500	varies	
Carbon Residue	% mass	D 524	0.35	D 4530	0.05	
Acid Number	mg KOH/g	-		D 664	0.8	
Free Glycerin	% mass	-		D 6584	0.02	
Total Glycerol	% mass	-		D 6584	0.24	
Phosphorous Content	% mass	-		D 4951	0.001	
Distillation Temp	°C	D86	282 - 338	D 1160	360	
Lower Heating Value,	Btu/gal		129500		11829	
Specific Gravity @ 60 °F	kg/L		0.85		0.88	
Density @ 15 °C	lb/gal		7.079		7.328	
Carbon	% mass		87		77	
Hydrogen	% mass		13		12	
Boiling Point	°C		180 to 340		315 to 350	
Pour Point	°C		- 35 to -15		-15 to 10	
Lubricity SLBOCLE	grams		2000 - 5000		> 7, 000	
Lubricity HFRR	microns		300 - 600		< 300	

Minimum flash points of both biodiesel and petrodiesel are required to meet fire safety specifications. The flash point for pure biodiesel (160 °C) is much higher than for petroleum diesel (70 °C). Minimum flash point is set to assure that excess methanol was removed during the manufacturing process, since methanol reduces the flash point. In addition, presence of methanol in biodiesel can also affect fuel pumps, seals and elastomers, and can result in poor combustion properties.

Requirements for free water droplets and levels of sediment-related particulate matter eliminate the use of improper processing such as poor drying techniques during manufacturing and improper handling during transport or storage. Excess water in the fuel cannot only lead to corrosion; it can foster the growth of microorganisms.

Fuels possessing a certain minimum viscosity as well as a certain maximum viscosity are required for proper engine performance. Fuels having viscosities that are too high or too low can induce problems with injection system operation. The maximum viscosity level is limited by the engine's fuel injection system design.

The amount of residual alkali catalyst and any other ash forming compounds present in the biodiesel could contribute to injector deposits or fuel system fouling.

Sulfur is limited in order to reduce sulfate and sulfuric acid pollutant emissions and to protect exhaust catalyst systems.

The copper strip corrosion test is an indicator of potential difficulties with copper and bronze fuel system components. Prolonged contact with these components can cause fuel degradation and sediment formation.

Cetane number is a measure of combustion quality for diesel fuel under compression. An adequate cetane number is required for good engine performance.

Cloud point is important for ensuring good performance in cold temperatures. Its value is determined by the local climate.

Carbon residue measures the tendency of a fuel to form carbon deposits in an engine.

Acid number is primarily an indicator of free fatty acids in biodiesel and increases if a fuel is not properly manufactured or has undergone oxidative degradation. Fuel system deposits and reduced life of fuel pumps and filters contribute to an acid number higher than 0.80.

Free and total glycerin numbers are a measure of the unconverted (triglyceride) or partially converted triglycerides (monoglycerides and diglycerides) as well as by-product triglycerols present in the fuel. High amounts of free and total glycerin can cause fouling in storage tanks, fuel systems, and engines, along with plugging filters and producing other problems.

Slight amount of phosphorous content in Biodiesel can damage catalytic converters. Phosphorous levels above 10 ppm are present in some vegetable oils, and this requirement ensures that a phosphorous level reduction process is conducted.

The T90 distillation specification prevents contamination in fuels with high boiling materials.

CHAPTER III
PROBLEM STATEMENT AND APPROACH

The overall goal of this work is to design and optimize a biodiesel (Fatty Acid Methyl Ester) production process from vegetable oil. The following are the specific objectives of the work:

- Develop a base-case design of the process
- Predict performance of the various units in the process
- Optimize the process by conserving resources and enhancing profitability
- Evaluation and analysis of process economics

In order to reach the aforementioned objectives, the following activities were undertaken:

- Synthesis of a base-case flowsheet
- Simulation of the base case and selection of appropriate thermodynamic databases
- Establishing tradeoffs among the various process objectives
- Identifying opportunities for process integration and cost minimization
- Development of integrated design strategies
- Development of a site-wide simulation of the process with various mass and energy integration projects
- Cost estimation and sensitivity analysis

Figure 3.1 shows a schematic diagram of the process design.
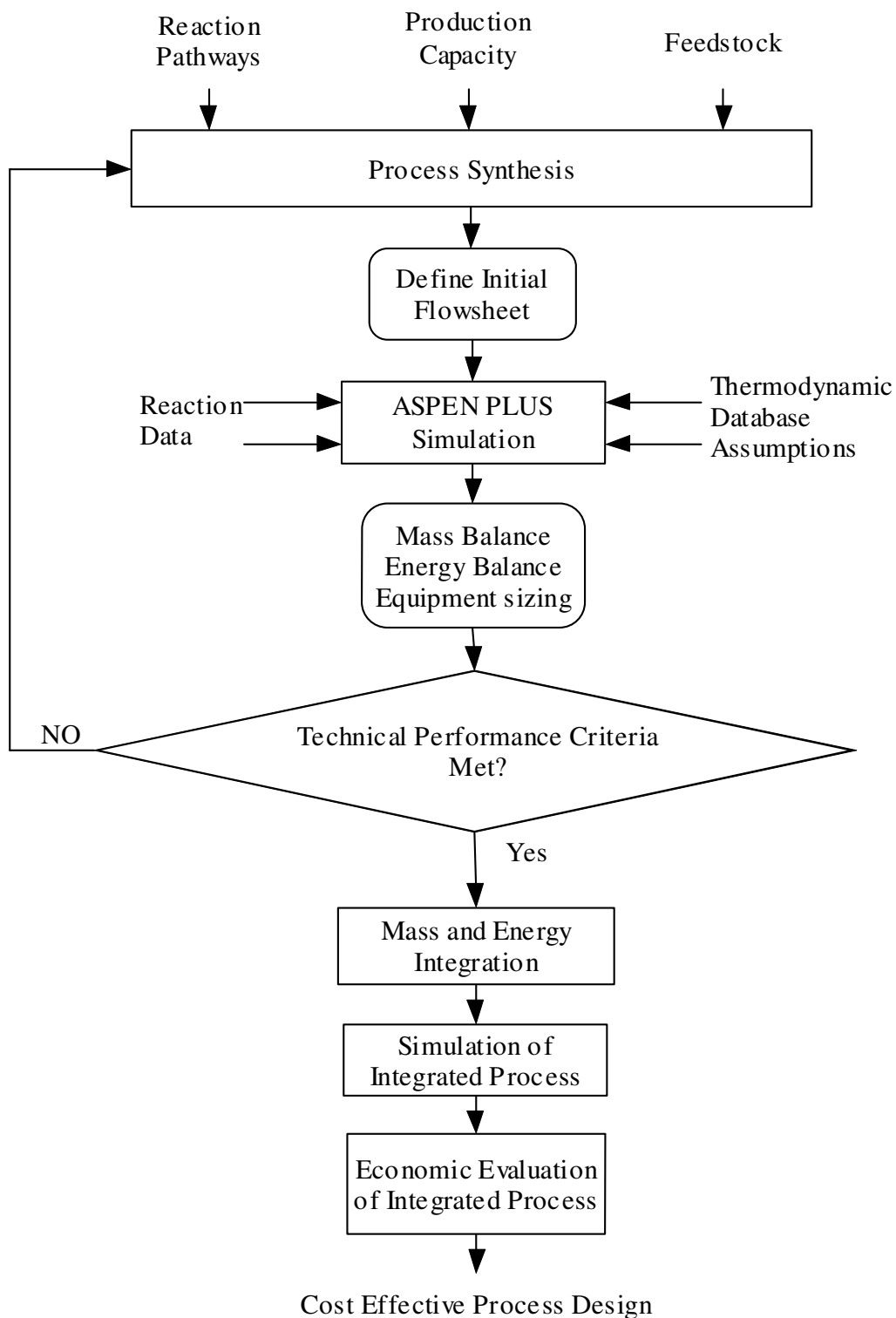
Figure 3.1 Schematic of Proposed Process Design

CHAPTER IV

METHODOLOGY

4.1 Process Synthesis

Many kinds of processing operations are applied to carry out chemical reactions and to separate products and byproducts from each other and from non-reacted raw materials. Structured methods of most economical process operations are identified systematically and put into flow sheets. The resulting flow sheet represents the configuration of the various pieces of equipment and their interconnections constructed so as to meet certain objectives. Synthesis of configurations that produce chemicals in a reliable, safe, and economical manner and at high yield with little or no waste has been one of the greatest challenges. This structured conceptual process design is also known as process synthesis.

In process synthesis, inputs and outputs are known as shown in Figure (4.1).

Process Input (Given) → Structure & Parameters (Unknown) → Process Output (Given)
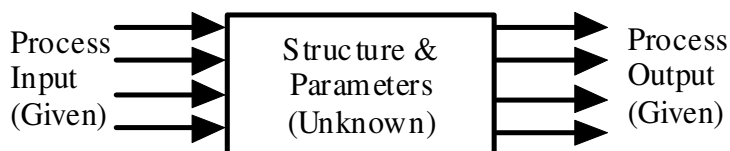
Figure 4.1 Process Synthesis (El-Halwagi, 2006)

Process synthesis methods and tools are used to design entirely new processes by synthesizing a process flow sheet from scratch for grassroot design of a new plant. The same techniques can also be applied to projects involving retrofitting within an existing plant environment, leading to significant savings in capital and operating costs, even in cases where many years of conventional optimization techniques and continuous improvement have already yielded savings (El-Halwagi, 2006).

The selection of the best process route to convert raw materials into desired products by a sequence of unit operations is a difficult task, as an infinite number of possible process alternatives exist. After the desired product is obtained, there are also numerous ways to separate the desired product from unwanted components. Table (4.1)

shows the alternative methods of separation for five components. For five components A, B, C, D and E, there are 14 possibilities of sequence for separation.

Table 4.1 Alternative Sequences for Separation of Compounds (Baldwin, 2006)

	Column 1	Column 2	Column 3	Column 4
1	A/BCDE	B/CDE	C/DE	D/E
2	A/BCDE	B/CDE	CD/E	C/D
3	A/BCDE	BC/DE	B/C	D/E
4	A/BCDE	BCD/E	B/CD	C/D
5	A/BCDE	BCD/E	BC/D	B/C
6	AB/CDE	A/B	C/DE	D/E
7	AB/CDE	A/B	CD/E	C/D
8	ABC/DE	A/BC	D/E	B/C
9	ABC/DE	AB/C	D/E	A/B
10	ABCD/E	A/BCD	B/CD	C/D
11	ABCD/E	A/BCD	BC/D	B/C
12	ABCD/E	AB/CD	A/B	C/D
13	ABCD/E	ABC/D	A/BC	B/C
14	ABCD/E	ABC/D	AB/C	A/B

The number of possible sequences for separation is described by equation (4-1) (Baldwin, 2006).

$$Ns = \sum_{j=1}^{P-1} Nj \, Np - j = \frac{[2(P-1)]!}{P!(P-1)!} \qquad (4\text{-}1)$$

where

P = number of product

N_s = number of different sequence

As shown in Table (4.2), the separation sequences increase as the number of components increases.

Table 4.2 Relationship Between Components and Design Alternatives (Baldwin, 2006)

Number of Products, P	Number of Separators in the Sequence	Number of different Sequences, N_s
2	1	1
3	2	2
4	3	5
5	4	14
6	5	42
7	6	132
8	7	429
9	8	1430
10	9	4862

There is a critical need to systematically extract the optimum solution from among the numerous alternatives without enumeration. The optimum solution may not be intuitively obvious and therefore it is necessary to understand and treat the process as an integrated system (El-Halwagi, 2006). Therefore, the objective of process synthesis includes the sequence of process steps (reaction, distillation, extraction, etc.), the choice of chemicals employed (including extraction agents), and the source and destination of recycle streams. Much decision-making is involved in rerouting streams, stream distribution, changes in design and operating variables, substitution of designs and reaction pathways, and the replacement or addition of units. While solving problems, instead of focusing on the symptoms of the process problems, root causes of the process deficiencies should be identified.

4.2 Process Analysis

After a process is synthesized, the whole process is decomposed into its constituent elements in order to analyze each individual element's performance. Detailed characteristics such as flow rates, compositions, temperatures, and pressures are predicted using analysis techniques which include mathematical models, empirical correlations, and computer aided process simulation tools as shown in Figure (4.2) (El-Halwagi, 2006).
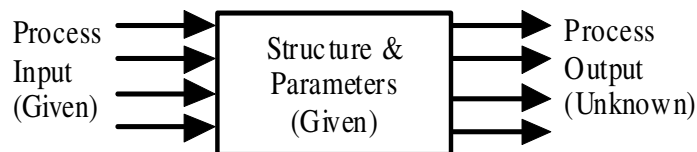
Figure 4.2 Process Analysis (El-Halwagi, 2006)

4.3 Process Integration

The traditional approach to process development and improvement includes (El-Halwagi, 2006):

1. Brainstorming and solution through scenarios: Relative conceptual design scenarios are constructed and synthesized then each generated scenario is ranked according to feasibility and performance evaluation to obtain an optimal solution.

2. Adopting/evolving earlier design: The solution already existed from previous related problems in the same plant or a solution from a different plant is copied, adopted, or evolved to suit the problem at hand and generate a similar solution.

3. Heuristics: Certain design problems are categorized into groups or regions and each has recommended solutions based on knowledge derived from experience and rules of thumb for a certain class of problems.

Although these approaches have added value to solving design problems, there are several serious limitations. The solution is not generated from infinite alternatives, and it is not the true optimal solution. The generated solution is only optimal among limited alternatives. Since the designs vary even for the same process, none of the generated solutions may be the optimal solution for a particular problem. The solution might work and it is financially reasonable, but it might not be a good solution for the long term. Although the symptoms of two problems may be the same, the source of the problem may be different and can result in misidentifying and correcting the wrong source.

The development of methodologies for energy conservation had been driven by increasing demand for expensive utilities within chemical industries. Heating and cooling utilities contribute greatly to the operation cost of a plant. By applying techniques for recovery of process heat, operating cost can be minimized. Therefore, in most chemical

process, it becomes essential to synthesize cost effective Heat Exchange Networks (HENs) which transfer heat among cold and hot streams as shown in Figure (4.3).
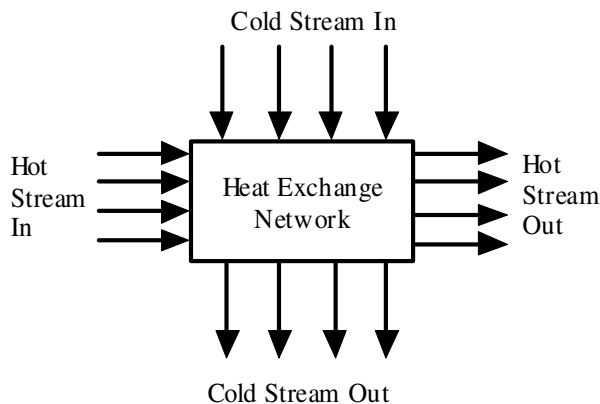
Figure 4.3 Heat Exchange Network (HEN) Synthesis (El-Halwagi, 2006)

For a given HEN, tasks such as identification of optimal heat load to be removed or added and optimal system configuration of cold and hot streams are required in order to optimize heat recovery and minimize cost. In order to accomplish these tasks, heat integration techniques have been developed. This systematic approach not only identifies a system that accomplishes energy reduction, but also a system that represents the most cost effective approach. In order to identify the targets, several methods can be utilized. These approaches include graphical methods (pinch diagram), algebraic methods (cascade diagram), and mathematical approaches (Lingo optimization software) (El-Halwagi, 2006).

4.3.1 Graphical Method

Graphical method can be applied by constructing "thermal pinch diagram" which is based on the work developed by Linnhoff and Hindmarsh (1983); Umeda et al. (1973) and Hohmann (1971) (El-Halwagi, 2006). The amount of heat loss from the hot streams and heat gained from the cold streams can be calculated by equations 4-2 and 4-3 as shown in Table (4.3).

$$Q_{Hi} = J_{Hi} \ x \ (T_{Hi}^{in} - T_{Hi}^{out}) \qquad i = 1,2,\ldots\ldots., N_H \qquad (4\text{-}2)$$

where

$Q_{Hk} =$ Heat loss from hot stream i

$J_{Hi} =$ (flow rate of hot stream i) x (specific heat of hot stream i)

$T_{Hi}^{in} =$ inlet (supply) temperature of hot stream i

$T_{Hi}^{out} =$ outlet (target) temperature of hot stream i

$$Q_{Ck} = J_{Ck} \; x \; (T_{Ck}^{out} - T_{Ck}^{in}) \qquad k = 1,2,\ldots\ldots., N_C \qquad (4\text{-}3)$$

where

$Q_{Ck} =$ Heat gained by cold stream k

$J_{Ck} =$ (flow rate of stream k) x (specific heat of stream k)

$T_{Ck}^{in} =$ inlet (supply) temperature of cold stream k

$T_{Ck}^{out} =$ outlet (target) temperature of cold stream k

Table 4.3 Stream Data for Pinch Diagram (El-Halwagi, 2006)

Cold Stream	Flow Rate x SpecificHeat (C_{Pj})	Supply Temperature	Target Temperature	Heat Need to be added to Cold Stream
C1	J_{C1}	T_{C1}^{in}	T_{C1}^{out}	$Q_{C1} = J_{C1}\, x\, (T_{C1}^{out} - T_{C1}^{in})$
C2	J_{C2}	T_{C2}^{in}	T_{C2}^{out}	$Q_{C2} = J_{C2}\, x\, (T_{C2}^{out} - T_{C2}^{in})$
C3	J_{C3}	T_{C3}^{in}	T_{C3}^{out}	$Q_{C3} = J_{C3}\, x\, (T_{C3}^{out} - T_{C3}^{in})$
………	………	………	………	………
C_i	J_{Ci}	T_{Ci}^{in}	T_{Ci}^{out}	$Q_{Ci} = H_{Ci}\, x\, (T_{Ci}^{out} - T_{Ci}^{in})$
Hot Stream	**Flow Rate x SpecificHeat (H_{pj})**	**Supply Temperature**	**Target Temperature**	**Heat Need to be removed From Hot Stream**
H1	J_{H1}	T_{H1}^{in}	T_{H1}^{out}	$Q_{H1} = J_{H1}\, x\, (T_{H1}^{in} - T_{H1}^{out})$
H2	J_{H2}	T_{H2}^{in}	T_{H2}^{out}	$Q_{H2} = J_{H2}\, x\, (T_{H2}^{in} - T_{H2}^{out})$
H3	J_{H3}	T_{H3}^{in}	T_{H3}^{out}	$Q_{H3} = J_{H3}\, x\, (T_{H3}^{in} - T_{H3}^{out})$
………	………	………	………	………
H_k	J_{Hk}	T_{Hk}^{in}	T_{Hk}^{out}	$Q_{Hk} = J_{Hk}\, x\, (T_{Hk}^{in} - T_{Hk}^{out})$

By setting a minimum heat exchange driving force, ΔT^{min}, corresponding temperatures of cold and hot streams for feasible heat transfer is established.

$$T_H = T_C + \Delta T^{min} \qquad (4\text{-}4)$$

where

T_H = temperature of hot stream

T_C = temperature of cold stream

ΔT^{min} = minimum heat exchange driving force

Then, both hot and cold composite streams are plotted on the same diagram versus their relative temperatures. Heat exchange is thermodynamically feasible at any point when the temperature of the cold composite stream is located to the left of the hot composite stream. The cold composite stream can be moved up and down until it touches the hot composite stream. The point where the two composite streams touch is known as the "Thermal Pinch Point." No heat should be passed through this point. Also, no cooling utilities should be used above the pinch or no heating utilities should be used below the pinch. Next, the minimum heating and cooling utilities are identified as shown in Figure (4.4).
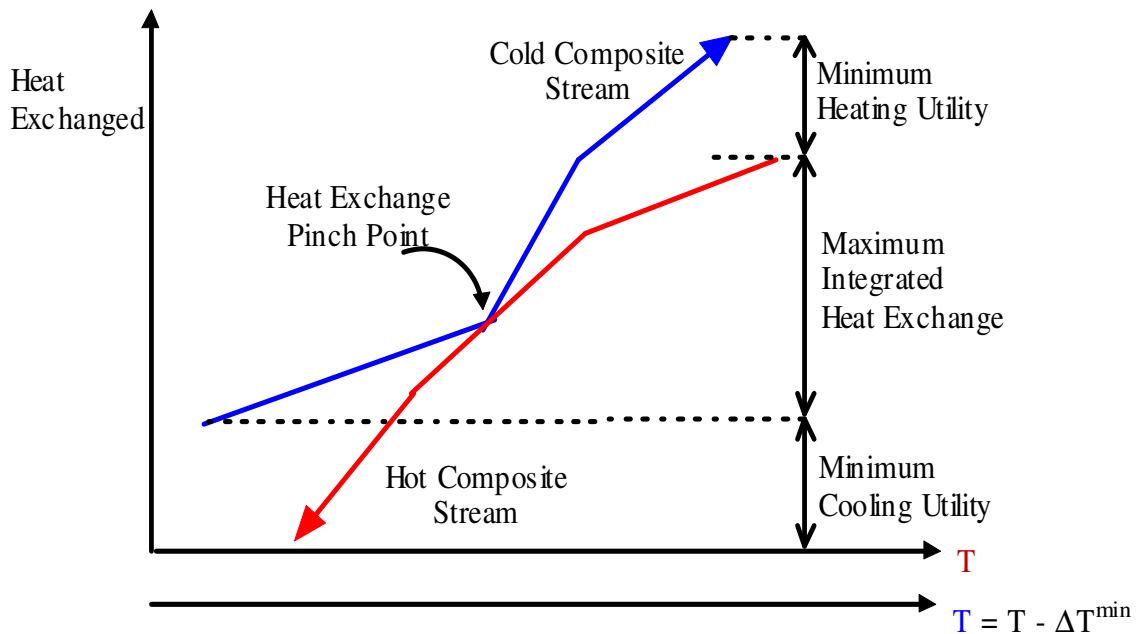
Figure 4.4 Thermal Pinch Diagram

4.3.2 Algebraic Method

In this approach, a temperature interval diagram (TID) with corresponding temperature scales are constructed, as shown in Figure (4.5). Horizontal lines define the series of temperature intervals. Heads of vertical arrows represent target temperatures of

the streams and tails represents the supply temperature of the stream. It is thermodynamically feasible to transfer heat from the hot stream to the cold stream within each interval. Also, heat from a hot stream in an interval can be transferred to any interval below it.

Intervel	Hot Stream		Cold Stream	
		T_{H1}^{in}	$T_{H1}^{in} - \Delta T^{min}$	
1		$T_{C1}^{in} + \Delta T^{min}$	T_{C1}^{out}	
2	H_{P1}	$T_{C2}^{out} + \Delta T^{min}$	T_{C2}^{out}	
3		T_{H2}^{in}	$T_{H2}^{in} - \Delta T^{min}$	C_{p1}
4		T_{H1}^{out}	T_{C1}^{in}	
5		$T_{C2}^{out} + \Delta T^{min}$	T_{C2}^{out}	
6	H_{P2}	T_{H3}^{int}	$T_{H3}^{in} - \Delta T_{min}$	C_{p2}
7		$T_{C2}^{in} + \Delta T^{min}$	T_{C2}^{in}	
8	H_{P3}	T_{H2}^{out}	T_{C3}^{out}	
9		$T_{C3}^{in} + \Delta T^{min}$	T_{C3}^{in}	C_{p3}
10		T_{H3}^{out}	$T_{H3}^{out} - \Delta T_{min}$	
	....		....	
			T_{CN}^{in}	
N		T_{HN}^{out}		

Figure 4.5 Temperature Interval Diagram (El-Halwagi, 2006)

Next, a table of exchangeable heat load is constructed, as shown in Table 4.4. The exchangeable heat load at each temperature interval can be calculated by the following equations.

For hot streams,

$$Q_{HN} = \Sigma J_{Hi} \times |\Delta T_{interval\_N}| \qquad\qquad i = 1,2,\ldots\ldots, n \qquad (4-5)$$

where

Q_{HN} = total exchangeable heat load for interval N for hot streams k

J_{Hi} = (flow rate of hot stream k) x (specific heat of hot stream k)

$|\Delta T_{interval\_N}|$ = temperature difference between interval N

For cold streams,

$$Q_{CN} = \Sigma \; J_{Ck} \; x \; |\Delta T_{interval\_N}| \qquad\qquad k = 1,2,\ldots\ldots, n \qquad (4\text{-}6)$$

where

Q_{CN} = total exchangeable heat load for interval N for cold streams j

J_{Ck} = (flow rate of hot stream j) x (specific heat of hot stream j)

$|\Delta T_{interval\_N}|$ = temperature difference between interval N

Table 4.4 Exchangeable Heat Load for Hot and Cold Streams

Interval	Hot Streams	Cold Streams
1	$Q_{H1} = H_{P1} \; x \; |\Delta T_{interval\_1}|$ $\Delta T_{interval1} = (T_{H1}^{in} - T_{C1}^{in} - \Delta T^{min})$	$Q_{C1} = 0$
2	$Q_{H2} = H_{P1} \; x \; |\Delta T_{interval\_2}|$ $\Delta T_{interval\_2} = T_{C1}^{in} + \Delta T^{min} - T_{C2}^{out} - \Delta T^{min}$	$Q_{C2} = C_{P1} \; x \; |\Delta T_{interval\_2}|$ $\Delta T_{interval\_2} = T_{C1}^{out} - T_{C2}^{out}$
3	$Q_{H3} = H_{P1} \; x \; |\Delta T_{interval\_3}|$ $\Delta T_{interval\_3} = T_{C2}^{out} + \Delta T^{min} - T_{H2}^{in}$	$Q_{C3} = C_{P1} \; x \; |\Delta T_{interval\_3}|$ $\Delta T_{interval\_3} = T_{C2}^{out} - T_{H2}^{in} + \Delta T^{min}$
4	$Q_{H4} = (H_{P1} + H_{p2}) \; x \; |\Delta T_{interval\_4}|$ $\Delta T_{interval\_4} = T_{H2}^{in} - T_{H1}^{out}$	$Q_{C4} = C_{P1} \; x \; |\Delta T_{interval\_4}|$ $\Delta T_{interval\_4} = T_{C1}^{in} - T_{H2}^{in} + \Delta T^{min}$
5	$Q_{H5} = H_{P2} \; x \; |\Delta T_{interval\_5}|$	$Q_{C5} = C_{P1} \; x \; |\Delta T_{interval\_5}|$
6	Q_{H6}	Q_{C6} ....
7	Q_{H7}	Q_{C7} ....
.....		
.....		
N	$Q_{HN} = H_p \; x \; |\Delta T_{interval\_N}|$	$Q_{CN} = C_p \; x \; |\Delta T_{interval\_N}|$

After calculation of exchangeable heat loads for hot and cold streams, a cascade diagram is developed, as shown in Figure (4.6). Residual heat, R_0, is zero, since no process stream exists above the first interval. A non-negative R_N assures that the intervals are thermodynamically feasible. A negative R_N denotes thermodynamic infeasibility and can be made non-negative by adding the most negative R_N value to the top of the cascade diagram. This value is also the minimum heating utility. The location where residual heat

has a value of zero designates the Thermal Pinch Location (previously the most negative residual heat). The residual heat at the end of the cascade diagram is the minimum-cooling load (El-Halwagi, 2006).

R e s i d u a l   H e a t   f r o m   P r e c e d i n g   I n t e r v a l

$$R_0 = 0$$

Heat Added by Process Hot Streams

Heat Removed By Process Cold Stream

Q_{H1}	Interval 1	Q_{C1}

$$R_1 = Q_{1in} - Q_{1out} + R_0$$

Q_{H2}	Interval 2	Q_{C2}

$$R_2 = Q_{2in} - Q_{2out} + R_1$$

Q_{H3}	Interval 3	Q_{C3}

$$R_3 = Q_{3in} - Q_{3out} + R_2$$

Q_{H4}	Interval 4	Q_{C4}

$$R_4 = Q_{4in} - Q_{4out} + R_3$$

Q_{HN}	Interval N	Q_{CN}

$$R_N = Q_{Nin} - Q_{Nout} + R_{N-1}$$

R e s i d u a l   H e a t   t o   S u b s e q u e n t   I n t e r v a l

Figure 4.6 Cascade Diagram for Heat Exchange Network

In order to determine how the cooling and heating loads can be distributed over multiple utilities, a grand composite curve (GCC) is constructed based upon the data obtained from the cascade diagram as shown in Figure (4.7). The temperature scale is adjusted to provide a single temperature representation by use of the following equation.

$$Adjusted \quad Temperature \quad = \quad \frac{T_H + T_C}{2} \qquad\qquad (4\text{-}7)$$

where

T_H = temperature of hot stream

T_C = temperature of cold stream

The adjusted temperature versus enthalpy is plotted with adjusted temperature values. Top and bottom residual values from cascade diagram indicate the minimum heating (Q_H^{min}) and cooling utility (Q_C^{min}), respectively. The pinch point designates the zero residual point.
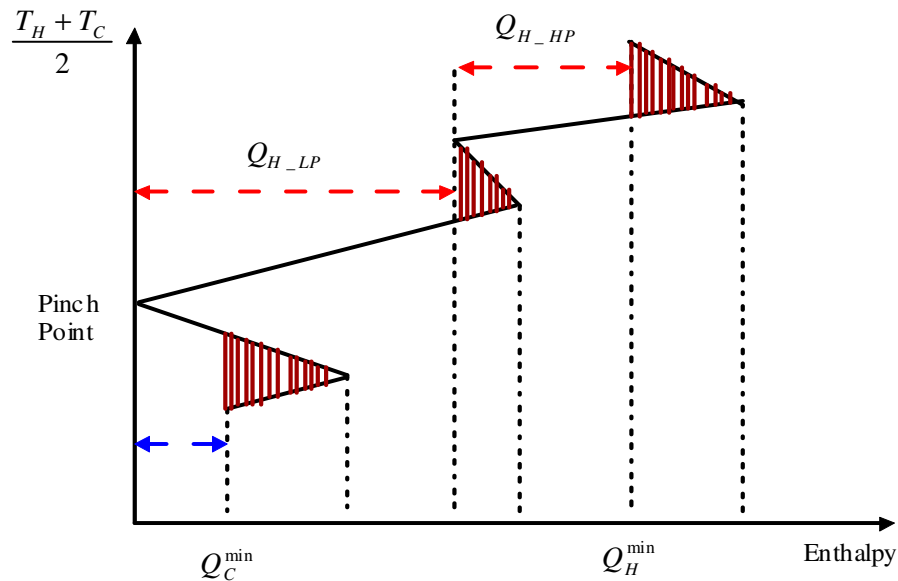
Figure 4.7 Grand Composite Curve of Heat Exchange Network (HEN) (El-Halwagi, 2006)

Whenever enthalpy line is drawn from left to right, there is a surplus of heat in that interval and a line drawn from right to left represents heat deficiency. The shaded pocket regions are completely integrated by transferring heat among the cold and hot streams. Then enthalpy deficiencies are filled up by moving up for heating utilities and down for cooling utility while maximizing the use of cheapest utility at the corresponding

temperature level. For example, $Q_H^{\min}$ can be divided among the low and high-pressure

steam (Q_{H_LP} and Q_{H_LP}) with low-pressure steam being cheaper.

CHAPTER V
CASE STUDY: BIODIESEL PRODUCTION

In order to evaluate the technical and economic aspects of the biodiesel production process, it is important to assess the performance of the various individual units in the process. In this regard, process simulation provides a convenient tool for predicting process characteristics and their dependence on design and operating variables. Previous simulation work of biodiesel processes (Zhang et al., 2003; Tapasvi et al, 2004; Hass et al., 2006) has used tools such as ASPEN Plus and HYSYS to gain insights into process attributes. However, there were limitations, including a lack of thermodynamic properties for some of the components involved in the simulations and a lack of detailed modeling of some separation units (instead, efficiency factors were used). When different scales of process design are considered, separation factors from a particular experiment may not be applicable since the ratios of the various components in the streams are no longer the same. This can result in low biodiesel yield or low quality product. Finally, earlier work also lacked process integration studies aimed at conserving resources, reducing waste, and improving profitability. Although the intent of earlier work was to get a process that basically works, more efficient biodiesel process designs must now be developed in order to enhance the economic performance of the process. In the following work, four process configurations will be synthesized and simulated. In the process simulations, the separation methods will be modeled in detail without fixing user-defined separation efficiency. The simulation will also be used to determine how different compounds interact with each other and how each of the compounds are separated when using different amount of water.

5.1 Determination of Feedstock

Based on the feedstock, process synthesis design is varied. Choosing the proper feedstock is very important since the feedstock cost is a major contributor to the production cost and affects the yield of the final product (Anderson et al., 2003). As described in section 2.8, there are many choices available for Biodiesel feedstock, varying from very cheap low quality waste cooking oil to high quality, yet costly,

vegetable oils. Although using low cost feedstock seems favorable, this practice has major drawbacks. Waste cooking oil (recycled frying oil), as well as animal fat, is very cheap to use as a feedstock compared to soy oil or canola oil. Not only does it result in lower yields as the content of FFA, water, phosphorus, sulfur, and other contaminants increase, but it also becomes more expensive due to the complexity of the requisite treatment process (Anderson et al, 2003).

Another important factor needing to be considered is the thermodynamic properties of the feedstock, such as gelling and oxidation. Biodiesel can gel in cold weather conditions similar to diesel. Gelling is a reversible process with the fuel returning to a liquid state following warming. Gelling is a function of the amount of saturated fats in the feedstock used. The higher the saturated fat of the feedstock, the higher the temperature at which gelling will occur (Kotrba, 2006). Therefore, even among the vegetable oils, oil enriched with saturated fats is a poor choice of feedstock for fuel to be utilized in climates characterized by cold weather conditions. However, the greater the unsaturated fat content in the feedstock, the more likely biodiesel is to experience oxidative degradation during a long period of storage.

With regards to high capacity commercial production of biodiesel, the use of a feedstock such as recycled frying oil has many limitations. Unlike the petroleum fuel market, biodiesel is new to consumers. Instability in product quality will jeopardize the comfort and trust of consumers using unconventional fuel. Therefore, producing a stable, quality product is extremely vital to the biodiesel market. The nature of the acquisition process for recycled frying oil produces inherent instability in quality. Collection of frying oil from different locations produces differing proportions of ingredients in the feedstock from day to day and place to place as well. Also, the presence of unknown components can affect problems with processing.

Since Biodiesel processing is not dynamic in nature, these changes can affect the quality of the Biodiesel. Although this low quality feedstock seems to provide a low cost solution, the costs associated with pretreatment should not be underestimated. It is also difficult to quantify the exact cost of pretreating these low quality feedstocks due to their significant variation (Anderson et. al, 2003)

Therefore, not only are the quality, availability, and cost of feedstocks determining factors in feedstock choice, but also the climate, storage duration, and local ASTM's specifications.

In this simulation, soybean oil was chosen as the feedstock for the following reasons:

- Major domestic crop in the United States, therefore independent of export
- Expandable harvest areas
- Cheapest feedstock among the vegetable oils
- High quality (low free fatty acid, high purity)

The harvested areas of soybean in the United States are shown in Figure (5.1). Total U.S. soybean production in 2004 was 3,124 million bushels with each bushel having produced 10.7 lb crude oil (USDA 2006). 1,103 million bushels were exported.
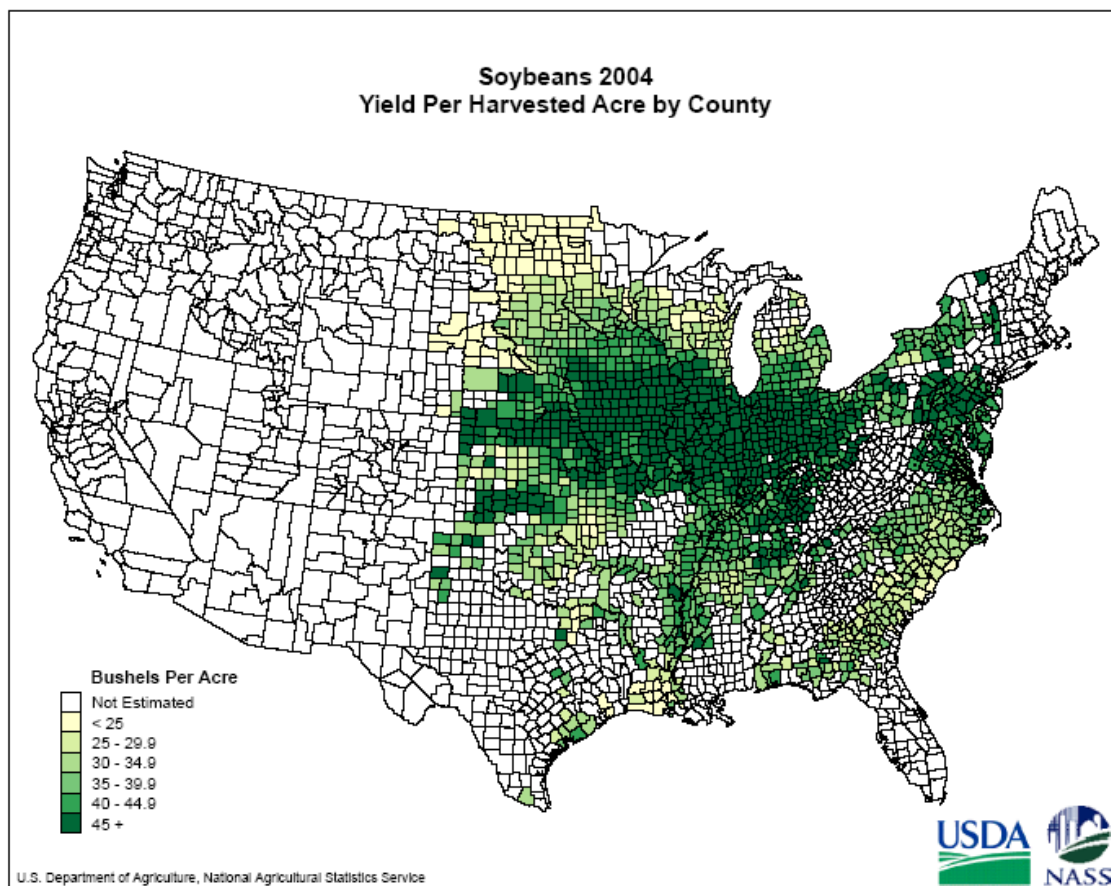
Figure 5.1 Soybean Harvested Area in the United States (USDA, 2006)

5.2 Determination of Feedstock's Compositions

Soybean oil consists of 22 to 31 % of oleic acid (C18: 1) and 49 to 53 % of linoleic acid along with myristic acid, palmitic acid, and linolenic acid, each ranging from 2 to 10%. Although the majority of triglycerides in soybean compose of oleic acid and linoleic fatty acids chain, only trioleic acid's (triolein, $C_{57}H_{104}O_6$) thermodynamic data is available in ASPEN plus simulation software. Trioleic acid is a triglyceride molecule made up of three oleic acid chains. Since the boiling points of oleic acid and linoleic acid are only 2 °F apart, (679.73 °F for oleic acid and 677.93 °F for linoleic acid), it is assumed that trioleic acid can represents the triglyceride content in soybean oil. Based on this assumption, triolein can represent most of the vegetable oils that have linoleic and oleic acids as their major components. Therefore, this simulation design is also valid for multiple feedstocks when the demand of the feedstock for the certain production capacity

cannot be provided by one feedstock alone. The biodiesel synthesized from trioleic acid will be oleic acid methyl ester ($C_{19}H_{36}O_2$). One mole of trioleic acid reacts with 3 moles of methanol and produces one mole of glycerol and three moles of Oleic Acid Methyl Ester as shown in Figure (5.2).
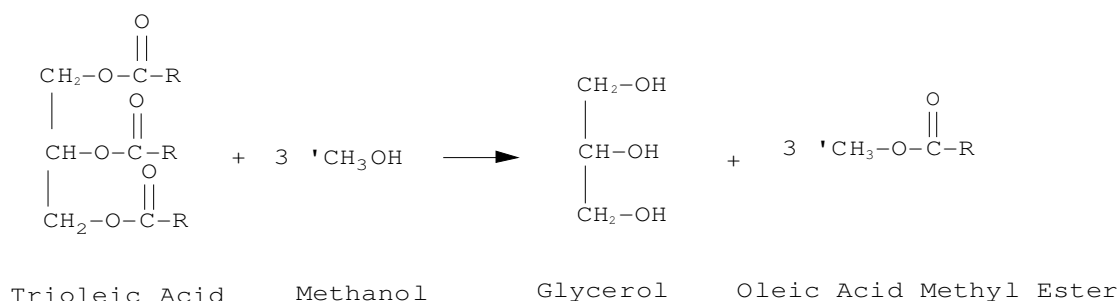
Figure 5.2 Transesterification of Trioleic Acid

where R in Oleic acid Methyl Ester is
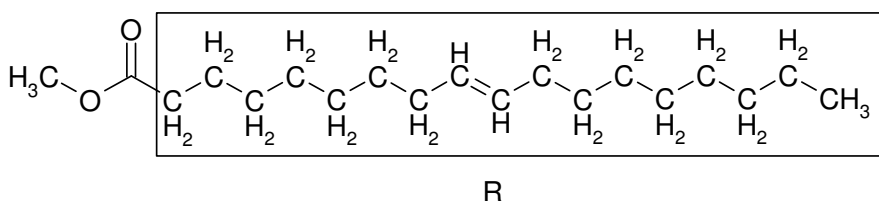
5.3 Determination of Catalyst

In a comparative study of different alkaline catalysts used in transesterification of vegetable oil with methanol (Vincete et al, 2004), (65 °C, 6:1 molar ratio of methanol to oil, and 1% wt catalyst) sodium methylate catalyst gives the highest yield (98.6%), 12% higher than sodium hydroxide. However, when changes in Biodiesel concentrations in a biodiesel layer with reaction time are compared, the results show that when hydroxides were used to catalyze the transesterification reaction, yields reached almost 100% in 5 minutes, while reactions catalyzed by sodium and potassium methoxide (methylate) reached the equivalent concentration in 60 and 240 minutes, respectively. Longer reaction time requires longer residence time or larger reactor volume, which might not be possible for large biodiesel production capacity. The cost and reality of the process using

sodium methoxide as the catalyst offset the resulting higher yield and decrease in saponification.

For this process simulation, NaOH catalyst at the optimal concentration of 1.0 wt % is used. Research has shown that excess NaOH catalyst has very little effect on methyl ester content in the product, but results in decreased product yield. Additionally, further cost related to removal of excess catalyst and soaps during the post treatment stage of product purification is required.

5.4 Estimation of Components' Thermodynamic Data

Although Aspen Plus has some incorporated thermodynamic data, not all the required thermodynamic data to conduct the simulation is included. The other thermodynamic properties have to either be entered by a user-defined method or estimated by Aspen after providing the molecular structure of the compounds. Combination NRTL and RK-Soave thermodynamic properties were used in the simulation. The molecular structures of trioleic acid (triolein), oleic acid, and oleic acid methyl ester were constructed by using ISIS draw and imported to ASPEN. Properties of these compounds were then estimated by Aspen's UNIFAC group contribution factor method based on provided molecular structures. Related thermodynamic data is incorporated into the user-defined method. Since Aspen does not have the option to identify the cis and trans of the compounds, deviations from real property and estimated thermodynamic data based on the molecular structures are expected.

During different trails of process synthesis, when NaOH (solid) in the ASPEN plus databank was used, it was found to not interact well during the separation process. Therefore, alternatives were considered. Since NaOH is a strong base and will dissociate into Na^+ and OH^- ions after mixing with methanol, 0.5 mol fraction for each of Na^+ and OH^- was used in place of NaOH. For HCl, H^+ and Cl^- ions were used instead of the HCl provided in the ASPEN Plus built-in properties. This was due to the fact that pure HCl exists as a vapor at room temp and pressure and that the concentration of the aqueous form present in ASPEN was unknown.

In this simulation, it was assumed that 97 % of the feed changed into fatty acid methyl ester while the remaining 3% underwent triglyceride saponification. This

assumption is based on the chromatography test results published by Leung and Guo (2006) which shows that all the reactant triglycerides react but not all the triglycerides undergo transesterifcation to form methyl ester. Complete transesterification is assumed for the 97% of triglyceride that forms methyl ester. Therefore, diglycerides and monoglycerides are neglected. It is also assumed that all the free fatty acid will react with NaOH and form soap.

According to previous assumptions, there is soap formation from both fatty acid saponification and triglyceride saponification. Since thermodynamic data of soap is not available and cannot be estimated by the group contribution factor, the simulation is designed in order to compensate for this limitation. Strong acid is added to reverse the saponification process and prevent soap interference in the separation process. In this process, hydrochloric acid is used to reverse soap formation and obtain free fatty acids and sodium chloride as shown in Figure (5.3).

```
                    O                        O
                    ||                       ||
    HCl     +     R-C-O-Na    ------>     R-C-OH      +      NaCl
Hydrochloric Acid     Soap              Free Fatty Acid   Sodium Chloride
```
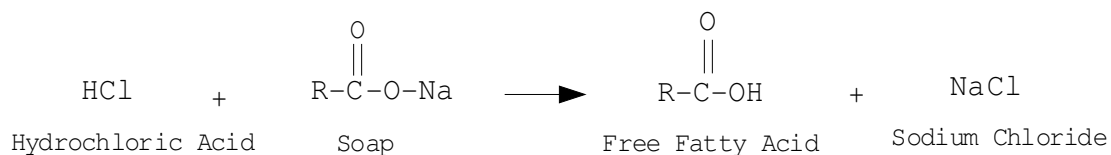
Figure 5.3 Reverse Saponification

5.5 Calculations of Feed Streams

The Biodiesel production plant is designed for 40 million gallons per year (mmgpy) or 500 gallons per hour based on 8000 operating hours per year.

5.5.1 Conversion

Various research efforts have shown that just for the base catalyst transesterification process the yield of Biodiesel varies from 80 to 99% based on the type and amount of catalyst (NaOH, KOH, NaOCH$_3$), feedstock quality (refined or raw vegetable oil, recycled oil, etc.), reaction parameters (temperature, pressure, agitation, flow rate), reactor types (Batch, CSTR, Plug), reaction steps (single or double reactors), and whether the process is conducted with or without solvent (Zhang et al., 2003; Tapasvi et al., 2004; Haas et al. 2006). Due to variations in the detailed mechanism and a lack of

accurate kinetic information for the reaction, a stoichiometric reactor with 97% conversion of triglyceride to methyl ester biodiesel is utilized in the ASPEN Plus simulation.

5.5.2 Free Fatty Acid

In order to see how free fatty acids interact during the separation process, or what percentage are recovered in the resulting biodiesel, 0.05 wt% of free fatty acid (oleic acids ($C_{18}H_{34}O_2$)) which is the maximum amount of free fatty acid in refined vegetable oil (Gerpen, 2005), is included in the feed.

5.5.3 Methanol to Oil Ratio

In order to shift the equilibrium forward, an excess stoichiometric ratio of methanol to oil is required as shown in section 2.9. Monoglycerides, diglycerides, and triglycerides are not water-soluble. Consequently, when transesterification is incomplete, these unreacted compounds are contained in the final biodiesel product, since they are not washed away by water (Kotrba, 2006). Therefore, it is vital to employ the reaction mechanism that provides a complete transesterification process. However, as the amount of excess methanol increases, not only does the cost for raw materials increase, but also the cost for methanol separation and purification. The optimal ratio of 6:1 of methanol to oil is used in this process simulation (Leung et al., 2006; Gerpen et al., 2004). For a molar ratio greater than 6:1, there is insignificant change on biodiesel yield and purity. When the transesterification is complete, there should be no or only small traces of monoglycerides and only a small amount of diglycerides in the reaction product stream (Vicente et al., 2004; Gerpen et al., 2004; Leung et al., 2006).

5.5.4 Hydrochloric Acid

In order to reverse the free fatty acid saponificaiton and fatty acid saponification, hydrochloric acid is used. Since hydrochloric acid is a very strong acid, it will react with the strong base catalyst present in the mixture to first form salt and water (neutralization) before it reacts with the soap, as seen in Figure (5.4).

HCl + NaOH ⟶ H$_2$O + NaCl

Hydrochloric Acid   Sodium Hydroxide   Water   Sodium Chloride
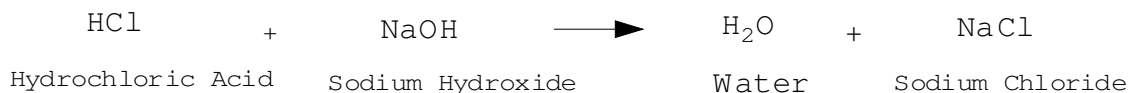
Figure 5.4 Neutralization Reaction

Therefore, the amount of hydrochloric acid required for this process is equivalent to the number of moles of NaCl present in the process.

Input calculation of the feed stream for the 97% conversion is shown in Table (5.1).

Table 5.1 Input Calculations of the Feed Streams for 97% Conversion

Methyl Oelate		
S.G	0.872422	
M.W	296.49364	lb/lbmol
Density	7.2646798	lb/gal
Production	5000	gal/hr
Total Flow	36323.399	lb/hr
	122.50988	lbmol/hr
Trioleic Acid		
M.W	885.449	lb/lbmol
Total Flow	42.102561	lbmol/hr
	37279.67	lb/hr
Methanol (1:6)		
M.W	32.04216	lb/lbmol
Total Flow	252.61536	lbmol/hr
	8094.3419	lb/hr
FFA		
M.W	282.46676	
wt%	0.05	wt %
Total Flow	0.0659895	lbmol/hr
	18.639835	lb/hr
Sodium Hydroxide		
M.W	39.9971	
wt%	1	wt%
Total Mol	9.3205933	lbmol/hr
	372.7967	lb/hr

5.6 Reactor Type and Operation Parameter

Batch reactors are used only in small production plants and continuous process is used in most of the larger plants (above 1 mmgpy). Although high pressures and high temperatures such as 90 bar (88 atm) and 240 ℃ can transesterify the fats without prior removal or treatment of FFA, lower temperatures, near atmospheric pressure, and longer reaction times are preferred due to the associated equipment and operating costs (Gerpen, 2005). A continuous process design is selected due to better performance in (Anderson et al, 2003)

- Heat economization
- Product purity from phase separation by removing only the portion of the layer furthest from the interface
- Recovery from excess methanol in order to save methanol cost
- Minimal operator interface in adjusting plant parameters
- Lower capital cost per unit of biodiesel produced

The reactor temperature in this process is an optimal temperature of 60 ℃, which is the near boiling point of methanol.

5.7 Process Simulations and Designs

The major steps of the biodiesel production process involve reaction (transesterification), methanol recovery, separation of biodiesel from the glycerol, biodiesel purification, and glycerol purification. After the transesterification reaction and biodiesel formation, separation of biodiesel from the rest of the products is required. Water is used either during the separation of biodiesel from the glycerol or during the Biodiesel purification process. The excess methanol used in the reaction can be removed and recycled back to the reactor unit. Methanol can be removed earlier or later in the process. The sequence of methanol recovery and water washing can be varied based on the objective and nature of the design. Numerous biodiesel purification methods include water washing as a step. Figure (5.5) illustrates the main alternatives of such methods.
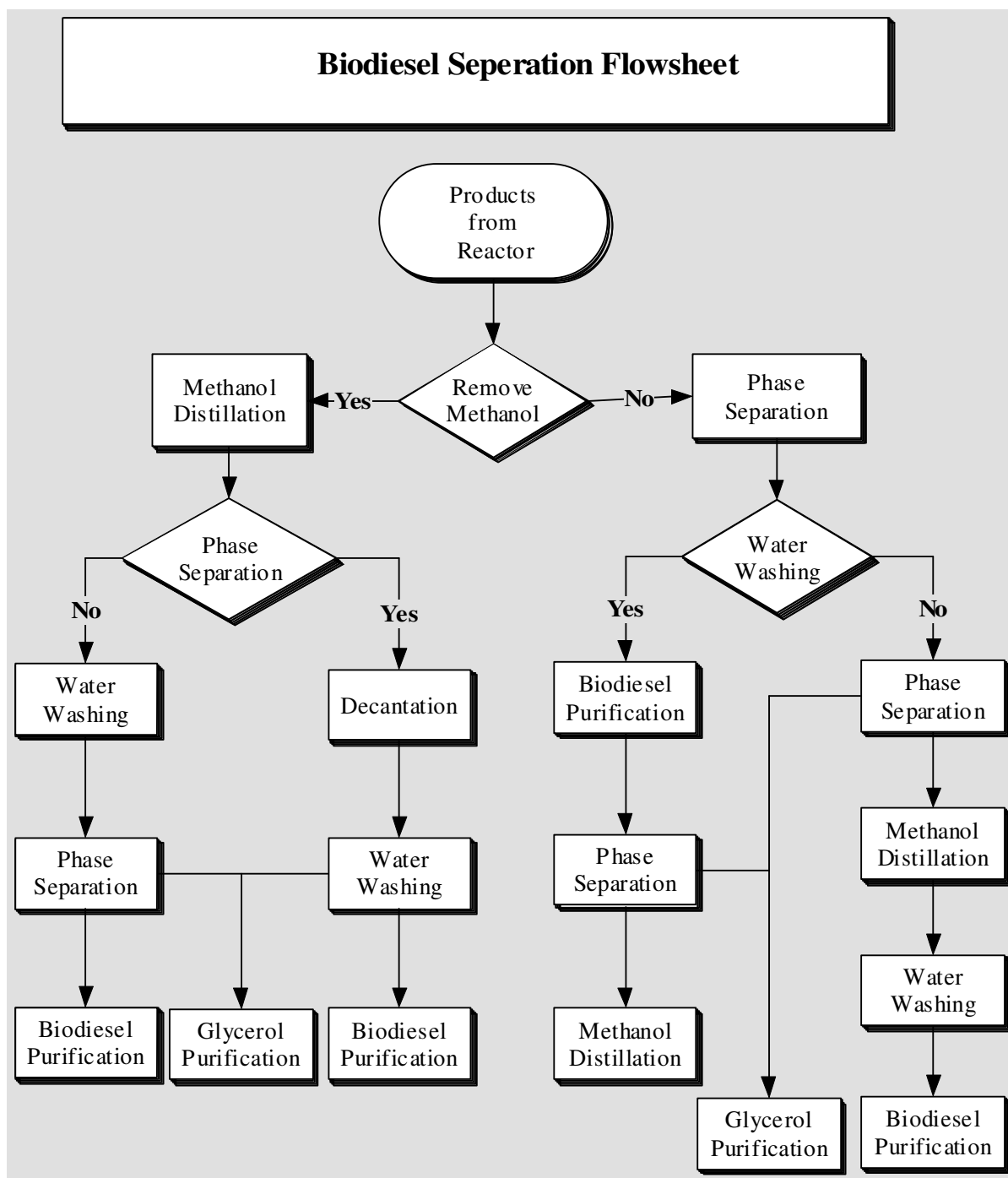
Figure 5.5 Proposed Approach to Synthesizing Separation Network

In order to compare the results, four different separation process scenarios are simulated:

1. Removal of methanol first: water washing at the presence of glycerol
2. Removal of methanol first: water washing after removal of glycerol
3. Biodiesel and glycerol separation first: water washing at the presence of methanol
4. Biodiesel and glycerol separation first: water washing after removal of methanol

The amount of triol (trioleic acid), methanol, and sodium hydroxide in the feed streams are the same for all four simulations. Since the simulation includes only the 0.05 % of free fatty acids (FFA), only an insignificant amount of NaOH catalyst (0.06 mol) is lost during reaction with FFA. Therefore, only 1wt% anhydrous sodium hydroxide is used in this process. Since it is received as solid flakes and needs to be dissolved in methanol, separate plant units are required for mixing. NaOH is mixed with methanol first before it is charged into the reactor at 60 °C and 1 atm. The triol is added to the reactor at 60 °C and 1 atm also. RK-Soave thermodynamic properties are used. Up to this point, all four simulations are identical. The four different ways of processing the exit stream from the reactor are as follows. Since the FAME and glycerol becomes unstable and prone to thermal decomposition at 250 °C (482 °F) and 150 °C (301 °F), respectively, it is necessary to keep the temperature below these temperatures during the process. Also, ASTM standards require biodiesel purification to be above 99.65 wt %. Additionally, glycerol purification needs to be greater than 90% in order to sell glycerol as a refined product.

RK-Soave thermodynamic data is used for all the heat exchangers and decanters in these four simulations. Specifying separation efficiencies on the "Input Efficiency" sheet is to account for departure from equilibrium. No separation efficiency is assigned to any of the decanters in this simulation and therefore, the outlet streams from the decanters are a result of equilibrium separation.
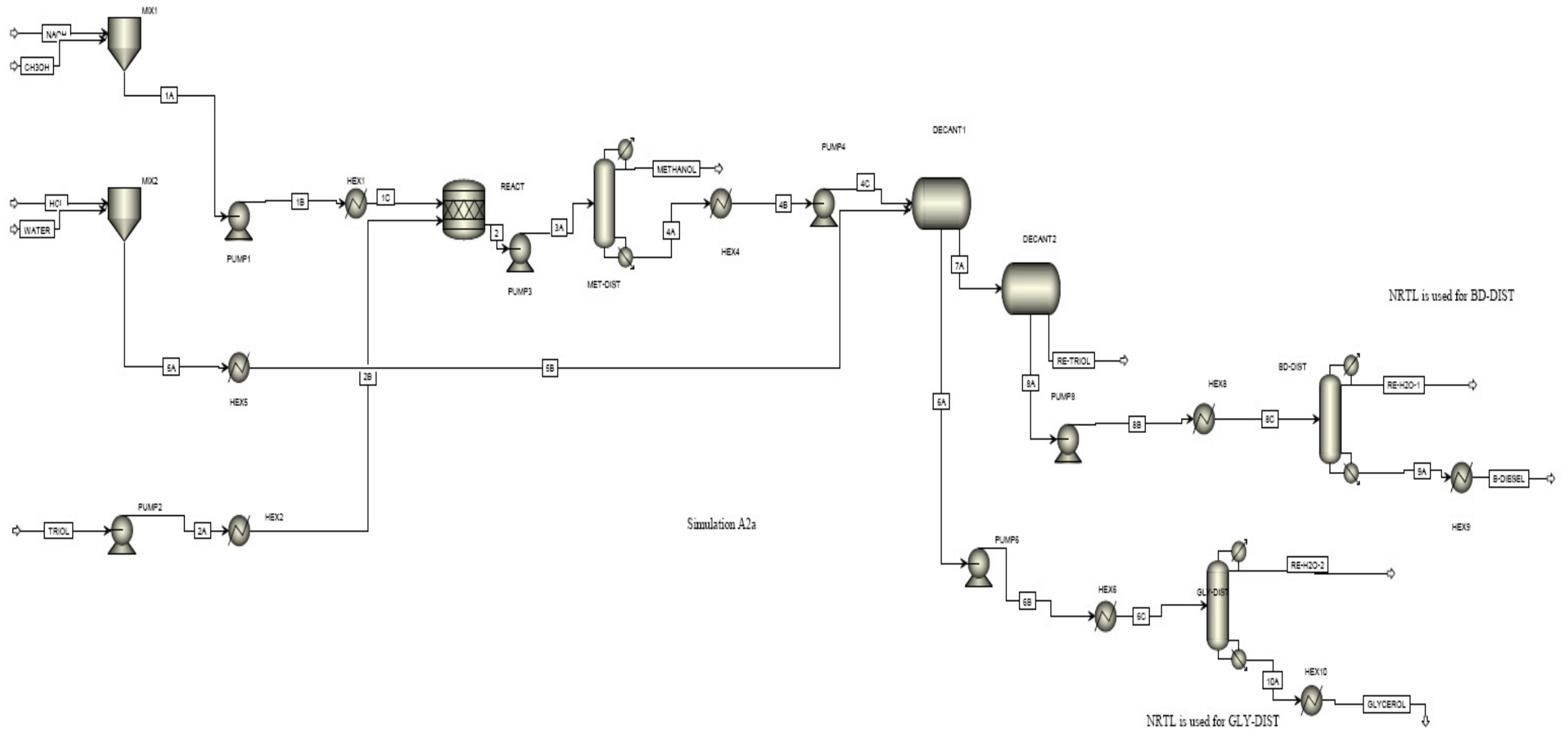
Figure 5.6 Scenario 1
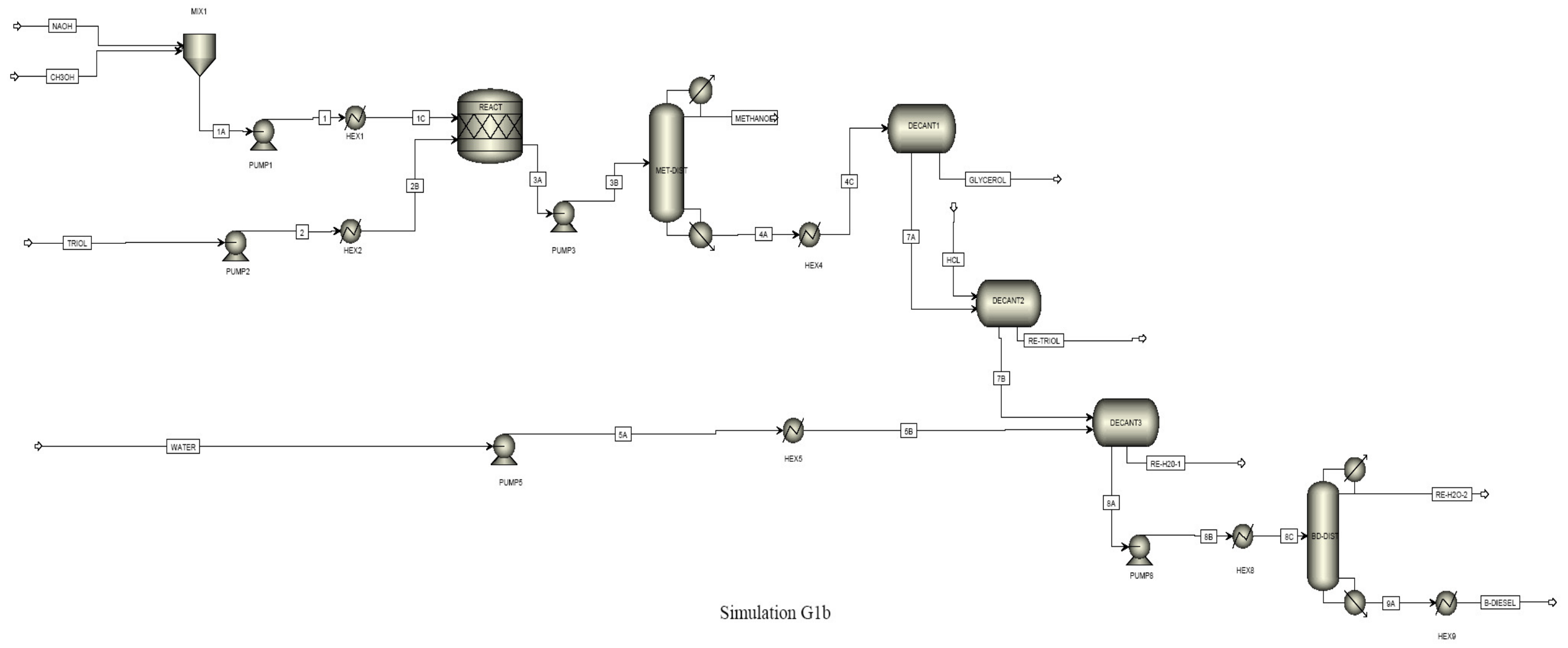
Simulation G1b

Figure 5.7 Scenario 2
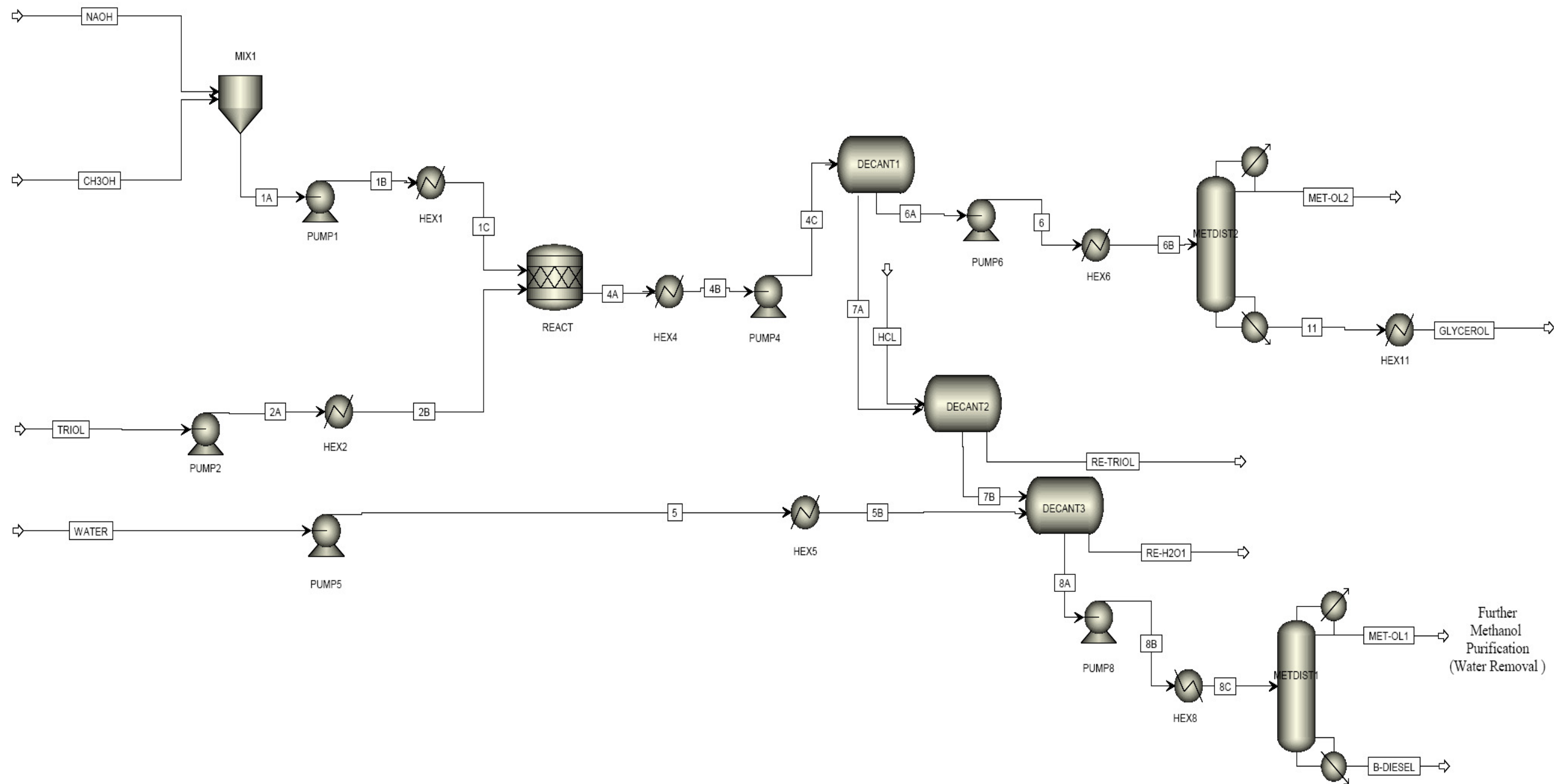
Figure 5.8 Scenario 3
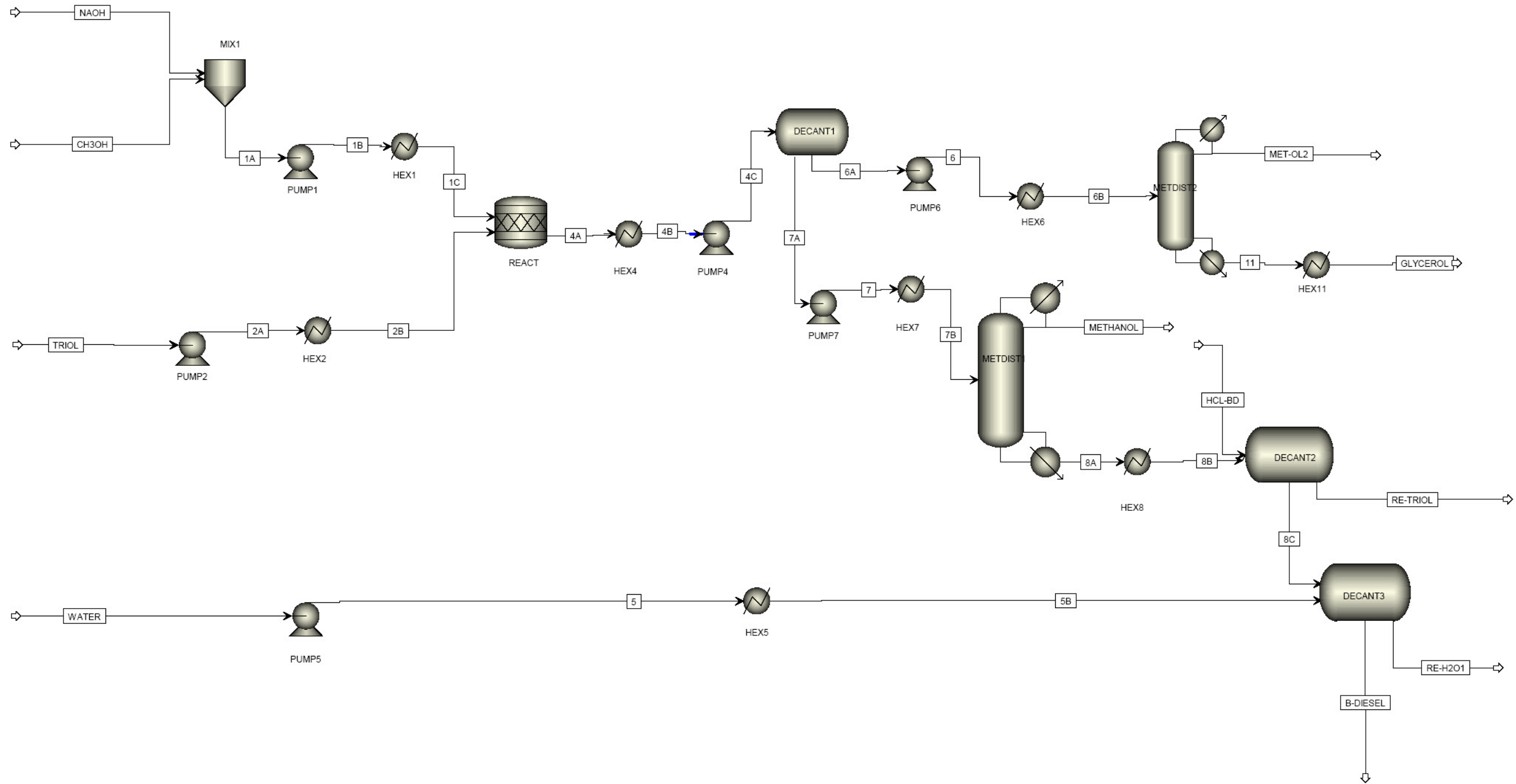
Figure 5.9 Scenario 4

5.7.1 Scenario 1: Removal of methanol first: water washing at the presence of glycerol

In this scenario, as shown in Figure (5.6), the exit stream from the reactor is sent to the methanol distillation column. In order to keep the temperature below 301 °F, a vacuum distillation column with 6 theoretical stages is used along with NRTL thermodynamic properties. The bottom stream of the methanol distillation column is cooled to 25 °C in a heat exchanger (HEX4) at atmospheric pressure before sending it to the first decanter (DECANT1) where the glycerol is separated from the biodiesel.

As soon as the methanol is separated, addition of hydrochloric acid and water washing is processed simultaneously to reverse any saponification during the washing process. The HCl, in equivalent moles to the NaOH present in the stream, is added to the washing water first and then mixes with the Biodiesel mixture in DECANT1.

In order to determine the optimal amount of water to remove the soap and catalyst from the biodiesel, water sensitivity analysis is conducted. Sensitivity analysis is used to determine the optimal amount of water needed in the washing process.

The biodiesel stream (7A) is sent to a second decanter (DECANT2) for further separation. In this step, triol is removed from the Biodiesel. Then the Biodiesel stream is heated in a heat exchanger, HEX8, and sent to a biodiesel distillation column. Again, in order to keep the temperature below biodiesel's thermal decomposition level of 250 °C, a vacuum distillation column is used. NRTL properties are used and the distillation column has 6 theoretical stages with a reflux ratio of 1.5.

The glycerol stream (6A) is heated in a heat exchanger (HEX6) before being sent to the glycerol distillation column (GLY-DIST) for further purification. Vacuum distillation with 5 theoretical stages is required to keep the temperature below 250 °C for GLY-DIST. Most of the water is removed.

5.7.2 Scenario 2: Removal of methanol first: water washing after removal of glycerol

In this scenario, as shown in Figure (5.7), every process design prior to methanol distillation is the same as in scenario (1). After the methanol is removed, the bottom stream from the methanol distillation column is cooled to 25 °C in the heat exchanger

(HEX4) at 1 atm. Instead of the simultaneous hydrochloric acid addition and water washing process, biodiesel and glycerol are separated in the decanter (DECANT1) first. The glycerol stream coming out of DECANT1 has above 90 wt % glycerol concentration and no further purification process is needed.

The biodiesel stream (7A) from DECANT1 is sent to a second decanter, DECANT2, in order to remove the triol. HCl in equivalent moles to NaOH is added to DECANT2 in order to reverse any saponification. After triol is removed, the biodiesel stream (7B) is sent to the third decanter (DECANT3) where water is added. Sensitivity analysis is conducted in order to determine the optimal amount of water to wash the Biodiesel. Water sensitivity analysis demonstrates that there is no instability in the biodiesel stream in this process. The optimal amount of 300 mol of water washing is used to wash NaOH in the biodiesel stream. The biodiesel stream, stream 8A, is heated in a heat exchanger (HEX8) before it is sent to the biodiesel distillation column (BD-DIST) for further purification. In order to keep the temperature below 250 °C, a vacuum distillation column with 8 theoretical stages and NRTL thermodynamic properties is used.

5.7.3 Scenario 3: Biodiesel and glycerol separation first: water washing at the presence of methanol

In this scenario, as shown in Figure (5.8), all the process design prior to the transesterification reactor unit is the same as in scenario (1) and (2). After the reactor unit, the product stream is sent to the heat exchanger (HEX4) at 1 atm and 25 °C with RK-Soave thermodynamic properties. The stream is then sent to the first decanter (DECANT1) for glycerol and biodiesel separation. The exit glycerol stream has only 60 wt % concentration of glycerol and therefore, further purification is required. The biodiesel stream (7A) from DECANT1 is sent to the second decanter (DECANT2) where HCl (in equivalent mol to NaOH present in 7A) is added and triol is removed. Then, the stream is sent to the third decanter (DECANT3) where water washing and decantation take place. The amount of water used is determined by the sensitivity analysis.

The same instability of stream observed in the first simulation occurred at 300 mol of water. However, glycerol is already removed in DECANT1, and the instability of the stream in DECANT3 did not result in mixing of glycerol and biodiesel. 300 mol of water is used in the process. Removal of methanol and water from biodiesel is used. The biodiesel stream from DECANT3 is then heated in HEX8 and sent to the methanol distillation column (MET-DIST1). Vacuum distillation with 8 theoretical stages and NRTL thermodynamic properties are used. The distillate contains water and methanol along with traces of other compounds. Therefore, methanol from this unit cannot be recycled directly and requires further purification.

5.7.4. Scenario 4: Biodiesel and glycerol separation first: water washing after removal of methanol

This process design is identical to the third scenario prior to glycerol and biodiesel separation in DECANT1. After the separation, instead of going through the multiple decantation process, methanol is removed from the biodiesel stream first. The stream components in the biodiesel stream (7A) and the glycerol stream (6A) exiting from DECANT1 are the same as in scenario 3. The glycerol stream has 60 % (mass) glycerol and therefore, further purification is conducted. This stream is sent to the heat exchanger (HEX6) before sending it to the glycerol distillation column (METDIST2) in order to remove methanol. In order to keep the glycerol below the thermal decomposition temperature (150 °C), a vacuum distillation column with 5 theoretical stages and NRTL thermodynamic properties are used.

The biodiesel stream (7A) from DECANT1 is sent to the heat exchanger (HEX7) to raise the temperature before being sent to the methanol distillation column (METDIST1) for methanol removal. In order to keep the Biodiesel below the thermal decomposition temperature of 250 °C, a vacuum distillation column with 6 theoretical stages and NRTL thermodynamic properties are used.

The bottom biodiesel stream from METDIST1 is cooled down in a heat exchanger (HEX8). Then, the stream is sent to the second decanter (DECANT2) where HCl in equivalent mol to the NaOH present is added. All the triol is removed from the Biodiesel stream in this decanter. Then, the stream is sent to the third decanter (DECENT3) where

water washing takes place. Water sensitivity analysis is conducted in order to determine the optimal amount of water needed to wash the biodiesel. As a result, 300 mol of water is used. The resulting Biodiesel stream already has 99.7% purification and therefore, no further Biodiesel purification is required.

CHAPTER VI
RESULTS AND DISCUSSION

6.1 Water Sensitivity Analysis

Water sensitivity analysis is conducted for each scenario to determine the optimal amount of water needed for removal of catalysts from biodiesel stream in order to meet the 99.65 wt % biodiesel purification. In this analysis, the amount of water used in the washing process is varied and the compositions of biodiesel stream coming out from the washing unit (decanter) are analyzed. Water washing is conducted in two different ways, isothermal and adiabatic for scenario (1). During the isothermal condition, the temperature of the decanter is kept constant at 25 ºC. The results show the existence of two-phase region and water and glycerol exit from the decanter as one stream while biodiesel exits as another stream. However as the amount of water used in the washing process increases, the two-phase region no longer exists and homogeneous region is obtained. As the result, biodiesel, water and glycerol exit from the decanter as one stream. The phase diagram can be constructed based on the results of the simulations as shown in Figure (6.1).
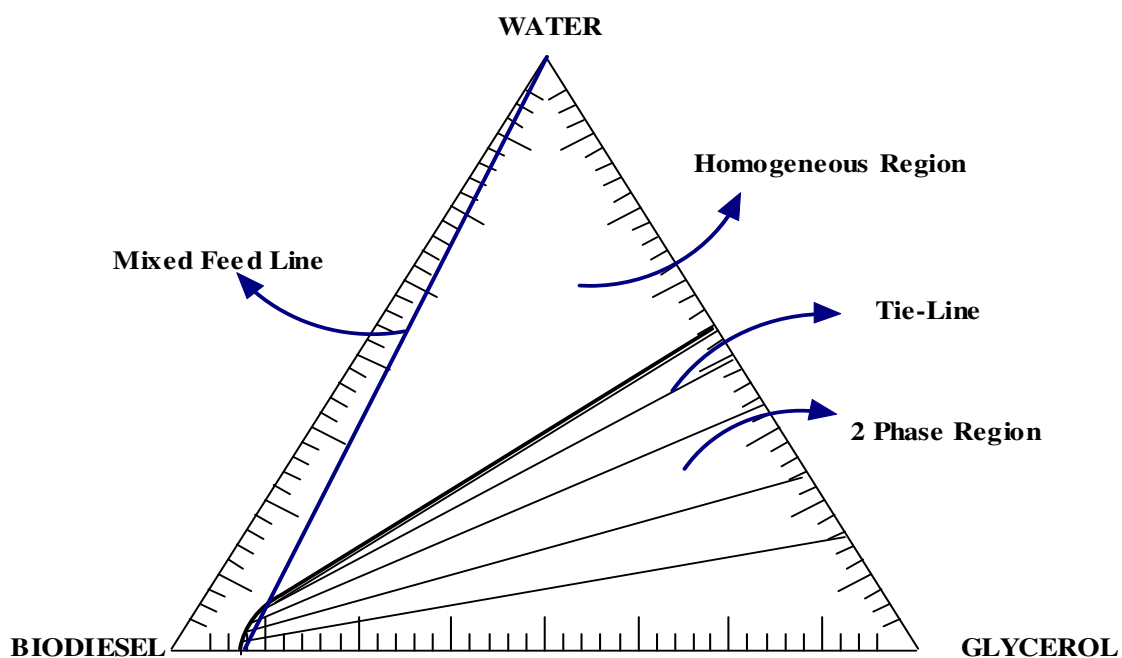
Figure 6.1 Phase Diagram at 25 ºC

When the water sensitivity analysis is conducted under adiabatic condition, it is independent of the amount of water used and the two-phase region exits through out. The phase diagram is constructed as shown in the Figure (6.2).
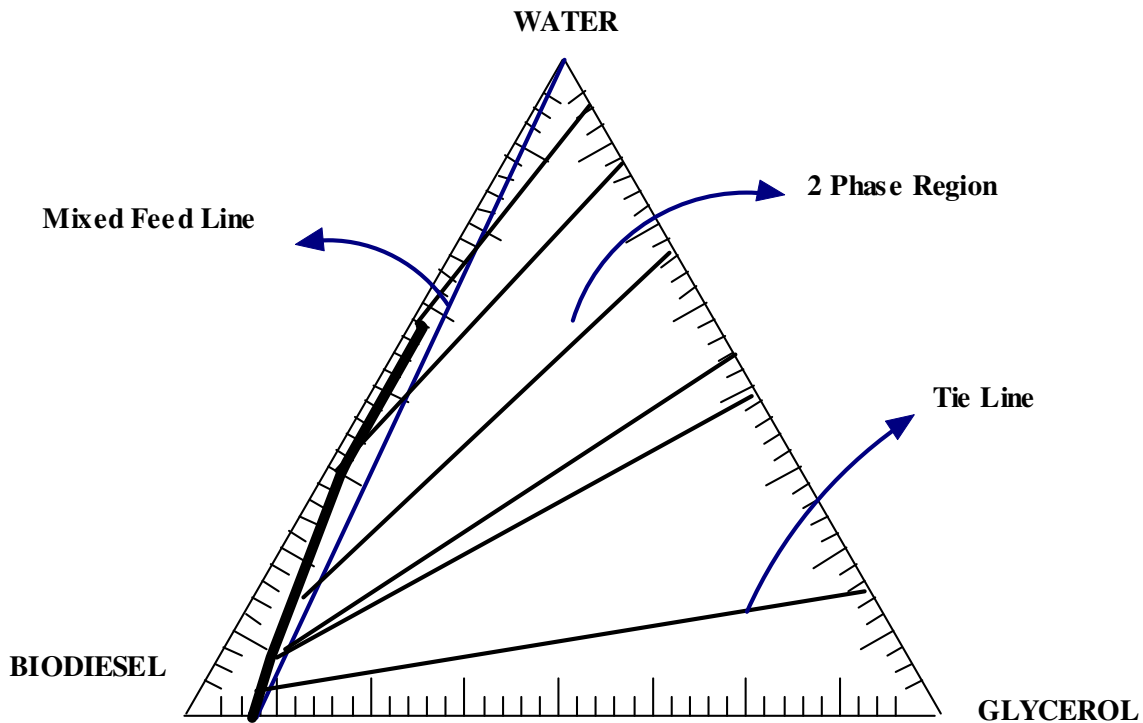
Figure 6.2 Phase Diagram at Adiabatic

Based on these results, all the water washing process is conducted under adiabatic condition for all scenarios. The result of the sensitivity analysis is plotted for each scenario and the optimal amount of water is determined as shown in Figure (6.3). In this figure, it can be seen that the amount of NaOH and HCl in the biodiesel stream decreases as the amount of water used in the washing process increases. However, after it reaches 300 mol of water, the catalyst amount removed from the biodiesel stream becomes less significant. Therefore, 300 mol of water is considered to be the optimal amount of water needed for the washing process. The results of water sensitivity analysis for all scenarios show the same optimal amount of water.
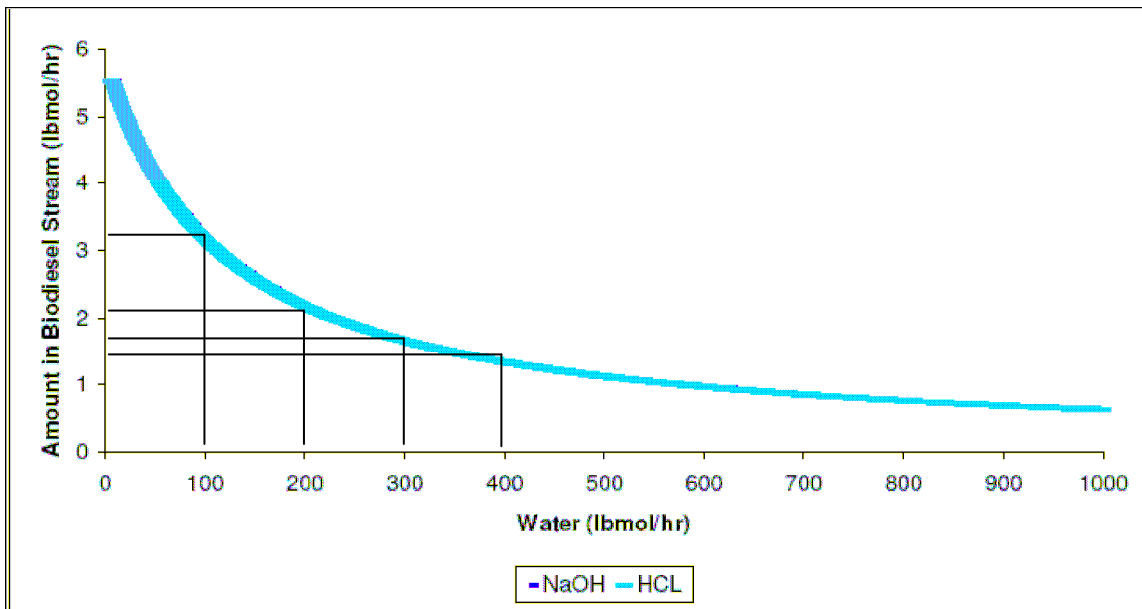
Figure 6.3 Water Sensitivity Analysis for Scenario 4

6.2 Comparison of Process Simulations

The removal of excess methanol at the beginning of the separation process is preferred, since the excess methanol tends to act as a solubilizer and interferes with the biodiesel separation by slowing down the process. However, according to Gerpen (2004), in the presence of catalysts, removing the excess methanol will shift the equilibrium towards the reactants and can reverse the transesterification. Due to that concern, excess methanol is usually not removed from the stream until the separation of glycerol and methyl ester is complete. Therefore, simulations 1 and 2 are both set aside for the same reason until more kinetic data is available for the transesterification process.

Comparing simulations 3 and 4, simulation 4 is considered to be the better process design. The difference between these two simulations is the timing of methanol removal. Simulation 4 positions methanol removal before water washing, while simulation 3 positions methanol removal after water washing. Placing a methanol distillation column before water washing is an inherently superior design. First, less heat duty is required for the methanol distillation since there is no water. Methanol exiting from the distillation column is recycled back to the reactor unit. It is vital that this recycled methanol stream be free of water. If the methanol distillation column is placed after the water washing process,

water vapor can be present in the recycle stream. If there is any equipment failure or misoperation, the methanol will be contaminated by water. If water is present in the methanol recycle stream, the transesterification reaction will be interrupted by a significant formation of soap. In simulation 3, the methanol exiting the methanol distillation column contains some water. Therefore, a purification process unit is required prior to recycling the stream back to the reactor.

Therefore, simulation 4 is chosen for further optimization via mass and energy integration and for performance of an economic evaluation.

6.3 Heat Integration and Utility Cost

In order to determine the minimum heating and cooling utilities, heat integration is conducted via an algebraic approach. The cold streams that need to be heated and the hot streams that need to be cooled are selected as shown in Table (6.1).

Table 6.1 Cold and Hot Stream of Scenario 4

	Supply Temp ($°F$)	Target Temp ($°F$)	Enthalpy Change $10^3 Btu.hr^{-1}$	Specific Heat $10^3 Btu.hr^{-1}.°F^{-1}$
Cold Streams				
HEX1	77	140	310.26	4.93
HEX2	77	140	875.27	13.89
HEX5	77	140	393.17	6.24
HEX6	130	140	195.25	19.53
HEX7	130	140	186.09	18.61
MET-DIST1 (Reboiler)	468	469	8788.50	8788.50
MET-DIST2 (Reboiler)	302	303	4084.08	4084.08
TOTAL HEATING UTILITY			**14832.61**	
Hot Streams				
HEX4	140	77	1435.99	22.793
HEX8	433	77	7993.29	22.45
HEX11	295	77	1372.04	6.29
MET-DIST1 (Condenser)	62	61	2195.27	2195.27
MET-DIST2 (Condenser)	62	61	3184.77	3184.77
REACT1	140	139	3706.88	3706.88
TOTAL COOLING UTILITY			**19888.24**	

The temperature interval is constructed with a minimum heat exchange driving force (Δ^{Tmin}) of 10 ºF as shown in Figure (6.4).

Intervals	Hot Streams			Cold Streams		
			479	469		
1			478	468		
2			433	423		
3			313	303		
4			312	302		
5			295	285		
6			150	140		
7			140	130		
8			139	129		
9			87	77		
10			77	67		
11			62	52		
12			61	51		

Figure 6.4 Temperature Interval Diagram for Scenario (4)

Then the cascade diagram is constructed to determine the Thermal Pinch as shown in Figure (6.5). Thermal Pinch is located between interval 4 and 5 and average temperature is 307 ºF.
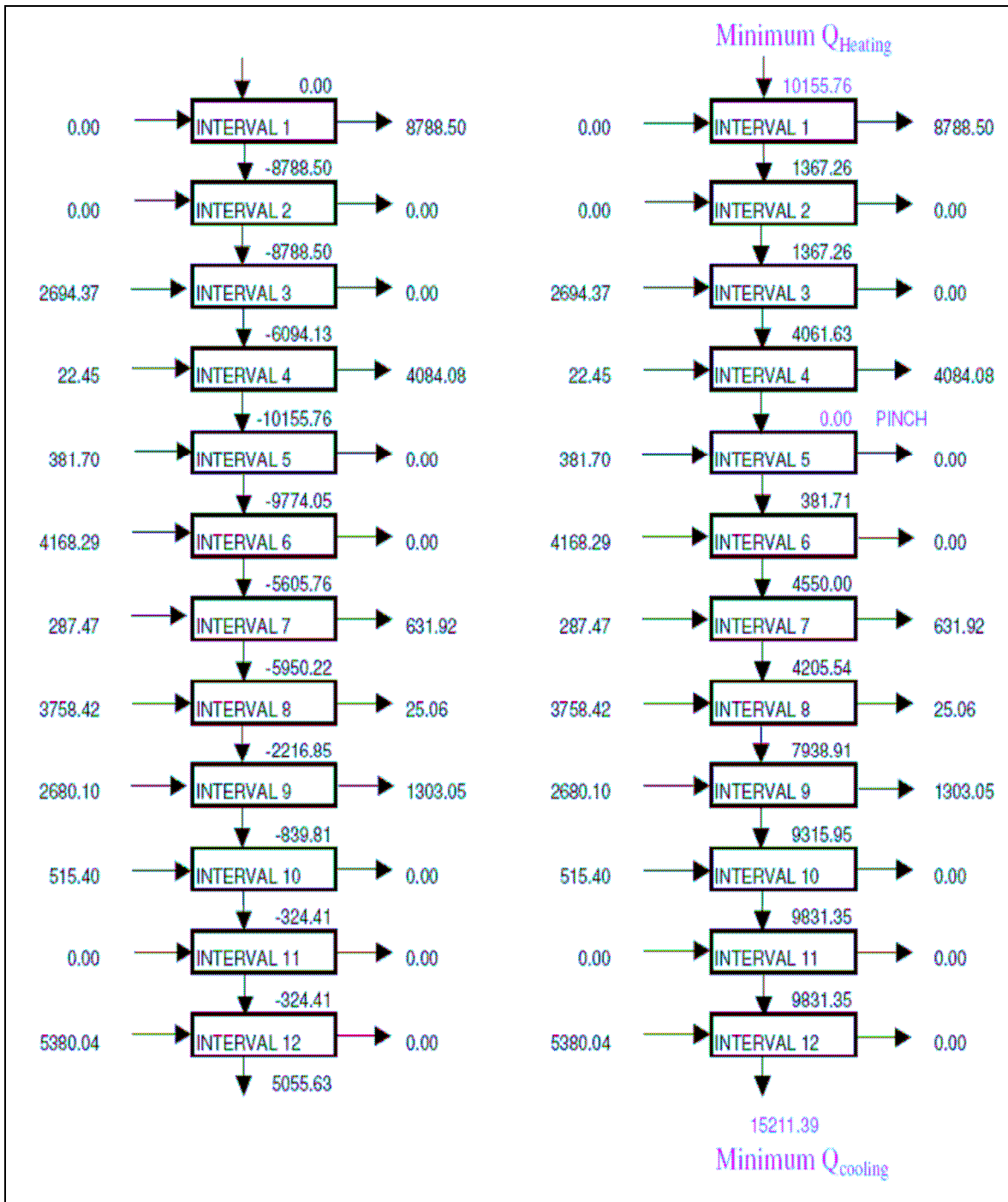
Figure 6.5 Cascade Diagram for Scenario (4)

From the cascade diagram, minimum heating utility (Q_H^{min}) and minimum cooling utility (Q_C^{min}) is determined. Then, the grand composite curve is constructed to determine the distribution of heating and cooling utilities, as shown in Figure (6.6).
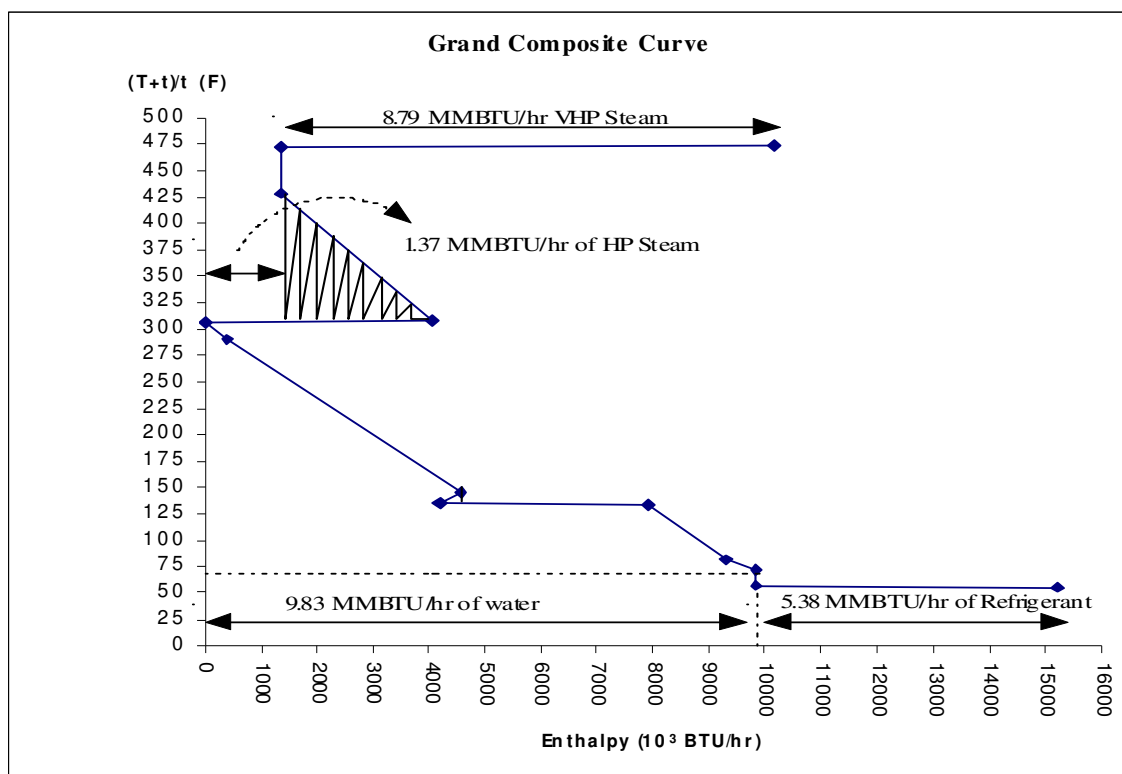
Figure 6.6 Grand Composite Curve for Scenario (4)

From this, total utility cost of biodiesel production before and after heat integration as well as total saving can be calculated as shown in Table (6.2).

Table 6.2 Total Utility Savings from HEN

HEN Claculation	Amount (10^3Btu / hr)	Unit Cost ($ / MMBtu)	Cost ($ / yr)
Heating Utility (HP Steam)	8,788.50	8.00	562,464
Heating Utility(MP Steam)	1,367.26	6.00	65,628
Cooling Utility (with water)	9,831.35	6.00	4,719,048
Cooling Utility (with refrigerant)	5,380.04	14.00	6,025,645
Total Utility Cost After Integration			11,372,785
Total Utility Cost Without Integration			16,860,000
Total Saving From HEN			5,487,000

A thermal pinch diagram shows the same minimum heating and cooling utilities as shown in Figure (6.7).
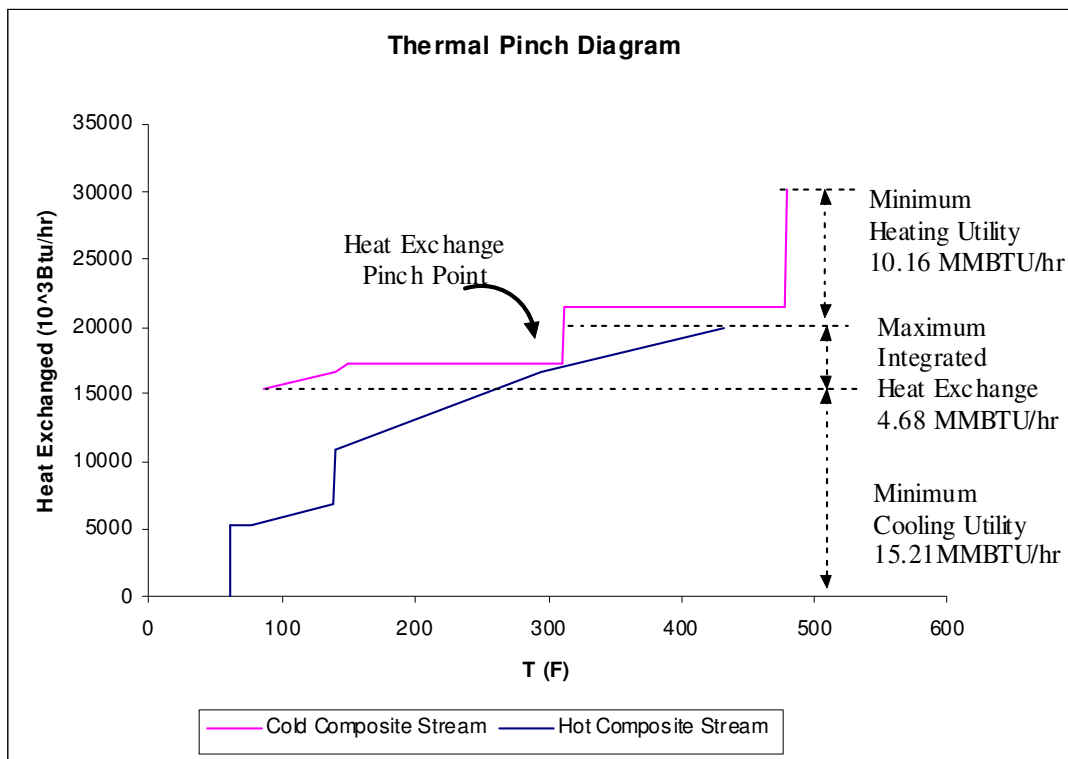
Figure 6.7 Thermal Pinch Diagram

6.4 Estimation of Capital Cost

Capital cost estimation was carried out using ICARUS Process Evaluator computer-aided tools linked to the results of the ASPEN simulation. Table (6.3) represents the total project cost of 40 million gallons per year biodiesel production scenario. A detailed itemization of equipment cost is shown in Table (6.4).

Table 6.3 Total Project Capital Cost

PROJECT	Total Cost ($)
Purchased Equipment	498,000.00
Equipment Setting	17,000.00
Piping	617,000.00
Civil	108,000.00
Steel	44,000.00
Instrumentation	862,000.00
Electrical	343,000.00
Insulation	212,000.00
Paint	363,000.00
Other	2,460,000.00
Subcontracts	0.00
G and A Overheads	116,000.00
Contract Fee	305,000.00
Escalation	0.00
Contingencies	1,070,000.00
Special Charges	0.00
Total Project Cost	7,015,000.00

Table 6.4 Total Equipment Cost

Equipment Name	Equipment Type	Total Direct Cost ($)	Equipment Cost ($)
DECANT1	DVT CYLINDER	68,500.00	10,900.00
DECANT2	DVT CYLINDER	85,600.00	14,000.00
DECANT3	DVT CYLINDER	85,600.00	14,000.00
HEX1	DHE FLOAT HEAD	55,500.00	15,900.00
HEX11	DHE FLOAT HEAD	62,300.00	13,300.00
HEX2	DHE FLOAT HEAD	53,200.00	12,700.00
HEX4	DHE FLOAT HEAD	95,500.00	28,700.00
HEX5	DHE FLOAT HEAD	46,000.00	16,300.00
HEX6	DHE FLOAT HEAD	46,900.00	17,400.00
HEX7	DHE FLOAT HEAD	56,200.00	15,900.00
HEX8	DHE FLOAT HEAD	96,700.00	23,500.00
METDIST1-tower	DTW TRAYED	288,900.00	78,200.00
METDIST1-cond	DHE FIXED T S	51,400.00	13,100.00
METDIST1-cond acc	DHT HORIZ DRUM	61,500.00	10,800.00
METDIST1-reflux pump	DCP CENTRIF	20,200.00	3,300.00
METDIST1-reb	DRB U TUBE	74,700.00	20,800.00
METDIST2-tower	DTW TRAYED	213,900.00	47,000.00
METDIST2-cond	DHE FIXED T S	52,600.00	14,300.00
METDIST2-cond acc	DHT HORIZ DRUM	61,500.00	10,800.00
METDIST2-reflux pump	DCP CENTRIF	20,700.00	3,800.00
METDIST2-reb	DRB U TUBE	71,800.00	20,500.00
PUMP1	DCP CENTRIF	22,700.00	2,900.00
PUMP2	DCP CENTRIF	28,000.00	3,600.00
PUMP4	DCP CENTRIF	28,100.00	3,700.00
PUMP5	DCP CENTRIF	22,700.00	2,900.00
PUMP6	DCP CENTRIF	22,700.00	2,900.00
PUMP7	DCP CENTRIF	27,300.00	3,600.00
REACT	DAT REACTOR	158,200.00	56,800.00
TOTOAL		1,978,900.00	481,600.00

6.5 Calculation of Annual Operating Cost

The raw material cost is calculated as shown in Table (6.5).

Table 6.5 Calculation of Raw Materials Cost

Description	Amount (lb/yr)	Unit Price ($/lb)	Annual Cost ($/yr)
Soy Bean Oil	290,587,200.00	0.28	81,364,416.00
Methanol	64,754,720.00	0.15	9,713,208.00
NaOH	74,560.00	1.80	134,208.00
HCL	815,840.00	0.63	509,900.00
Water	43,236,640.00	0.00	5,188.40
Total Raw Materials Cost			91,727,000.00

Discharge water from the process is treated by a single stage Reverse Osmosis Network (RON) (El-Halwagi, 1997). 41 % of the discharge water can be recycled and the remaining 60% sent to wastewater treatment. Wastewater treatment with and without recycling is compared. The savings obtained from including water recycling can be seen in Table (6.6).

Table 6.6 Total Saving from Recycling Water

Description	Amount (lb/yr)	Unit Price ($/lb)	Annual Cost ($/yr)
Waste water treatment (without recycle)	44,168,000.00	0.001200	53,001.60
Waste water treatment (with recycle)	25,992,000.00	0.001200	31,190.40
Recycled Water	18,160,000.00	0.000120	2,179.20
Savings from Recycling Water			23,990.40

Annual operating cost is calculated as shown in Table 6.7. Savings from selling the glycerol byproduct (above 92% purity), methanol recycling, and water recycling are included in the operating cost.

Table 6.7 Calculation of Annual Operating Cost

Description	Cost	Unit
Raw Materials Cost	91,727,000.00	$/yr
Operating Labor Cost	340,000.00	$/yr
Maintainance Cost	26,000.00	$/yr
Electricity	21,000.00	$/yr
Utilities Cost	16,860,000.00	$/yr
Total Operating Cost Without Process Integration	**108,974,000.00**	**$/yr**
Savings From Process Integration		
Heat Integration	5,487,000.00	
Water Recycling	24,000.00	$/yr
Methanol Recycling	4,985,000.00	$/yr
Glycerol	15,987,000.00	$/yr
Total Operating Cost With Process Integration	**82,491,000.00**	**$/yr**

6.6 Calculation of Total Annualized Cost

Annualized fixed cost is calculated in Table 6.8. Salvage value is 10% of the total capital cost and a 5 years useful life period is used. Then, the total annualized cost is calculated as shown in Table 6.9.

Table 6.8 Calculation of Annualized Fixed Cost (AFC)

Annualized Fixed Cost (AFC) = (Total Capital Cost-Salvage Value) / (Useful life Period)		
Description	Cost	Unit
Total Capital Cost	7,015,002.20	$
Salvage Value	701,500.22	$
Useful life Period	5.00	yr
Annualized Fixed Cost (AFC)	1,262,700.40	$/yr

Table 6.9 Calculation of Total Annualized Cost (TAC)

Total Annualized Cost (TAC) = Annualized Fixed Cost + Annual Operating Cost+Interceptor		
Description	Cost	Unit
Annualized Fixed Cost (AFC)	1,263,000.00	$/yr
Annual Operating Cost	82,491,000.00	$/yr
Total Annualized Cost (TAC)	83,754,000.00	$/yr

6.7 Calculation of Return of Investment (ROI) and Payback Period (PP)

In order to determine the ROI and PP, production cost and annual gross profit are calculated first, as shown in Table (6.10) and Table (6.11). Selling prices of $2.75 and $3.00 per gallon are used for the comparison.

Table 6.10 Calculation of Production Cost

Production Cost = TAC / Annual Production Rate		
Description	Cost	Unit
TAC	83,754,000.00	$
Actual Production Rate	40,144,000.00	gal /yr
Production Cost	2.09	$/gal

Table 6.11 Calculation of Annual Gross Profit

Annual Gross Profit = Annual Production Income - TAC			
	2.75	3.00	$/gal
Annual Production Income	110,396,000.00	120,432,000.00	$/yr
TAC	83,754,000.00	83,754,000.00	$/yr
Annual Goss Profit	26,642,000.00	36,678,000.00	$/yr

Next, the ROI and PP are calculated as shown in Tables (6.12) and (6.13). Sensitivity analysis based on the price of the soybean is conducted for both since the pice of the soy bean is the main contributing factor for the production cost. The results are plotted in Figure (6.8) and (6.9).

Table 6.12 Calculation of ROI

ROI = [Annual Gross Profit/Capital Investment] x 100			
	2.75	3.00	$/gal
Annual Goss Profit	26,642,000.00	36,678,000.00	$/yr
Capital Investment	7,015,000.00	7,015,000.00	$/yr
ROI	380	523	%
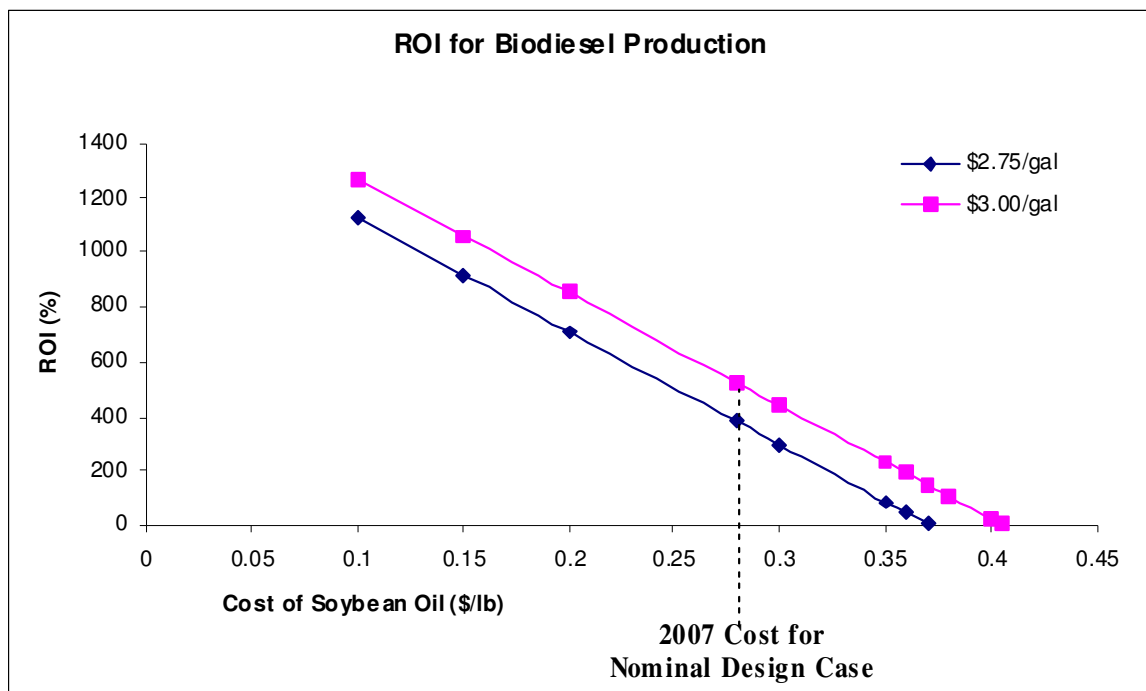
Figure 6.8 Sensitivity Analysis of ROI

Table 6.13 Calculation of Pay Back Period (PP)

Payback period (yrs) = Fixed Capital Investment/ Annual after-tax cash flow			
Annual after tax cash flow = Annual income - Annual operating cost – tax			
Description	Cost ($ 2.75/gal)	Cost ($3/gal)	Unit
Fixed Capital Investment	7,015,000.00	7,015,000.00	$
Annual Income	110,396,000.00	120,432,000.00	$/yr
Annual Operating Cost	82,491,000.00	82,491,000.00	$/yr
PayBack Period	0.25	0.18	

In calculation of payback period, it is assumed that the tax credit for biodiesel production by using soybean oil is equivalent to the tax.
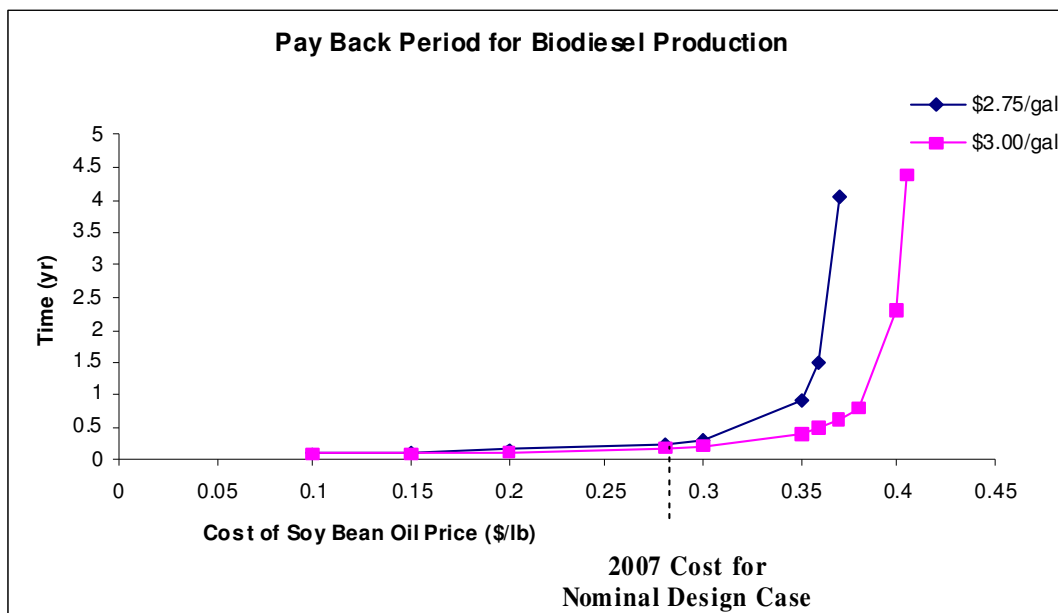
Figure 6.9 Sensitivity Analysis of PP

CHAPTER VII

CONCLUSIONS AND RECOMMENDATIONS FOR FUTURE WORK

This work focused on the design, analysis, and optimization of biodiesel production from soybean oil. Four process flowsheets were synthesized. The performance of these flowsheets, along with the key design and operating criteria, were identified by conducting computer-aided simulations using ASPEN Plus. By comparing the technical and economic aspects of the four scenarios, a process configuration was recommended. Next, mass and energy integration studies were performed to reduce the consumption of heating and cooling utilities, to conserve fresh water, and to reduce wastewater discharge. Capital cost estimation was completed using ICARUS Process Evaluator computer-aided tools linked to the results of the ASPEN simulation. The operating cost of the process was estimated using key information concerning process operations, such as raw materials, utilities, and labor. A profitability analysis was performed by examining the ROI and PP. Under current market conditions, both the ROI and PP were found to be very attractive (ROI of about 380% and a PP of about 0.25 year). It was determined that the single most important economic factor is the cost of soybean oil, which accounted for more than 90% of the total annualized cost. Consequently, a sensitivity analysis was performed to examine the effect of soybean oil cost on profitability. Both ROI and PP quickly deteriorate as the cost of soybean oil increases. A break-even point is reached with a soybean oil cost of $0.37/lb, when the biodiesel selling price is $2.75/gal. When the biodiesel selling price is $3.00/gal, a break-even point is reached with a soybean oil cost of $0.40/lb.

The following research topics are proposed for future work:

- Multi-feedstock plants considering segregated, co-fed raw materials
- Dynamic operations and scheduling of a process whose feedstock varies throughout the year
- Life cycle analysis to evaluate environmental impact, especially green house gas (GHG) emissions, of renewable feedstocks versus fossil fuel feedstocks
- A detailed kinetic study of the effect of methanol removal on rates of glycerol/biodiesel formation versus reverse reaction to monoglyceride and methanol (This study will help in the analysis of the first two process configurations examined

in this work.)

- Exploration of new reaction pathways and processing schemes (This entails a combination of experimental and theoretical work.)

REFERENCES

Anderson, D., Masterson, D., McDonald, B., and Sullivan, L., 2003. Industrial Biodiesel Plant Design and Engineering: Practical Experience. Crown Iron Works Company. Presented at International Palm Oil Conference (PIPOC), Malaysia.

Allen, M. and Prateepchaikul,G., 2006. The modeling of the biodiesel reaction, Report Entry, Department of Mechanical Engineering, Prince of Songkla University, Hadyai, Thailand.

API, Available at http://www.api.org/aboutoilgas/diesel/index.cfm. Accessed October 13, 2006.

Agency for Toxic Substances and Disease Registry (ATSDR), 1995. Toxicological profile for fuel oils. Atlanta, GA: U.S. Department of Health and Human Services, Public Health Service.

Baldwin, J., 2006. Plant Design: Separation synthesis assessment, Class notes, CHEN 426, Chemical Engineering, Texas A&M University.

Billen, J., Nuijsenburg, M., Oomen, A., Reniers, J., Schmeits, J. and Wezel, R., 2004. Biodiesel II or Vegetable Oil. Multi Disciplinary Project. Eindhoven University of Technology, Eindhoven, The Netherlands.

Brevard Biodiesel: Stability of Biodiesel and the 'Iodine Value'. Available at http://www.brevardbiodiesel.org/iv.html. Accessed March 10, 2006.

Earth Biofuels: better living through Biodiesel. Available at www.earthbiofuesl.net. Accessed March 21, 2006.

EIA, 2005. International Energy Annual 2003: System for the analysis of Global Energy Market. Available at www.eia.doe.gov/eia/2003.2030. Accessed March 21, 2006.

EIA, 2006. International Energy Annual 2004: World Consumption of Primary Energy by Energy Type and Selected Country Groups (U.S. Physical Units), 1980-2004. Available at http://www.eia.doe.gov/iea/wec.html. Accessed March 21, 2006.

El-Halwagi, M. M., 2006. Process Integration, Academic Press, New York.

El-Halwagi, M. M., 1997. Pollution Prevention Through Process Integration, Academic Press, San Diego, California.

Freudenrich,C., 2001. How Oil Refining Works. Web site available at http://www/howstuffworks.com/oil-refining2.htm. Accessed July 6, 2006.

Gerpen, J. V., 2005. Biodiesel processing and production. Fuel Processing Technology 86, 1097-1107.

Gerpen, J, Shanks, B, Pruszko, R., 2004. Biodiesel Production Technology, National Renewable Energy Laboratory. Subcontractor Report, NREL/SR-510-36244.

Ghadge, S. V. and Raheman, H., 2006. Process optimization for biodiesel production from mahua (Madhuca indica) oil using response surface methodology. Bioresource Technology 97, 379-384.

Hass, M. J., McAloon, A. J., Yee, W. C., Foglia T. A., 2006. A process model to estimate biodiesel production costs. Bioresource Technology 97, 671-678.

He, B., 2006. Biodiesel stability & Storage, Report entry, Biological and Agricultural Engineering, University of Idaho.

Jackson, S., 2006. Standard for Good Reason, Biodiesel Magazine, February, 36.

Knothe, G., Dunn, R. O., Bagby, M.O., 1997. Biodiesel: The use of vegetable oils and their derivatives as alternative diesel fuels. Fuels and Chemicals from Biomass. Presented at American Chemical Society Symposium, Ser. 666. Washington, D.C.

Kotrba, R., 2006. Bound by Determination. Biodiesel Magazine, October, 42.

Leung, D. and Guo, Y., 2006. Transesterification of neat and used frying oil: Optimization for biodiesel production. Fuel Processing Technology 87, 883-890.

Meher, L., Sagar, D., and Naik S., 2006. Technical aspects of biodiesel production by transesterification: a review. Renewable and Sustainable Energy Reviews, 10, 248-268 (2006).

Noureddini, H., and Zhu, D., 1997. Kinetics of transesterificaiton of soybean oil. Journal of the American Oil Chemists' Society (JAOCS), Vol. 74, 1457-1463 (1997).

NBB. National Biodiesel Board. Biodiesel Production and Quality. Available at http://www.nrel.gov/vehiclesandfuels/npbf/pdfs/40555.pdf. Accessed October 9, 2006.

OTM, 1999. OSHA Technical Manual. U.S. Department of Labor. Occupational Safety & Health Adminstration. TED 01-00-015.

Schuchardt, U., Ricardo, S., and Vargas, R. Instituto de Quimica., 1997. Transesterification of vegetable oils: a Review. Report entry, Universidade Estadual de Campinas, Campus de Ondina, Brazil.

Tapasvi, D., Wiesenborn, D. and Gustafson, 2004. Process Modeling Approach for Evaluating the Economic Feasibility of Biodiesel Production. Presented at 2004 North Central ASAE/CSAE Conference, Winnipeg, Canada.

Tyson, K.S., McCormick, R.L., 2006. Biodiesel Handling and Use Guide, Third Edition, National Renewable Energy Laboratory. Technical Report, NREL/TP-450-40555.

Tyson, K.S, Bozell, J., Wallace, R., Petersen, E., and Moens, L., 2004. Biomass Oil Analysis: Research Needs and Recommendations, National Renewable Energy Laboratory. Technical Report, NREL/TP-510-34796.

USDA, 2006. Oil Crops Situation and Outlook Yearbook, Economic Research Service. Outlook Report, OCS-2006. Washington, D.C.

Vicente, G. , Martínez, M. and Aracil, J., 2004. Integrated Biodiesel production: a comparison of different homogeneous catalyst system. Bioresource Technology 92, 297-305.

West, H., 2006. What is Biodiesel, Research Report, Chemical Engineering Department, Texas A&M University.

Zang, Y., Dube´, M., Mclean, D., and Kates, M., 2003. Biodiesel production from waste cooking oil: 1. Process design and technological assessment. Bioresource Technology 89, (1-16).

Zadra, R., 2006. Improving Process efficiency by the usage of alcholates in the Biodiesel production, Marketing and Sales Industrial Chemicals, BASF. Presented at IV Forum Brasil-Alemanha sobre Biodiesel, Aracatuba.

APPENDIX A

Table A.1 Stream Table for Simulation 1

Sim 1	1A	1B	1C	2	2A	2B	3A	4A	4B	4C	5A	5B	6A	6B	6C	7A	8A	8B	8C	9A	10A	B-DIESEL	CH3OH	GLYCEROL	HCL	METHANOL	NAOH	RE-H2O-1	RE-H2O-2	RE-TRIOL	TRIOL	WATER
Temperature F	77	77.2	140	140	76.9	140	140.1	301.8	77	77.1	52.8	140	137	137.1	140	137	144	144	194	442.6	291.4	77	77	77	77	41	77	85.7	91.1	144	77	77
Pressure psi	14.5	29.39	14.7	14.7	29.39	14.7	29.39	0.73	14.7	29.39	14.7	14.7	14.7	29.39	14.7	14.7	14.7	29.39	14.7	0.73	0.73	14.7	14.5	14.7	14.7	0.73	14.5	0.73	0.73	14.7	14.5	15.95
Vapor Frac	0	0	0	0	0	0	0	0	0	0	0	0	0	0	0	0	0	0	0	0	0	0	0	0	1	0	0	0	0	0	0	0
Mole Flow lbmol/hr	261.935	261.935	261.935	304.103	42.168	42.168	304.103	174.586	174.586	174.586	309.32	309.32	350.629	350.629	350.629	133.277	131.948	131.948	131.948	127.872	55.689	127.872	252.615	55.689	9.32	129.517	9.32	4.076	294.941	1.329	42.168	300
Mass Flow lb/hr	8280.717	8280.717	8280.717	45578.717	37298	37298	45578.717	41428.717	41428.717	41428.717	5574.491	5574.491	9363.314	9363.314	9363.314	37639.904	36520.198	36520.198	36520.198	36445.198	4043.314	36445.198	8094.33	4043.314	169.907	4150	186.387	75	5320	1119.707	37298	5404.584
Volume Flow cuft/hr	183.126	183.163	193.658	986.977	658.807	667.034	987.007	922.349	840.772	840.79	103.377	108.879	163.062	163.074	163.36	739.822	714.338	714.353	729.231	811.798	84.616	688.949	165.177	75.06	3550.997	82.274	19.666	1.232	86.545	20.98	658.817	87.181
Enthalpy MMBtu/hr	-25.062	-25.06	-24.626	-61.916	-34.065	-33.194	-61.911	-44.398	-50.408	-50.404	-34.693	-33.924	-46.294	-46.293	-46.266	-38.037	-37.055	-37.051	-36.142	-29.622	-8.989	-37.746	-25.996	-10.323	2.61	-13.448	0.934	-0.498	-36.166	-0.986	-34.069	-37.303
Mass Flow lb/hr																																
WATER	0	0	0	0	0	0	0	0	0	0	5404.584	5404.584	5329.241	5329.241	5329.241	75.342	75.084	75.084	75.084	3.688	24.234	3.688	0	24.234	0	0	0	71.396	5305.007	0.259	0	5404.584
METHA-01	8094.33	8094.33	8094.33	4168.609	0	0	4168.609	18.609	18.609	18.609	0	0	14.993	14.993	14.993	3.615	3.606	3.606	3.606	0.001	0	0.001	8094.33	0	0	4150	0	3.604	14.993	0.01	0	0
METHY-01	0	0	0	36325.624	0	0	36325.624	36325.624	36325.624	36325.624	0	0	0	0	0	36325.635	36325.544	36325.544	36325.544	36325.544	0	36325.544	0	0	0	0	0	0	0	0.091	0	0
NACL	0	0	0	0	0	0	0	0	0	0	0	0	0	0	0	0	0	0	0	0	0	0	0	0	0	0	0	0	0	0	0	0
GLYCE-01	0	0	0	3761.068	0	0	3761.068	3761.068	3761.068	3761.068	0	0	3760.903	3760.903	3760.903	0.164	0.164	0.164	0.164	0.164	3760.903	0.164	0	3760.903	0	0	0	0	0	0	0	0
NA+	107.13	107.13	107.13	107.13	0	0	107.13	107.13	107.13	107.13	0	0	77.624	77.624	77.624	29.506	29.211	29.211	29.211	29.211	77.624	29.211	0	77.624	0	0	107.13	0	0	0.294	0	0
OH-	79.257	79.257	79.257	79.257	0	0	79.257	79.257	79.257	79.257	0	0	57.428	57.428	57.428	21.829	21.611	21.611	21.611	21.611	57.428	21.611	0	57.428	0	0	79.257	0	0	0.218	0	0
H+	0	0	0	0	0	0	0	0	0	0	4.694	4.694	3.401	3.401	3.401	1.293	1.28	1.28	1.28	1.28	3.401	1.28	0	3.401	4.694	0	0	0	0	0.013	0	0
CL-	0	0	0	0	0	0	0	0	0	0	165.212	165.212	119.71	119.71	119.71	45.503	45.049	45.049	45.049	45.049	119.71	45.049	0	119.71	165.212	0	0	0	0	0.454	0	0
SODIU-01	0	0	0	0	0	0	0	0	0	0	0	0	0	0	0	0	0	0	0	0	0	0	0	0	0	0	0	0	0	0	0	0
OLEIC-01	0	0	0	18.649	18.649	18.649	18.649	18.649	18.649	18.649	0	0	0	0	0	18.649	18.649	18.649	18.649	18.649	0	18.649	0	0	0	0	0	0	0	0	18.649	0
TRIOL-01	0	0	0	1118.381	37279.351	37279.351	1118.381	1118.381	1118.381	1118.381	0	0	0.013	0.013	0.013	1118.368	0	0	0	0	0.013	0	0	0.013	0	0	0	0	0	0	1118.368	37279.351	0
Mass Frac																																
WATER	0	0	0	0	0	0	0	0	0	0	0.97	0.97	0.569	0.569	0.569	0.002	0.002	0.002	0.002	0	0.006	0	0	0.006	0	0	0	0.952	0.997	0	0	1
METHA-01	0.977	0.977	0.977	0.091	0	0	0.091	0	0	0	0	0	0.002	0.002	0.002	0	0	0	0	0	0	0	1	0	0	1	0	0.048	0.003	0	0	0
METHY-01	0	0	0	0.797	0	0	0.797	0.877	0.877	0.877	0	0	0	0	0	0.965	0.995	0.995	0.995	0.997	0	0.997	0	0	0	0	0	0	0	0	0	0
NACL	0	0	0	0	0	0	0	0	0	0	0	0	0	0	0	0	0	0	0	0	0	0	0	0	0	0	0	0	0	0	0	0
GLYCE-01	0	0	0	0.083	0	0	0.083	0.091	0.091	0.091	0	0	0.402	0.402	0.402	0	0	0	0	0	0.93	0	0	0.93	0	0	0	0	0	0	0	0
NA+	0.013	0.013	0.013	0.002	0	0	0.002	0.003	0.003	0.003	0	0	0.008	0.008	0.008	0.001	0.001	0.001	0.001	0.001	0.019	0.001	0	0.019	0	0	0.575	0	0	0	0	0
OH-	0.01	0.01	0.01	0.002	0	0	0.002	0.002	0.002	0.002	0	0	0.006	0.006	0.006	0.001	0.001	0.001	0.001	0.001	0.014	0.001	0	0.014	0	0	0.425	0	0	0	0	0
H+	0	0	0	0	0	0	0	0	0	0	0.001	0.001	0	0	0	0	0	0	0	0	0.001	0	0	0.001	0.028	0	0	0	0	0	0	0
CL-	0	0	0	0	0	0	0	0	0	0	0.03	0.03	0.013	0.013	0.013	0.001	0.001	0.001	0.001	0.001	0.03	0.001	0	0.03	0.972	0	0	0	0	0	0	0
SODIU-01	0	0	0	0	0	0	0	0	0	0	0	0	0	0	0	0	0	0	0	0	0	0	0	0	0	0	0	0	0	0	0	0
OLEIC-01	0	0	0	0	0.001	0.001	0	0	0	0	0	0	0	0	0	0	0.001	0.001	0.001	0.001	0	0.001	0	0	0	0	0	0	0	0	0.001	0
TRIOL-01	0	0	0	0.025	1	1	0.025	0.027	0.027	0.027	0	0	0	0	0	0.03	0	0	0	0	0	0	0	0	0	0	0	0	0	0	0.999	1	0
Mole Flow lbmol/hr																																
WATER	0	0	0	0	0	0	0	0	0	0	300	300	295.818	295.818	295.818	4.182	4.168	4.168	4.168	0.205	1.345	0.205	0	1.345	0	0	0	3.963	294.473	0.014	0	300
METHA-01	252.615	252.615	252.615	130.098	0	0	130.098	0.581	0.581	0.581	0	0	0.468	0.468	0.468	0.113	0.113	0.113	0.113	0	0	0	252.615	0	0	129.517	0	0.112	0.468	0	0	0
METHY-01	0	0	0	122.517	0	0	122.517	122.517	122.517	122.517	0	0	0	0	0	122.517	122.517	122.517	122.517	122.517	0	122.517	0	0	0	0	0	0	0	0	0	0
NACL	0	0	0	0	0	0	0	0	0	0	0	0	0	0	0	0	0	0	0	0	0	0	0	0	0	0	0	0	0	0	0	0
GLYCE-01	0	0	0	40.839	0	0	40.839	40.839	40.839	40.839	0	0	40.837	40.837	40.837	0.002	0.002	0.002	0.002	0.002	40.837	0.002	0	40.837	0	0	0	0	0	0	0	0
NA+	4.66	4.66	4.66	4.66	0	0	4.66	4.66	4.66	4.66	0	0	3.377	3.377	3.377	1.283	1.271	1.271	1.271	1.271	3.377	1.271	0	3.377	0	0	4.66	0	0	0.013	0	0
OH-	4.66	4.66	4.66	4.66	0	0	4.66	4.66	4.66	4.66	0	0	3.377	3.377	3.377	1.283	1.271	1.271	1.271	1.271	3.377	1.271	0	3.377	0	0	4.66	0	0	0.013	0	0
H+	0	0	0	0	0	0	0	0	0	0	4.66	4.66	3.377	3.377	3.377	1.283	1.271	1.271	1.271	1.271	3.377	1.271	0	3.377	4.66	0	0	0	0	0.013	0	0
CL-	0	0	0	0	0	0	0	0	0	0	4.66	4.66	3.377	3.377	3.377	1.283	1.271	1.271	1.271	1.271	3.377	1.271	0	3.377	4.66	0	0	0	0	0.013	0	0
SODIU-01	0	0	0	0	0	0	0	0	0	0	0	0	0	0	0	0	0	0	0	0	0	0	0	0	0	0	0	0	0	0	0	0
OLEIC-01	0	0	0	0.066	0.066	0.066	0.066	0.066	0.066	0.066	0	0	0	0	0	0.066	0.066	0.066	0.066	0.066	0	0.066	0	0	0	0	0	0	0	0	0.066	0
TRIOL-01	0	0	0	1.263	42.102	42.102	1.263	1.263	1.263	1.263	0	0	0	0	0	1.263	0	0	0	0	0	0	0	0	0	0	0	0	0	0	1.263	42.102	0

Table A.2 Stream Table for Simulation 2

SIM 2 (G1C)	1	1A	1C	2	2B	3A	3B	4A	4C	5A	5B	7A	7B	8A	8B	8C	9A	B-DIESEL	CH3OH	GLYCEROL	HCL	METHANOL	NAOH	RE-H2O-2	RE-H2O-1	RE-TRIOL	TRIOL	WATER
Temperature F	133.9	77	140	76.9	140	140	140.1	301.8	77	77.1	140	129.5	140.1	128.5	128.5	194	435.3	77	77	129.5	77	41	77	109.3	128.5	140.1	77	77
Pressure psi	29.2	14.5	14.7	29.2	14.7	14.7	29.39	0.73	29.39	30.65	14.7	14.7	14.7	14.7	29.39	14.7	1.47	14.7	14.5	14.7	14.7	0.73	14.5	1.47	14.7	14.7	14.5	15.95
Vapor Frac	0	0	0	0	0	0	0	0	0	0	0	0	0	0	0	0	0	0	1	0	0	0	0	0	0	0	0	0
Mole Flow lbmol/hr	261.935	261.935	261.935	42.168	42.168	304.103	304.103	174.586	174.586	300	300	131.308	138.909	131.042	131.042	131.042	127.227	127.227	252.615	43.279	7.008	129.517	9.32	3.815	305.867	1.407	42.168	300
Mass Flow lb/hr	8260.717	8260.717	8260.717	37298	37298	45578.717	45578.717	41428.717	41428.717	5404.584	5404.584	37617.89	36624.435	36502.416	36502.416	36502.416	36432.416	36432.416	8094.33	3810.824	127.758	4150	186.387	70	5526.603	1121.213	37298	5404.584
Volume Flow cuft/hr	192.544	193.126	193.658	658.907	667.034	986.977	987.007	922.349	840.772	87.185	90.308	738.234	739.551	706.481	706.495	725.714	905.111	685.972	165.177	53.846	2870.106	82.274	19.666	1.163	107.876	22.158	658.817	87.181
Enthalpy MMBtu/hr	-25.06	-25.062	-24.626	-34.065	-33.194	-61.916	-61.911	-44.398	-50.405	-37.303	-36.91	-38.024	-35.092	-37.498	-37.494	-36.312	-29.964	-37.944	-25.996	-12.382	1.962	-13.448	0.934	-0.465	-34.507	-0.969	-34.069	-37.303
Mass Flow lb/hr																												
WATER	0	0	0	0	0	0	0	0	0	5404.584	5404.584	0	0	75.772	75.772	75.772	8.682	8.682	0	0	0	0	0	67.09	5328.812	0	0	5404.584
METHA-01	8094.33	8094.33	8094.33	0	0	4168.609	4168.609	18.609	18.609	0	0	14.154	14.116	2.913	2.913	2.913	0.003	0.003	8094.33	4.455	0	4150	0	2.91	11.203	0.038	0	0
METHY-01	0	0	0	0	0	36325.624	36325.624	36325.624	36325.624	0	0	36325.62	36325.537	36325.536	36325.536	36325.536	36325.536	36325.536	0	0	0	0	0	0	0	0.083	0	0
NACL	0	0	0	0	0	0	0	0	0	0	0	0	0	0	0	0	0	0	0	0	0	0	0	0	0	0	0	0
GLYCE-01	0	0	0	0	0	3761.068	3761.068	3761.068	3761.068	0	0	0.919	0.919	0	0	0	0	0	0	3760.151	0	0	0	0	0	0.919	0	0
NA+	107.13	107.13	107.13	0	0	107.13	107.13	107.13	107.13	0	0	80.573	79.753	23.92	23.92	23.92	23.92	23.92	0	26.557	0	0	107.13	0	55.833	0.82	0	0
OH-	79.257	79.257	79.257	0	0	79.257	79.257	79.257	79.257	0	0	59.61	59.003	17.697	17.697	17.697	17.697	17.697	0	19.647	0	0	79.257	0	41.306	0.606	0	0
H+	0	0	0	0	0	0	0	0	0	0	0	0	3.494	1.048	1.048	1.048	1.048	1.048	0	0	3.53	0	0	0	2.446	0.036	0	0
CL-	0	0	0	0	0	0	0	0	0	0	0	0	122.964	36.881	36.881	36.881	36.881	36.881	0	0	124.228	0	0	0	86.084	1.264	0	0
SODIU-01	0	0	0	0	0	0	0	0	0	0	0	0	0	0	0	0	0	0	0	0	0	0	0	0	0	0	0	0
OLEIC-01	0	0	0	18.649	18.649	18.649	18.649	18.649	18.649	0	0	18.649	18.649	18.649	18.649	18.649	18.649	18.649	0	0	0	0	0	0	0	0	18.649	0
TRIOL-01	0	0	0	37279.351	37279.351	1118.381	1118.381	1118.381	1118.381	0	0	1118.366	0	0	0	0	0	0	0.015	0	0	0	0	0	0	0	1118.366	37279.351	0
Mass Frac																												
WATER	0	0	0	0	0	0	0	0	0	1	1	0	0	0.002	0.002	0.002	0	0	0	0	0	0	0	0.958	0.964	0	0	1
METHA-01	0.977	0.977	0.977	0	0	0.091	0.091	0	0	0	0	0	0	0	0	0	0	0	1	0.001	0	1	0	0.042	0.002	0	0	0
METHY-01	0	0	0	0	0	0.797	0.797	0.877	0.877	0	0	0.966	0.992	0.995	0.995	0.995	0.997	0.997	0	0	0	0	0	0	0	0	0	0
NACL	0	0	0	0	0	0	0	0	0	0	0	0	0	0	0	0	0	0	0	0	0	0	0	0	0	0	0	0
GLYCE-01	0	0	0	0	0	0.083	0.083	0.091	0.091	0	0	0	0	0	0	0	0	0	0	0.987	0	0	0	0	0	0	0	0
NA+	0.013	0.013	0.013	0	0	0.002	0.002	0.003	0.003	0	0	0.002	0.002	0.001	0.001	0.001	0.001	0.001	0	0.007	0	0	0.575	0	0.01	0.001	0	0
OH-	0.01	0.01	0.01	0	0	0.002	0.002	0.002	0.002	0	0	0.002	0.002	0	0	0	0	0	0	0.005	0	0	0.425	0	0.007	0.001	0	0
H+	0	0	0	0	0	0	0	0	0	0	0	0	0	0	0	0	0	0	0	0	0.028	0	0	0	0	0	0	0
CL-	0	0	0	0	0	0	0	0	0	0	0	0	0.003	0.001	0.001	0.001	0.001	0.001	0	0	0.972	0	0	0	0.016	0.001	0	0
SODIU-01	0	0	0	0	0	0	0	0	0	0	0	0	0	0	0	0	0	0	0	0	0	0	0	0	0	0	0	0
OLEIC-01	0	0	0	0.001	0.001	0	0	0	0	0	0	0	0.001	0.001	0.001	0.001	0.001	0.001	0	0	0	0	0	0	0	0	0.001	0
TRIOL-01	0	0	0	1	1	0.025	0.025	0.027	0.027	0	0	0.03	0	0	0	0	0	0	0	0	0	0	0	0	0	0	0.997	1	0
Mole Flow lbmol/hr																												
WATER	0	0	0	0	0	0	0	0	0	300	300	0	0	4.206	4.206	4.206	0.482	0.482	0	0	0	0	0	3.724	295.794	0	0	300
METHA-01	252.615	252.615	252.615	0	0	130.098	130.098	0.581	0.581	0	0	0.442	0.441	0.091	0.091	0.091	0	0	252.615	0.139	0	129.517	0	0.091	0.35	0.001	0	0
METHY-01	0	0	0	0	0	122.517	122.517	122.517	122.517	0	0	122.517	122.517	122.517	122.517	122.517	122.517	122.517	0	0	0	0	0	0	0	0	0	0
NACL	0	0	0	0	0	0	0	0	0	0	0	0	0	0	0	0	0	0	0	0	0	0	0	0	0	0	0	0
GLYCE-01	0	0	0	0	0	40.839	40.839	40.839	40.839	0	0	0.01	0.01	0	0	0	0	0	0	40.829	0	0	0	0	0.01	0	0	0
NA+	4.66	4.66	4.66	0	0	4.66	4.66	4.66	4.66	0	0	3.505	3.469	1.041	1.041	1.041	1.041	1.041	0	1.155	0	0	4.66	0	2.429	0.036	0	0
OH-	4.66	4.66	4.66	0	0	4.66	4.66	4.66	4.66	0	0	3.505	3.469	1.041	1.041	1.041	1.041	1.041	0	1.155	0	0	4.66	0	2.429	0.036	0	0
H+	0	0	0	0	0	0	0	0	0	0	0	0	3.468	1.04	1.04	1.04	1.04	1.04	0	0	3.504	0	0	0	2.428	0.036	0	0
CL-	0	0	0	0	0	0	0	0	0	0	0	0	3.468	1.04	1.04	1.04	1.04	1.04	0	0	3.504	0	0	0	2.428	0.036	0	0
SODIU-01	0	0	0	0	0	0	0	0	0	0	0	0	0	0	0	0	0	0	0	0	0	0	0	0	0	0	0	0
OLEIC-01	0	0	0	0.066	0.066	0.066	0.066	0.066	0.066	0	0	0.066	0.066	0.066	0.066	0.066	0.066	0.066	0	0	0	0	0	0	0	0	0.066	0
TRIOL-01	0	0	0	42.102	42.102	1.263	1.263	1.263	1.263	0	0	1.263	0	0	0	0	0	0	0	0	0	0	0	0	0	0	1.263	42.102	0

Table A.3 Stream Table for Simulation 3

SIM 3 (A4C)	1A	1B	1C	2A	2B	4A	4B	4C	5	5B	6	6A	6B	7A	7B	8A	8B	8C	11	B-DIESEL	CH3OH	GLYCEROL	HCL	MET-OL1	MET-OL2	NAOH	RE-H2O1	RE-TRIOL	TRIOL	WATER
Temperature F	77	133.9	140	76.9	140	140	77	77.1	77.1	140	130.6	130.4	140	130.4	140.4	138.6	138.7	140	325.4	417.2	77	77	77	69.2	61.9	77	138.6	140.4	77	77
Pressure psi	14.5	29.2	14.7	29.2	14.7	14.7	14.7	29.39	30.65	14.7	29.39	14.7	14.7	14.7	14.7	14.7	29.39	14.7	1.47	1.47	14.5	14.7	14.7	1.47	1.47	14.5	14.7	14.7	14.5	15.95
Vapor Frac	0	0	0.07	0	0	0	0	0	0	0	0	0	0.103	0	0	0	0	0	0	0	0	0	1	0	0	0	0	0	0	0
Mole Flow lbmol/hr	261.935	261.935	261.935	42.168	42.168	304.103	304.103	304.103	300	300	121.457	121.457	121.457	182.646	186.794	140.593	140.593	140.593	44.715	126.355	252.615	44.715	5.598	14.238	78.743	9.32	346.201	1.449	42.168	300
Mass Flow lb/hr	8280.717	8280.717	8280.717	37298	37298	45578.717	45578.717	45578.717	5404.584	5404.584	6301.985	6301.985	6301.985	39276.728	38258.854	36809.95	36809.95	36809.95	3842.985	36415.95	8094.33	3842.985	102.053	394	2459	186.387	6853.478	1119.928	37298	5404.584
Volume Flow cuft/hr	183.126	192.544	8089.832	658.807	667.034	986.977	961.397	961.422	97.185	90.308	105.659	105.65	5482.051	811.902	802.746	723.231	723.246	723.634	63.115	793.483	165.177	55.516	2132.884	7.688	49.562	19.666	134.653	22.262	658.817	87.181
Enthalpy MMBtu/hr	-25.062	-25.06	-24.752	-34.065	-33.194	-61.916	-63.352	-63.347	-37.303	-36.91	-20.051	-20.052	-19.958	-43.295	-40.742	-38.531	-38.527	-38.506	-10.955	-30.487	-25.996	-12.403	1.588	-1.561	-7.928	0.934	-39.121	-0.985	-34.069	-37.303
Mass Flow lb/hr																														
WATER	0	0	0	0	0	0	0	0	5404.584	5404.584	0	0	0	0	0	89.705	89.705	89.705	0	9.803	0	0	0	79.902	0	0	5314.879	0	0	5404.584
METHA-01	8094.33	8094.33	8094.33	0	0	4168.609	4168.609	4168.609	0	0	2464.216	2464.216	2464.216	1704.393	1701.063	314.721	314.721	314.721	5.216	0.623	8094.33	5.216	0	314.098	2459	0	1386.342	3.331	0	0
METHY-01	0	0	0	0	0	36325.624	36325.624	36325.624	0	0	0	0	0	36325.619	36325.555	36325.545	36325.545	36325.545	0	36325.545	0	0	0	0	0	0	0	0.064	0	0
NACL	0	0	0	0	0	0	0	0	0	0	0	0	0	0	0	0	0	0	0	0	0	0	0	0	0	0	0	0	0	0
GLYCE-01	0	0	0	0	0	3761.068	3761.068	3761.068	0	0	3759.832	3759.832	3759.832	1.237	1.237	0	0	0	3759.832	0	0	3759.832	0	0	0	0	1.237	0	0	0
NA+	107.13	107.13	107.13	0	0	107.13	107.13	107.13	0	0	42.787	42.787	42.787	64.343	63.947	18.44	18.44	18.44	42.787	18.44	0	42.787	0	0	0	107.13	45.407	0.495	0	0
OH-	79.257	79.257	79.257	0	0	79.257	79.257	79.257	0	0	31.655	31.655	31.655	47.602	47.235	13.642	13.642	13.642	31.655	13.642	0	31.655	0	0	0	79.257	33.593	0.367	0	0
H+	0	0	0	0	0	0	0	0	0	0	0	0	0	0	2.798	0.808	0.808	0.808	0	0.808	0	0	2.82	0	0	0	1.99	0.022	0	0
CL-	0	0	0	0	0	0	0	0	0	0	0	0	0	0	98.47	28.439	28.439	28.439	0	28.439	0	0	99.234	0	0	0	70.03	0.764	0	0
SODIU-01	0	0	0	0	0	0	0	0	0	0	0	0	0	0	0	0	0	0	0	0	0	0	0	0	0	0	0	0	0	0
OLEIC-01	0	0	0	18.649	18.649	18.649	18.649	18.649	0	0	0	0	0	18.649	18.649	18.649	18.649	18.649	0	18.649	0	0	0	0	0	0	0	0	18.649	0
TRIOL-01	0	0	0	37279.351	37279.351	1118.381	1118.381	1118.381	0	0	3.495	3.495	3.495	1114.885	0	0	0	0	3.495	0	0	3.495	0	0	0	0	0	1114.885	37279.351	0
Mass Frac																														
WATER	0	0	0	0	0	0	0	0	1	1	0	0	0	0	0	0.002	0.002	0.002	0	0	0	0	0	0.203	0	0	0.776	0	0	1
METHA-01	0.977	0.977	0.977	0	0	0.091	0.091	0.091	0	0	0.391	0.391	0.391	0.043	0.044	0.009	0.009	0.009	0.001	0	1	0.001	0	0.797	1	0	0.202	0.003	0	0
METHY-01	0	0	0	0	0	0.797	0.797	0.797	0	0	0	0	0	0.925	0.949	0.987	0.987	0.987	0	0.998	0	0	0	0	0	0	0	0	0	0
NACL	0	0	0	0	0	0	0	0	0	0	0	0	0	0	0	0	0	0	0	0	0	0	0	0	0	0	0	0	0	0
GLYCE-01	0	0	0	0	0	0.083	0.083	0.083	0	0	0.597	0.597	0.597	0	0	0	0	0	0.978	0	0	0.978	0	0	0	0	0	0	0	0
NA+	0.013	0.013	0.013	0	0	0.002	0.002	0.002	0	0	0.007	0.007	0.007	0.002	0.002	0.001	0.001	0.001	0.011	0.001	0	0.011	0	0	0	0.575	0.007	0	0	0
OH-	0.01	0.01	0.01	0	0	0.002	0.002	0.002	0	0	0.005	0.005	0.005	0.001	0.001	0	0	0	0.008	0	0	0.008	0	0	0	0.425	0.005	0	0	0
H+	0	0	0	0	0	0	0	0	0	0	0	0	0	0	0	0	0	0	0	0	0	0	0.028	0	0	0	0	0	0	0
CL-	0	0	0	0	0	0	0	0	0	0	0	0	0	0	0.003	0.001	0.001	0.001	0	0.001	0	0	0.972	0	0	0	0.01	0.001	0	0
SODIU-01	0	0	0	0	0	0	0	0	0	0	0	0	0	0	0	0	0	0	0	0	0	0	0	0	0	0	0	0	0	0
OLEIC-01	0	0	0	0.001	0.001	0	0	0	0	0	0	0	0	0	0	0.001	0.001	0.001	0	0.001	0	0	0	0	0	0	0	0	0.001	0
TRIOL-01	0	0	0	1	1	0.025	0.025	0.025	0	0	0.001	0.001	0.001	0.028	0	0	0	0	0.001	0	0	0.001	0	0	0	0	0	0.995	1	0
Mole Flow lbmol/hr																														
WATER	0	0	0	0	0	0	0	0	300	300	0	0	0	0	0	4.979	4.979	4.979	0	0.544	0	0	0	4.435	0	0	295.021	0	0	300
METHA-01	252.615	252.615	252.615	0	0	130.098	130.098	130.098	0	0	76.905	76.905	76.905	53.192	53.088	9.822	9.822	9.822	0.163	0.019	252.615	0.163	0	9.803	76.743	0	43.266	0.104	0	0
METHY-01	0	0	0	0	0	122.517	122.517	122.517	0	0	0	0	0	122.517	122.517	122.517	122.517	122.517	0	122.517	0	0	0	0	0	0	0	0	0	0
NACL	0	0	0	0	0	0	0	0	0	0	0	0	0	0	0	0	0	0	0	0	0	0	0	0	0	0	0	0	0	0
GLYCE-01	0	0	0	0	0	40.839	40.839	40.839	0	0	40.826	40.826	40.826	0.013	0.013	0	0	0	40.826	0	0	40.826	0	0	0	0	0.013	0	0	0
NA+	4.66	4.66	4.66	0	0	4.66	4.66	4.66	0	0	1.861	1.861	1.861	2.799	2.777	0.802	0.802	0.802	1.861	0.802	0	1.861	0	0	0	4.66	1.975	0.022	0	0
OH-	4.66	4.66	4.66	0	0	4.66	4.66	4.66	0	0	1.861	1.861	1.861	2.799	2.777	0.802	0.802	0.802	1.861	0.802	0	1.861	0	0	0	4.66	1.975	0.022	0	0
H+	0	0	0	0	0	0	0	0	0	0	0	0	0	0	2.777	0.802	0.802	0.802	0	0.802	0	0	2.799	0	0	0	1.975	0.022	0	0
CL-	0	0	0	0	0	0	0	0	0	0	0	0	0	0	2.777	0.802	0.802	0.802	0	0.802	0	0	2.799	0	0	0	1.975	0.022	0	0
SODIU-01	0	0	0	0	0	0	0	0	0	0	0	0	0	0	0	0	0	0	0	0	0	0	0	0	0	0	0	0	0	0
OLEIC-01	0	0	0	0.066	0.066	0.066	0.066	0.066	0	0	0	0	0	0.066	0.066	0.066	0.066	0.066	0	0.066	0	0	0	0	0	0	0	0	0.066	0
TRIOL-01	0	0	0	42.102	42.102	1.263	1.263	1.263	0	0	0.004	0.004	0.004	1.259	0	0	0	0	0.004	0	0	0.004	0	0	0	0	0	1.259	42.102	0

Table A.4 Stream Table for Simulation 4

SIM4 (A5C)	1A	1B	1C	2A	2B	4A	4B	4C	5	5B	6	6A	6B	7	7A	7B	8A	8B	8C	11	B-DIESEL	CH3OH	GLYCEROL	HCL-BD	MET-OL2	METHANOL	NAOH	RE-H2O1	RE-TRIOL	TRIOL	WATER
Temperature F	77	133.9	140	76.9	140	140	77	77.1	77.1	140	130.8	130.4	140	130.5	130.4	140	399.9	77	87.8	325.4	92.5	77	77	77	61.9	61.9	77	92.5	67.8	77	77
Pressure psi	14.5	29.2	14.7	29.2	14.7	14.7	14.7	29.39	30.65	14.7	29.39	14.7	14.7	29.39	14.7	14.7	1.47	14.7	14.7	1.47	14.7	14.5	14.7	14.7	1.47	1.47	14.5	14.7	14.7	14.5	15.95
Vapor Frac	0	0	0.07	0	0	0	0	0	0	0	0	0	0.103	0	0	0	0	0	0	0	0	0	0	0	1	0	0	0	0	0	0
Mole Flow lbmol/hr	261.935	261.935	261.935	42.168	42.168	304.103	304.103	304.103	300	300	121.457	121.457	121.457	182.646	182.646	182.646	129.747	129.747	133.968	44.715	128.216	252.615	44.715	5.594	76.743	52.899	9.32	305.752	1.373	42.168	300
Mass Flow lb/hr	8280.717	8280.717	8280.717	37298	37298	45578.717	45578.717	45578.717	5404.584	5404.584	6301.985	6301.985	6301.985	39276.728	39276.728	39276.728	37581.728	37581.728	36586.827	3842.985	38450.041	8094.33	3842.985	101.98	2459	1695	186.387	5821.153	1117.081	37298	5404.584
Volume Flow cuft/hr	183.126	192.544	8099.832	658.807	667.034	966.977	961.307	961.422	87.185	90.308	105.659	105.65	5482.051	811.921	811.902	815.031	824.214	717.908	714.096	63.115	689.982	165.177	55.516	2131.36	49.562	34.163	19.666	102.353	21.452	658.817	87.181
Enthalpy MMBtu/hr	-25.082	-25.06	-24.752	-34.065	-33.194	-61.916	-63.352	-63.347	-37.303	-36.91	-20.051	-20.052	-19.858	-43.291	-43.295	-43.112	-31.867	-39.048	-38.488	-10.955	-38.059	-25.996	-12.403	1.567	-7.928	-5.465	0.934	-35.339	-0.993	-34.069	-37.303
Mass Flow lb/hr																															
WATER	0	0	0	0	0	0	0	0	5404.584	5404.584	0	0	0	0	0	0	0	0	0	0	41.567	0	0	0	0	0	0	5363.018	0	0	5404.584
METHA-01	8094.33	8094.33	8094.33	0	0	4168.609	4168.609	4168.609	0	0	2464.216	2464.216	2464.216	1704.393	1704.393	1704.393	9.393	9.393	9.38	5.216	1.673	8094.33	5.216	0	2459	1695	0	7.707	0.014	0	0
METHY-01	0	0	0	0	0	36325.624	36325.624	36325.624	0	0	0	0	0	36325.619	36325.619	36325.619	36325.619	36325.619	36325.607	0	36325.599	0	0	0	0	0	0	0	0.012	0	0
NACL	0	0	0	0	0	0	0	0	0	0	0	0	0	0	0	0	0	0	0	0	0	0	0	0	0	0	0	0	0	0	0
GLYCE-01	0	0	0	0	0	3761.068	3761.068	3761.068	0	0	3759.832	3759.832	3759.832	1.237	1.237	1.237	1.237	1.237	1.237	3759.832	0	0	3759.832	0	0	0	0	1.237	0	0	0
NA+	107.13	107.13	107.13	0	0	107.13	107.13	107.13	0	0	42.787	42.787	42.787	64.343	64.343	64.343	64.343	64.343	63.69	42.787	18.817	0	42.787	0	0	0	107.13	44.873	0.653	0	0
OH-	79.257	79.257	79.257	0	0	79.257	79.257	79.257	0	0	31.655	31.655	31.655	47.602	47.602	47.602	47.602	47.602	47.119	31.655	13.921	0	31.655	0	0	0	79.257	33.198	0.483	0	0
H+	0	0	0	0	0	0	0	0	0	0	0	0	0	0	0	0	2.789	0	0.824	0	0	0	0	2.818	0	0	0	1.965	0.029	0	0
CL-	0	0	0	0	0	0	0	0	0	0	0	0	0	0	0	0	98.157	0	29	0	0	99.163	0	0	0	0	0	89.156	1.006	0	0
SODIU-01	0	0	0	0	0	0	0	0	0	0	0	0	0	0	0	0	0	0	0	0	0	0	0	0	0	0	0	0	0	0	0
OLEIC-01	0	0	0	18.649	18.649	18.649	18.649	18.649	0	0	0	0	0	18.649	18.649	18.649	18.649	18.649	18.649	0	18.649	0	0	0	0	0	0	0	0	18.649	0
TRIOL-01	0	0	0	37279.351	37279.351	1118.381	1118.381	1118.381	0	0	3.495	3.495	3.495	1114.885	1114.885	1114.885	1114.885	1114.885	0	3.495	0	0	3.495	0	0	0	0	0	1114.885	37279.351	0
Mass Frac																															
WATER	0	0	0	0	0	0	0	0	1	1	0	0	0	0	0	0	0	0	0	0	0.001	0	0	0	0	0	0	0.971	0	0	1
METHA-01	0.977	0.977	0.977	0	0	0.091	0.091	0.091	0	0	0.391	0.391	0.391	0.043	0.043	0.043	0	0	0	0.001	0	1	0.001	0	1	1	0	0.001	0.001	0	0
METHY-01	0	0	0	0	0	0.797	0.797	0.797	0	0	0	0	0	0.925	0.925	0.925	0.967	0.967	0.993	0	0.997	0	0	0	0	0	0	0	0	0	0
NACL	0	0	0	0	0	0	0	0	0	0	0	0	0	0	0	0	0	0	0	0	0	0	0	0	0	0	0	0	0	0	0
GLYCE-01	0	0	0	0	0	0.083	0.083	0.083	0	0	0.597	0.597	0.597	0	0	0	0	0	0	0.978	0	0	0.978	0	0	0	0	0	0	0	0
NA+	0.013	0.013	0.013	0	0	0.002	0.002	0.002	0	0	0.007	0.007	0.007	0.002	0.002	0.002	0.002	0.002	0.002	0.011	0.001	0	0.011	0	0	0	0.575	0.008	0.001	0	0
OH-	0.01	0.01	0.01	0	0	0.002	0.002	0.002	0	0	0.005	0.005	0.005	0.001	0.001	0.001	0.001	0.001	0.001	0.008	0	0	0.008	0	0	0	0.425	0.006	0	0	0
H+	0	0	0	0	0	0	0	0	0	0	0	0	0	0	0	0	0	0	0	0	0	0	0	0.028	0	0	0	0	0	0	0
CL-	0	0	0	0	0	0	0	0	0	0	0	0	0	0	0	0	0.003	0	0.001	0	0	0.972	0	0	0	0	0	0.013	0.001	0	0
SODIU-01	0	0	0	0	0	0	0	0	0	0	0	0	0	0	0	0	0	0	0	0	0	0	0	0	0	0	0	0	0	0	0
OLEIC-01	0	0	0	0.001	0.001	0	0	0	0	0	0	0	0	0	0	0	0	0	0.001	0	0.001	0	0	0	0	0	0	0	0	0.001	0
TRIOL-01	0	0	0	1	1	0.025	0.025	0.025	0	0	0.001	0.001	0.001	0.028	0.028	0.028	0.03	0.03	0	0.001	0	0	0.001	0	0	0	0	0	0.998	1	0
Mole Flow lbmol/hr																															
WATER	0	0	0	0	0	0	0	0	300	300	0	0	0	0	0	0	0	0	0	0	2.307	0	0	0	0	0	0	297.693	0	0	300
METHA-01	252.615	252.615	252.615	0	0	130.098	130.098	130.098	0	0	76.905	76.905	76.905	53.192	53.192	53.192	0.293	0.293	0.293	0.163	0.052	252.615	0.163	0	76.743	52.899	0	0.241	0	0	0
METHY-01	0	0	0	0	0	122.517	122.517	122.517	0	0	0	0	0	122.517	122.517	122.517	122.517	122.517	122.517	0	122.517	0	0	0	0	0	0	0	0	0	0
NACL	0	0	0	0	0	0	0	0	0	0	0	0	0	0	0	0	0	0	0	0	0	0	0	0	0	0	0	0	0	0	0
GLYCE-01	0	0	0	0	0	40.839	40.839	40.839	0	0	40.826	40.826	40.826	0.013	0.013	0.013	0.013	0.013	0.013	40.826	0	0	40.826	0	0	0	0	0.013	0	0	0
NA+	4.66	4.66	4.66	0	0	4.66	4.66	4.66	0	0	1.861	1.861	1.861	2.799	2.799	2.799	2.799	2.799	2.77	1.861	0.819	0	1.861	0	0	0	4.66	1.952	0.028	0	0
OH-	4.66	4.66	4.66	0	0	4.66	4.66	4.66	0	0	1.861	1.861	1.861	2.799	2.799	2.799	2.799	2.799	2.77	1.861	0.819	0	1.861	0	0	0	4.66	1.952	0.028	0	0
H+	0	0	0	0	0	0	0	0	0	0	0	0	0	0	0	0	2.769	0	0.818	0	0	0	0	2.797	0	0	0	1.951	0.028	0	0
CL-	0	0	0	0	0	0	0	0	0	0	0	0	0	0	0	0	2.769	0	0.818	0	0	2.797	0	0	0	0	0	1.951	0.028	0	0
SODIU-01	0	0	0	0	0	0	0	0	0	0	0	0	0	0	0	0	0	0	0	0	0	0	0	0	0	0	0	0	0	0	0
OLEIC-01	0	0	0	0.066	0.066	0.066	0.066	0.066	0	0	0	0	0	0.066	0.066	0.066	0.066	0.066	0.066	0	0.066	0	0	0	0	0	0	0	0	0.066	0
TRIOL-01	0	0	0	42.102	42.102	1.263	1.263	1.263	0	0	0.004	0.004	0.004	1.259	1.259	1.259	1.259	1.259	0	0.004	0	0	0.004	0	0	0	0	0	1.259	42.102	0

APPENDIX B

Storage and Handling of Product

It is important to monitor oxidative stability and prevent oxidative degradation, which is the formation of peroxides, acids, and gums. One of the best ways to prevent this occurrence is to not expose the biodiesel to air at high temperatures during processing. The more double bonds a substance possesses, the more prone it is to oxidation. The relative rate of oxidation for C18:1 : C18:2 : C18:3 is 1: 15: 25. Less poly saturation increases the oxidative stability of Biodiesel. As a result of oxidation, aliphatic alcohols, aldehydes, and short chain fatty acids are formed. This formation reduces the flash point of biodiesel, causing rancidity or bad smell, and corrosion. Increased acidity is the primary indicator of biodiesel oxidative degradation and therefore should be monitored (He, 2006). Instability affects the level of precipitates dropping out of the methyl ester solution. When biodiesel is oxidized, double bonds in unsaturated fatty acid chains form epoxides. This temporary molecule is unstable and either breaks off entirely to make a carboxylic acid, or the oxygen will find another molecule containing a double bond and a temporary bridge between two separate esters is formed. Those initial bridges are the beginning formations of polymers, which also precipitate out of the fuel, causing severe filter-plugging problems. Increased viscosity of the stored biodiesel is an indicator of oxidative polymerization.

Metals such as copper and copper containing materials such as brass and bronze have a catalytic effect on the biodiesel oxidation process. Contact with these materials should be avoided during long-term storage. Lead, tin, and zinc are also cited as having some incompatibility with biodiesel. Aluminum, steel, and stainless steel are acceptable for tank materials, while stainless steel and black iron are commonly used for piping (Tyson, 2006).

Other preventive measures for the storage of biodiesel involve (He, 2006, Tyson, 2006):

- Putting antioxidant immediately at the point of manufacture before oxidation has a chance to start
- Cleaning tanks thoroughly before initial fillings so that there are no oxidizing agents

- Storage in underground tanks to avoid severe environmental change

- Preventing exposure to air by using nitrogen blankets

- Monitoring pH and viscosity levels regularly

- Applying biocides to prevent biological contamination

Safety

Biodiesel popularity stems from several characteristics. It is simple to manufacture, biodegradable, nontoxic, and essentially free of sulfur and aromatics. Although biodiesel is non-flammable and non-reactive, manufacturing of biodiesel poses processing hazards and therefore careful attention is necessary to manufacture biodiesel safely. The following safety issues are identified from Material Safety Data Sheets (MSDSs).

Methanol (flash point 12.2 ^{o}C) is classified as a Class IB flammable liquid. According to OSHA, Class IB substances have flash points below 73 ^{o}F (22.8 ^{o}C) and boiling points higher than 100 ^{o}F (37.8 ^{o}C) and subsequently can readily catch fire at room temperature. The flame above burning methanol is virtually invisible, so it is not always easy to determine whether a methanol flame is still alight. The explosion limits for methanol (the lower and upper percentage limits of methanol in an air-methanol mixture giving a vapor that can explode) are unusually wide. Methanol's lower flammability limit (LFL) is 7.3 (vol% in fuel air) and its upper flammability limit (UFL) is 36. Methanol's autoignition temperature is 574 °C. The reaction temperature can exceed the boiling point of methanol (64.8 $^.$C /148.64 F) and therefore, a blanket of nitrogen is recommended.

Methanol is toxic. If ingested or inhaled, it can cause a wide range of harmful effects, from headache to death. Contact with methanol can cause skin diseases such as defatting of the skin and dermatitis.

Hydrochloric acid is a very strong acid and corrosive. Ingestion can cause circulatory system failure, severe digestive tract burns with abdominal pain, vomiting, and possible death. Vapors have an irritating effect on the respiratory tract, causing coughing, burns, breathing difficulty, and possible coma. Contact with skin produces

irritation and burns of the skin and mucous membranes. Contact with the eyes can cause severe burns, which may result in prolonged or permanent visual impairment or loss of sight.

NaOH solid is very corrosive and an irritant. Inhalation of dust or mist can cause symptoms ranging from mild irritation to serious damage of the upper respiratory tract. Ingestion may cause severe burns of the mouth, throat, and stomach. Skin contact can cause irritation or severe burns and scarring with greater exposures. Contact with the eyes can cause burns that may result in permanent impairment of vision or even blindness.

Also, mixing NaOH and methanol is an exothermic reaction that generates heat. As a result, cooling jackets are recommended for the mixing tank.

The severity of safety issues related to these compounds are determined by concentration and duration of exposure. Therefore, special care should be taken while handling these compounds in a biodiesel production unit.

Iodine Number

The number of unsaturated double bonds is described by "Iodine Value" or "Iodine Number", a measure of how many grams of iodine are absorbed when 100 grams of sample are introduced to the iodine. Although United States ASTM D6751 does not specify Iodine Value, the maximum Iodine Number, according to Europe's EN14214 specification is 120. According to Germany's DIN 51606 specifications, the maximum Iodine Number is 115 (Brevard Biodiesel, 2006).

Glycerol Index

ASTM's total glycerin spec of 0.24 is not widely understood. When the bonded glycerin value is calculated, only the fractions that make up the backbones (actual glycerin portion) of monoglycerides, diglycerides, and triglycerides are included in the spec calculations, while the connected long fatty acids chains are not. The sum of these three individual numbers is the bond glycerin value. Then the number of bond glycerin is added to the free glycerin to get the value of total glycerin. This is the reason why 96 or 97 % transesterification can still meet the ASTM total glycerin spec of 0.24 % (Kotrba, 2006).

Calculation of Total NaOH for High FFA Concentration

Extra amount of NaOH to neutralize the FFA

$$= Wt \ of \ FFA \ x \ \frac{1 \ mol \ of \ FFA}{1 \ mol \ of \ NaOH} \ x \ \frac{M.W \ of \ NaOH}{M.W \ of \ FFA}$$

$$= Wt \ of \ FFA \ x \ \frac{1 \ mol \ of \ FFA}{1 \ mol \ of \ NaOH} \ x \ \frac{39.9971 \ lb \ of \ NaOH}{282.46676 \ lb \ of \ FFA}$$

$$\boxed{Total \ Amount \ of \ NaOH \ = \ Wt \ of \ FFA \ x \ 0.1416}$$

where

$$Wt \ of \ FFA = \frac{Wt \ of \ FFA}{Wt \ of \ Triol} \ x \ Wt \ of \ Triol = \frac{\% \ Wt \ of \ FFA}{100} \ x \ Wt \ of \ Triol$$

From this general equation, the total amount of NaOH can be calculated as follows:

Total % of NaOH = Extra amount to neutralize FFA + 1 wt % of Trioleic

$$\boxed{Total \ Amount \ of \ NaOH \ (lb) \ = \ \frac{(\% \ Wt \ of \ FFA \ x \ 0.1416 + 1)}{100} \ x \ Wt \ of \ Trioleic}$$

VITA

Name: Lay L. Myint

Address: 15910 FM 529, Houston, TX 77095

Email Address: Lmyint2001@yahoo.com

Education: B.S., Biology, Purdue University, 1998
                                M.S., Chemical Engineering, Texas A&M,
                                2007